Functional characterisation of RNA helicases in the remodelling of pre-ribosomal subunits

Dissertation

for the award of the degree

"Doctor rerum naturalium"

of the Georg-August-Universität Göttingen

within the doctoral program *Molecular Biology of Cells*

of the Georg-August University School of Science (GAUSS)

submitted by

Lukas Brüning

from Gelnhausen

Göttingen 2017

Promovierenden-Erklärung

Georg-August-Universität Göttingen

Name: Brüning, Lukas

(Name, Vorname)

Anschrift: Humboldtallee 4, 37073 Göttingen

(Straße, PLZ, Wohnort)

Ich beabsichtige, eine Dissertation zum Thema "Functional characterisation of RNA helicases in the remodelling of pre-ribosomal complexes" an der Georg-August-Universität Göttingen anzufertigen. Dabei werde ich von Herrn Prof. Dr. Markus Bohnsack betreut.

Ich gebe folgende Erklärung ab:

1. Die Gelegenheit zum vorliegenden Promotionsvorhaben ist mir nicht kommerziell vermittelt worden. Insbesondere habe ich keine Organisation eingeschaltet, die gegen Entgelt Betreuerinnen und Betreuer für die Anfertigung von Dissertationen sucht oder die mir obliegenden Pflichten hinsichtlich der Prüfungsleistungen für mich ganz oder teilweise erledigt.

2. Hilfe Dritter wurde bis jetzt und wird auch künftig nur in wissenschaftlich vertretbarem und prüfungsrechtlich zulässigem Ausmaß in Anspruch genommen. Insbesondere werden alle Teile der Dissertation selbst angefertigt; unzulässige fremde Hilfe habe ich dazu weder unentgeltlich noch entgeltlich entgegengenommen und werde dies auch zukünftig so halten.

3. Die Richtlinien zur Sicherung der guten wissenschaftlichen Praxis an der Universität Göttingen werden von mir beachtet.

4. Eine entsprechende Promotion wurde an keiner anderen Hochschule im In- oder Ausland beantragt; die eingereichte Dissertation oder Teile von ihr wurden nicht für ein anderes Promotionsvorhaben verwendet.

Mir ist bekannt, dass unrichtige Angaben die Zulassung zur Promotion ausschließen bzw. später zum Verfahrensabbruch oder zur Rücknahme des erlangten Grades führen.

Göttingen, den 29.09.2017

(Unterschrift)

<u>Table of Contents</u>

List of Figures

List of Tables

Abbreviation	Meaning
Bp	Basepair
cDNA	Complementary DNA
CLASH	Crosslinking and analysis of sequence hybrids
CLIP	Crosslinking and immunoprecipitation
CP	Central protuberance
CRAC	Crosslinking and analysis of cDNA
Cryo-EM	Cryo-electron microscopy
DMS	Dimethyl sulfate
DNA	Deoxyribonucleic acid
Dox	Doxycycline
ES	Expansion segment
ETS	External transcribed spacer
EV	Empty vector
HTP	His_6-TEV cleavage site-ProteinA
ITS	Internal transcribed spacer
lncRNA	Long non-coding RNA
LSU	Large ribosomal subunit
mRNA	Messenger RNA
NES	Nuclear export signal
NLS	Nuclear localisation signal
NPC	Nuclear pore complex
nt	Nucleotide
NTP	Nucleotide triphosphate
ORF	Open reading frame
PAGE	Polyacrylamide gel electrophoresis
PAR-CRAC	Photoactivatable ribonucleoside-enhanced CRAC
PCR	Polymerase chain reaction
Pol I / II / III	RNA polymerases I / II / III
PTC	Peptidyl transferase center
qPCR	Quantitative PCR
RBP	RNA binding protein
RNA	Ribonucleic acid
RNP	Ribonucleoprotein particle
RP	Ribosomal protein
rRNA	Ribosomal RNA
S	Svedberg units
SF	Superfamily
snoRNA	Small nucleolar RNA
snRNA	Small nuclear RNA
SSU	Small ribosomal subunit
TEV	Tobacco etch virus
tRNA	Transfer RNA
UTR	Untranslated region
UV	Ultra violet

<u>Abstract</u>

DEAD/H-box RNA helicases are ubiquitously expressed enzymes, which are characterised by a conserved helicase core of two RecA-like domains containing sequence motifs required for substrate binding and hydrolysis of NTP. Since this helicase core predominantly interacts with the sugar phosphate backbone of its target RNA, additional N- and/or C-terminal ancillary domains are thought to confer substrate specificity and/or mediate cofactor interactions. On the molecular level, some RNA helicases were shown to have unwinding activity, but others can also anneal RNA duplexes or mediate the release of proteins from protein-RNA complexes. Through their key functions in structural remodelling of RNAs and RNP complexes, RNA helicases are implicated in all aspects of RNA metabolism including transcription, translation, pre-mRNA splicing, RNA turnover and ribosome biogenesis.

The biogenesis of ribosomes is a complex and energy-consuming process, which involves the synthesis and processing of four ribosomal RNAs (rRNAs) and their assembly with approximately 80 ribosomal proteins. Ribosome synthesis involves in excess of 200 biogenesis cofactors, including snoRNPs that introduce rRNA modifications co-transcriptionally as well as enzymes such as nucleases, NTPases and RNA helicases, which act in a strict hierarchical order to mediate the correct assembly and maturation of 40S and 60S subunits. In the yeast *Saccharomyces cerevisiae*, 21 RNA helicases are proposed to act during the synthesis of ribosomes, where they likely contribute to different steps along the maturation pathway. Some RNA helicases are required for the release of specific snoRNPs from pre-ribosomal complexes, whereas other RNA helicases are suggested to be involved in structural rearrangements of rRNA and remodelling of pre-ribosomal complexes. However, many of the RNA helicases implicated in ribosome biogenesis remain uncharacterised and the lack of information about their binding sites on pre-ribosomal complexes has impeded further functional characterisation of these proteins.

In this work, we focused on three essential RNA helicases, Has1, Spb4 and Mak5, which are implicated in both SSU and LSU biogenesis (Has1) or in the later stages of LSU biogenesis (Spb4 and Mak5). Using a crosslinking technique with subsequent analysis of cDNA (CRAC) we revealed their putative binding sites on pre-ribosomal complexes. The observed CRAC sites for Has1 were consistent with its previously reported functions in the release the U14 snoRNA from pre-40S particles and regulating the release of a subset of *trans*-acting ribosome biogenesis factors from pre-60S complexes, but the identification of two Has1 crosslinking sites in the 18S rRNA suggests that Has1 may have an additional function in the biogenesis of small ribosomal subunits. DMS structure probing experiments demonstrated that the crosslinking sites identified for Spb4 and Mak5 by CRAC are *bona-fide* protein binding sites. In the case of Spb4, the structure probing data further suggest that one of the identified

crosslinking sites likely represents a binding platform for the helicase whereas the other crosslinking site might represent a region of the pre-rRNA that is remodelled by Spb4. Interestingly, this rRNA region is in close proximity to the known binding site of the ribosome biogenesis factors Nog2 and Arx1, suggesting that Spb4 may play a direct role in recruitment or release of these proteins from pre-60S complexes. Excitingly, for Mak5, our data have revealed a function of the helicase in restructuring a region of the pre-ribosome to enable recruitment of the ribosomal protein Rpl10 to cytoplasmic ribosomal particles. Together, these findings extend the range of functions linked to RNA helicases in ribosome biogenesis and add to the understanding of important events during assembly of the large ribosomal subunit.

1   Introduction

1.1   RNA helicases

The functions of RNA extend from being solely the messenger between the genetic information in DNA and the ribosome where proteins are produced (messenger RNAs; mRNAs) to also include various non-coding RNAs, such as ribosomal RNAs (rRNAs), transfer RNAs (tRNAs), small nuclear RNAs (snRNAs), small nucleolar RNAs (snoRNAs) and long non-coding RNAs (lncRNAs). RNA therefore plays important roles in facilitating and regulating almost all aspects of gene expression. These various functions of RNAs require correct folding into secondary and finally tertiary structures, as well as assembly with protein components to form larger ribonucleoprotein complexes (RNPs). Nascent transcripts, produced by any of the three RNA polymerases (Pol I, II or III), can immediately fold into secondary structures. However, in the case of longer transcripts that form long-range intramolecular interactions in their final topology, it is possible that aberrant basepairing interactions are formed first because of the low variety of bases in the RNA. These kinetic traps necessitate RNA structural transitions to enable the RNAs to establish their correct folds (Russell, 2008). Furthermore, most RNPs are highly dynamic and require numerous structural rearrangements during their biogenesis to fulfil their functions. Such RNA remodelling often requires assistance by proteins. RNA helicases, which are ubiquitous enzymes that are best known for their functions in unwinding double-stranded nucleic acids by cooperative binding and hydrolysis of nucleotide triphosphates (NTPs), are major contributors to chaperoning RNA folding or conformational rearrangements of RNAs (Banroques *et al*., 2008; Jankowsky, 2011).

1.1.1   Helicase families

RNA and DNA helicases are highly related but sequence alignments have allowed classification of these proteins into six superfamilies (SF), SF1 to SF6 (Gorbalenya and Koonin, 1993; Singleton *et al.,* 2007). All eukaryotic RNA helicases belong to SF1 and SF2, and are characterised by a conserved helicase core, which consists of two RecA-like domains. Both RecA-like domains are crucial for helicase function as they provide the binding sites for NTP and nucleic acids (Fig. 1.1). The helicase core contains up to twelve consensus sequence motifs, which are similar in number and type within families, but differ between families (Fairman-Williams *et al*., 2010). Accordingly, helicases from SF2 can be subdivided into nine families (DEAD-box, DEAH-box, Ski2-like, RecQ-like, RecG-like, T1R, Swi/Snf, RIG-I-like and Rad3/XPD). The vast majority of RNA helicases are found in DEAD- and DEAH-box families, which can be collectively described as DExD/H-box proteins. The DExD/H-box RNA helicases commonly contain eight conserved sequence motifs. Motifs I and II (Walker A and B), which are also found in non-helicase proteins, are required for NTP binding and its hydrolysis (Fig.

1.1; Walker *et al.,* 1982). Energetic coupling of NTP binding and hydrolysis with helicase activity is suggested to be mediated by motif III (Pause and Sonenberg, 1992). Although motif VI was initially thought to participate in RNA binding, it is also implicated in the hydrolysis of NTP (Pause *et al.*, 1993). The remaining motifs Ia, Ib, IV and V constitute the scaffold for RNA substrate binding (Cordin *et al.*, 2006). Interestingly, these motifs contact only the sugar-phosphate backbone of RNAs, which suggests that most RNA helicases have little or no sequence specificity. However, an important feature of RNA helicases is that their function as NTPases is stimulated by RNA (Hilbert *et al.*, 2009). Additionally, a ninth conserved motif, which only occurs in DEAD-box proteins and is characterised by an invariant glutamine, was identified (Tanner *et al.*, 2003). This Q motif is thought to sense the NTP bound state, suggesting a role in functional regulation of RNA helicase activity (Tanner *et al.*, 2003; Cordin *et al.*, 2004). Furthermore, many SF2 helicases contain ancillary domains at the carboxyl-terminus that are structurally conserved and are characteristic features of DEAH-box and Ski2-like proteins (Fig. 1.1A). Several RNA helicases also contain additional N- and/or C-terminal extensions, which are more flexible and heterogeneous (Fairman-Williams *et al.*, 2010; He *et al.*, 2010; Walbott *et al.*, 2010).

1.1.2   Structure and molecular function of RNA helicases

Responsible for the mode of action and common for all RNA helicases of SF1 and SF2 is their conserved helicase core with its tandem RecA-like domains, which are in juxtaposition with each other. In absence of either NTP or RNA, the helicase core adopts an inactive, open conformation presenting an inter-domain cleft. Binding of NTP cooperatively enhances RNA substrate binding, which subsequently results in a conformational change inducing closure of the inter-domain cleft (ON conformation). In this conformation, the interaction between the protein and the sugar-phosphate backbone of the RNA substrate introduces a kink, which compromises basepairing between the two strands of the RNA duplex and is therefore key for the unwinding mechanism. Hydrolysis of NTP triggers a conformational switch back to the open conformation (OFF conformation), bringing about release of inorganic phosphate and the dissociated RNA strands. This substrate release enables the RNA helicase to be recycled and available for additional rounds of unwinding.

Conventionally, DNA helicases separate duplexes by translocation along a single nucleic acid strand and DEAH-box and Ski2-like RNA helicases also unwind RNA duplexes by this mechanism (Singleton *et al.*, 2007). For unwinding, they require a single stranded extension adjacent to the RNA duplex, which allows loading of the helicase and translocation in 3' to 5' or 5' to 3' directionality (Jankowsky *et al.*, 2000). In DEAH-box proteins, the inter-domain cleft is rather narrow in the OFF conformation due to their family specific C-terminal domains, which keep the two RecA-like domains in close proximity (He *et al.*, 2010; Walbott *et al.*, 2010).

Several rounds of NTP binding and hydrolysis suggest a stepping model along the loading RNA strand, which leads to dissociation of the top strand (Myong and Ha, 2010).
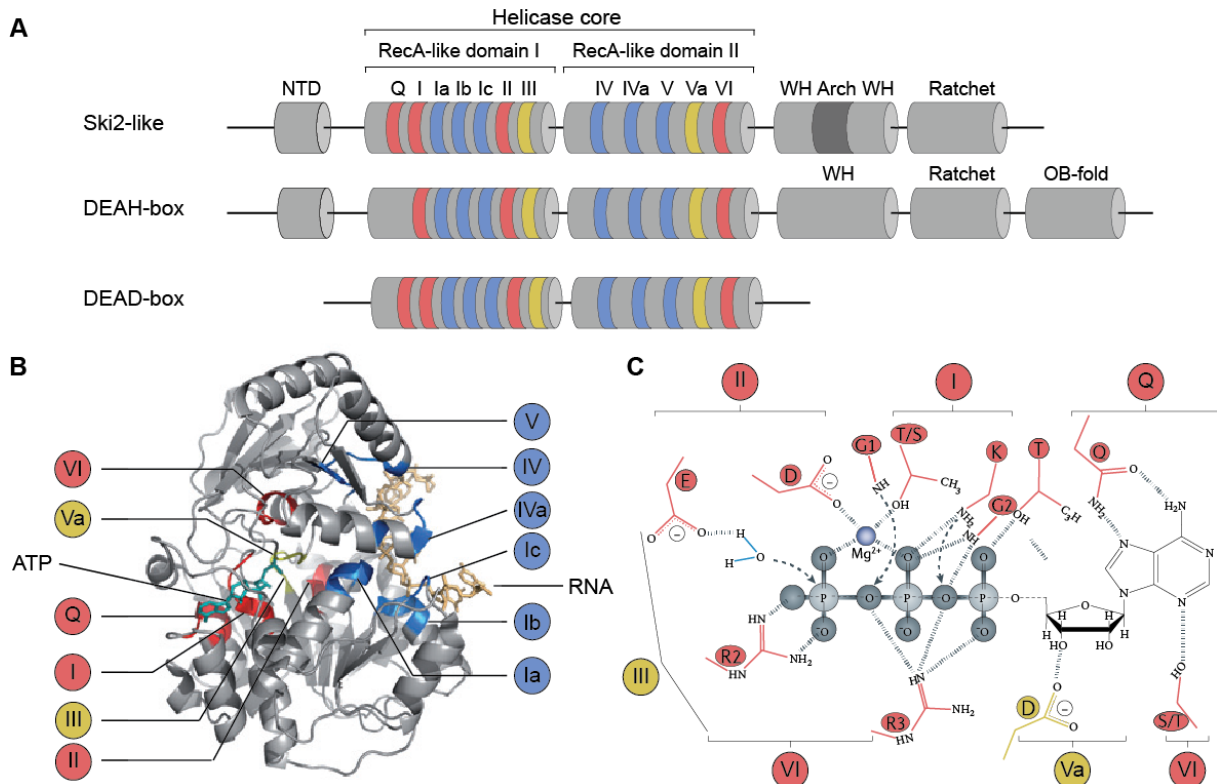
Figure 1.1: Structural composition of RNA helicases. (A) Arrangement of structural domains of members of the helicase SF2 (Ski2-like, DEAH-box and DEAD-box proteins). Conserved motifs in the helicase core are indicated in red (implicated in NTP binding), in blue (implicated in RNA binding) and yellow (implicated in coupling of NTP hydrolysis and helicase activity). NTD = N-terminal domain; WH = winged helix; OB-fold = oligonucleotide/oligosaccharide-binding fold (modified from Jarmoskaite and Russell, 2014). **(B)** Helicase core domain of the *Drosophila melanogaster* DEAD-box protein Vasa. Conserved motifs are coloured as in (A). **(C)** Schematic view of key residues of the ATP binding pocket of Vasa. Conserved motifs and the corresponding residues are coloured as in (A). Modified from Linder and Jankowsky, 2011.

In contrast, DEAD-box proteins promote RNA duplex unwinding by non-processive local strand separation (Bizebard *et al.*, 2004; Yang and Jankowsky, 2006). Loading of a DEAD-box protein locally opens the RNA duplex, and this can occur irrespective of whether the duplex is at the end of an RNA molecule or internal (Yang *et al.*, 2007). Further unwinding of neighbouring basepairs can often occur without the direct action of the protein (Yang *et al.*, 2007). As a result, DEAD-box proteins have relatively low unwinding efficiency for longer RNA duplexes and ATP hydrolysis by DEAD-box proteins is not required for the unwinding mechanism (Rogers *et al.*, 1999; Chen *et al.*, 2008; Liu *et al.*, 2008; Henn *et al.*, 2010). As they are connected by a flexible linker sequence, the two RecA-like domains of DEAD-box proteins confer high mobility towards each other (Caruthers *et al.*, 2000). Although double stranded RNA is unwound by directly loading onto the RNA helix, it is suggested that ancillary protein sequences bind single stranded RNA regions, bringing the helicase core in close proximity to

its site of action, thereby promoting efficient duplex unwinding (Jankowsky, 2006; Yang and Jankowsky, 2006; Halls *et al.*, 2007; Hilbert *et al.*, 2009; Jarmoskaite and Russell, 2011). Consistent with this hypothesis, such single stranded regions do not have to be contiguous with the target RNA duplex (Yang and Jankowsky, 2006; Halls *et al.*, 2007).

In addition, binding of cofactor proteins to the catalytic core of RNA helicases can influence their NTPase activity by modulating the transition between the open and closed conformational states by providing a structural scaffold that is similar to the ON conformation of the two RecA-like domains (Oberer *et al.*, 2005; Schütz *et al.*, 2008). Various RNA helicase cofactors are known, many of which are characterised by specific protein domains, such as the G-patch or MIF4G-domain, that mediate interactions with the corresponding RNA helicases. For example, substrate release by Dbp5 was shown to be stimulated by an interaction with its MIF4G-domain-containing cofactor Gle1 and the molecule inositol hexakisphosphate (IP_6; Alcazar-Roman *et al.*, 2006; Weirich *et al.*, 2006; Montpetit *et al.*, 2011). Reciprocally, cofactors can also stabilise the closed ON conformation preventing recycling of the protein, or can out-compete RNA helicases for RNA substrate binding, causing inhibitory effects on RNA helicase activity (Von Moeller *et al.*, 2009). The human DEAD-box protein eIF4AIII (DDX48), an RNA helicase involved in pre-mRNA splicing as a component of exon junction complexes, was reported to be negatively regulated by the MIF4G domain of CWC22 by holding eIF4AIII in an inactive conformation (Buchwald *et al.*, 2013)

1.1.3 Cellular functions

Due to their mechanistic features and modes of action, the functions of RNA helicases are not limited to RNA duplex unwinding. Instead, there is evidence for a broad diversity of functions concerning RNA remodelling, such as RNA strand annealing (Yang and Jankowsky, 2005), displacement of proteins (Jankowsky and Bowers, 2006) or RNA clamping (Liu *et al.*, 2014), which stabilises pathway intermediates during assembly of ribonucleoprotein complexes. RNA helicases are therefore present throughout the cell and play important roles in all aspects of RNA metabolism from transcription to pre-mRNA splicing, RNA editing, ribosome biogenesis, RNA export, translation and RNA decay. Since the helicase core only forms contacts with the sugar-phosphate backbone of RNA and helicases show almost no sequence specificity *in vitro*, an important question is how these proteins are distributed to their sites of action to fulfil very specific functions. Protein cofactors can not only stimulate or inhibit helicase activity, but they can also confer substrate specificity by increasing the binding selectivity of the protein to its particular RNA substrate. The DEAD-box protein Dbp8, for example, physically interacts with Esf2, which directs the helicase to ribosome biogenesis, where it is essential for 18S rRNA maturation within pre-40S particles (Hoang *et al.*, 2005; Granneman *et al.*, 2006). Recruitment to specific substrates by cofactors is particularly important as some RNA helicases are known

to be multifunctional, being required for several pathways of RNA metabolism. The Ski2-like RNA helicase Mtr4 is a component of the TRAMP complex that functions together with the nuclear exosome in RNA processing and the degradation of structured non-coding or aberrant RNAs (Schuch *et al.*, 2014; Wasmuth *et al.*, 2017). Nop53 and Utp18 share a consensus motif that mediates their interaction with Mtr4 and recruits the nuclear exosome either to pre-rRNA processing or rRNA degradation respectively (Thoms *et al.*, 2015). Furthermore, Dbp2 was reported to participate in RNA decay as well as in ribosome biogenesis (Bond *et al.*, 2001; Cloutier *et al.*, 2012). RNA export and pre-mRNA splicing both require Sub2 (Jensen *et al.*, 2001; Cordin and Beggs, 2013) and the DEAD-box protein Dbp5 is proposed to function in nuclear RNA export, translation termination and ribosome biogenesis (Tseng *et al.*, 1998; Gross *et al.*, 2007; Neumann *et al.*, 2016). The DEAH-box RNA helicase Prp43, which has various functions in ribosome biogenesis and pre-mRNA splicing, is directed to its diverse cellular functions by a set of G-patch protein cofactors, which compete for helicase binding in order to regulate its subcellular localisation (Heininger *et al.*, 2016). Pxr1 (Gno1) and Sqs1 (Pfa1) act together with Prp43 in ribosome biogenesis and Prp43 is bound by Spp382 (Ntr1) in order to direct the helicase to post-catalytic spliceosomes, where the helicase is required for release of the intron-lariat (Lebaron *et al.*, 2009; Tsai *et al.*, 2007; Chen *et al.*, 2014).

Indeed, pre-mRNA splicing is a well-characterised process that relies on several helicase-mediated structural transitions. Eight RNA helicases are known to function in different steps of spliceosome assembly, rearrangement and factor recycling. Here, the DEAD-box proteins Sub2 and Prp5 chaperone the assembly of spliceosomes on pre-mRNAs by promoting branchpoint recognition (Ruby *et al.*, 1993; Kistler and Guthrie, 2001). Prp28, another DEAD-box protein, facilitates the release of U1 snRNP to expose the 5' splice site for binding of U6 snRNP (Staley and Guthrie, 1999). More extensive remodelling events at intermediate and late steps of pre-mRNA splicing are mediated by DEAH-box proteins, including dissociation of proteins from the branchpoint region by Prp2 (Warkocki *et al.*, 2009; Lardelli *et al.*, 2010) and intron-lariat release by Prp43 (Arenas and Abelson, 1997). However, the cellular process that involves the most RNA helicases is the synthesis of ribosomes.

1.2   Ribosomes: structure and function

Mature eukaryotic ribosomes consist of two ribosomal subunits, named according to their sedimentation coefficient in sucrose density gradients: the 40S or small ribosomal subunit (SSU) and 60S or large ribosomal subunit (LSU). For translating the genetic information encoded in mRNA into proteins, the two subunits engage to form a catalytically active 80S ribosome (Fig. 1.2). The SSU harbours the mRNA entry and exit sites and decodes the mRNA by selection of complementary aminoacyl-tRNAs in the decoding centre. Peptide bond formation is catalysed in the peptidyl-transferase centre (PTC) of LSU, which additionally

contains the polypeptide exit tunnel and provides binding sites for GTPases that promote translation.

Constituents of the *Saccharomyces cerevisiae* (yeast) SSU are the 18S ribosomal RNA (rRNA) and 33 ribosomal proteins (RPs), whereas the yeast LSU is composed of three ribosomal RNAs (25S, 5.8S and 5S) and 46 RPs. Recent advances in cryo-electron microscopy (cryo-EM) and crystallographic methods, which were applied to yeast and *Tetrahymena* ribosomes, rapidly enhanced the understanding of ribosome architecture (Armache *et al*., 2010a,b; Ben-Shem *et al*., 2011; Klinge *et al*., 2011, Rabl *et al*., 2011; Jenner *et al*., 2012; Klinge *et al*., 2012; Melnikov *et al*., 2012). There are four phylogenetically conserved secondary structural domains in the 18S rRNA (Petrov *et al*., 2014a), called the 5', central, 3' major and 3' minor domains, which fold together with RPs into tertiary structures termed the body, shoulder, platform, head and beak. In LSU, there are six defined conserved secondary structure elements (domain I – VI), which includes basepairing of 25S with 5.8S rRNA in domain I. Besides the central protuberance (CP), which is formed by the 5S rRNA together with its associated RPs, Rpl5 (uL18) and Rpl11 (uL5), there are two other defined tertiary features: the L1 and the acidic stalks. Prokaryotic and eukaryotic ribosomes share a conserved structural core, mostly devoid of RPs, containing the sites of ribosome function (Melnikov *et al*., 2012; Petrov *et al*., 2014b). Rather than having a catalytic function, RPs create a protein-RNA interaction network, which provides a stable structural scaffold that ensures correct positioning of the RNA core and shields it from the solvent exposed surface.
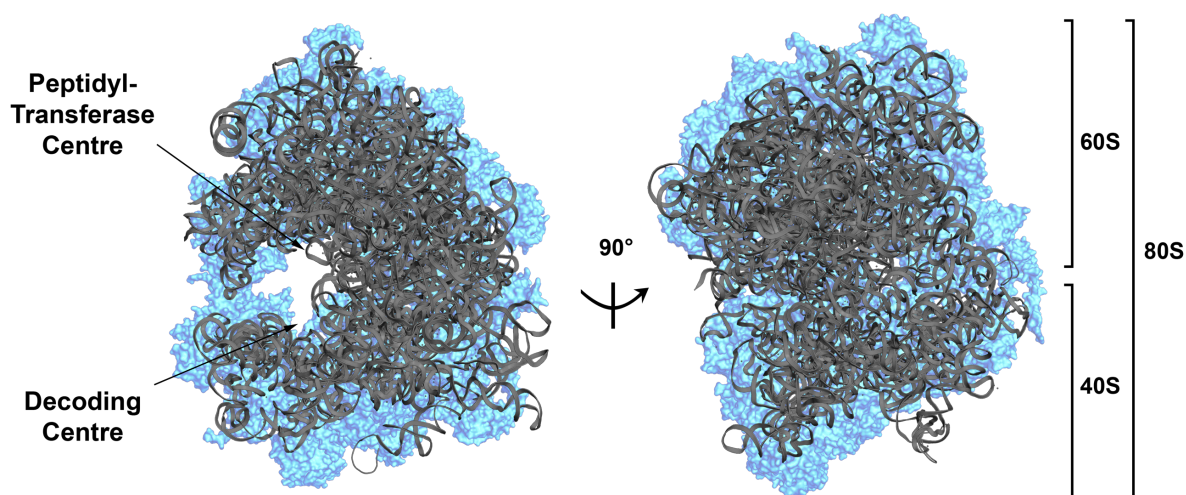
Figure 1.2: Structure of the yeast 80S ribosome. 3D structure depicting the 80S yeast ribosome, composed of the large ribosomal 60S subunit (LSU) and small ribosomal 40S Subunit (SSU; Ben-Shem *et al*., 2011; PDB-ID: 4V88). Ribosomal RNA is shown in grey, ribosomal proteins in blue.

1.2.1 Yeast ribosome biogenesis

Ribosome biogenesis is an energy-consuming process that requires the action of all three cellular RNA polymerases to produce the necessary components. Pol I and III transcribe rRNAs, whereas Pol II transcribes mRNAs coding for RPs and *trans*-acting ribosome biogenesis factors. More than 2,000 ribosomes are synthesised per minute in actively proliferating yeast cells to meet the constant demand for functional ribosomes (Warner, 1999) and therefore, approximately 70 % of cellular RNAs are directed to the synthesis of ribosomes (Li *et al.*, 1999; Warner, 1999). Ribosome biogenesis takes place in three different cellular compartments as it is initiated in the nucleolus, and continues in the nucleoplasm but final maturation steps occur in the cytoplasm.

Correct pre-rRNA processing, modification and folding as well as assembly of the 79 RPs require a multitude of cofactors, including 76 small nucleolar RNAs (snoRNAs) and more than 200 *trans*-acting ribosome biogenesis cofactors (Fromont-Racine *et al.*, 2003). Already co-transcriptionally, early RPs and ribosome biogenesis factors assemble with the nascent transcript, which forms the earliest detectable intermediate, the 90S pre-ribosome (Grandi *et al.*, 2002). After a central pre-rRNA cleavage event at site A_2, the pathways of 40S and 60S biogenesis diverge and subsequent maturation steps are independent (Turowski and Tollervey, 2015). While pre-40S subunits are rapidly exported from the nucleus for final maturation in the cytoplasm, pre-60S subunits undergo several compositional and structural changes in the nucleoplasm, including assembly of the 5S RNP (Zhang *et al.*, 2007), before they reach their final destination in the cytoplasm.

1.2.2 Transcription and pre-rRNA processing

The process of ribosome biogenesis starts with the synthesis of a pre-rRNA transcript from the *RDN* locus, which in yeast appears in approximately 150 tandem repeats on chromosome XII (Long and Dawid, 1980). A single repeat contains the genetic information for the 18S, 5.8S and 25S rRNAs, which are transcribed by RNA Pol I as a 35S primary transcript, also containing several spacer elements (Fig. 1.3). Internal transcribed spacers (ITS1 and ITS2) separate the mature rRNA sequences, whereas external transcribed spacers (5'ETS and 3'ETS) constitute the ends of this transcript. The 5S rRNA is transcribed by RNA Pol III in reverse orientation and is separated within the *RDN* locus by a non-transcribed spacer region (NTS). To allow a high rate of rRNA transcription, multiple transcripts can be simultaneously produced from a single *RDN* repeat, creating a high density of involved factors around these gene loci. This generates a non-membrane delimited sub-compartment within the nucleus, known as the nucleolus (Thiry and Lafontaine, 2005). Early RPs and ribosome biogenesis factors that associate with the nascent transcript already co-transcriptionally are important for

structural assembly and subsequent pre-rRNA processing events (Chaker-Margot *et al.*, 2015).
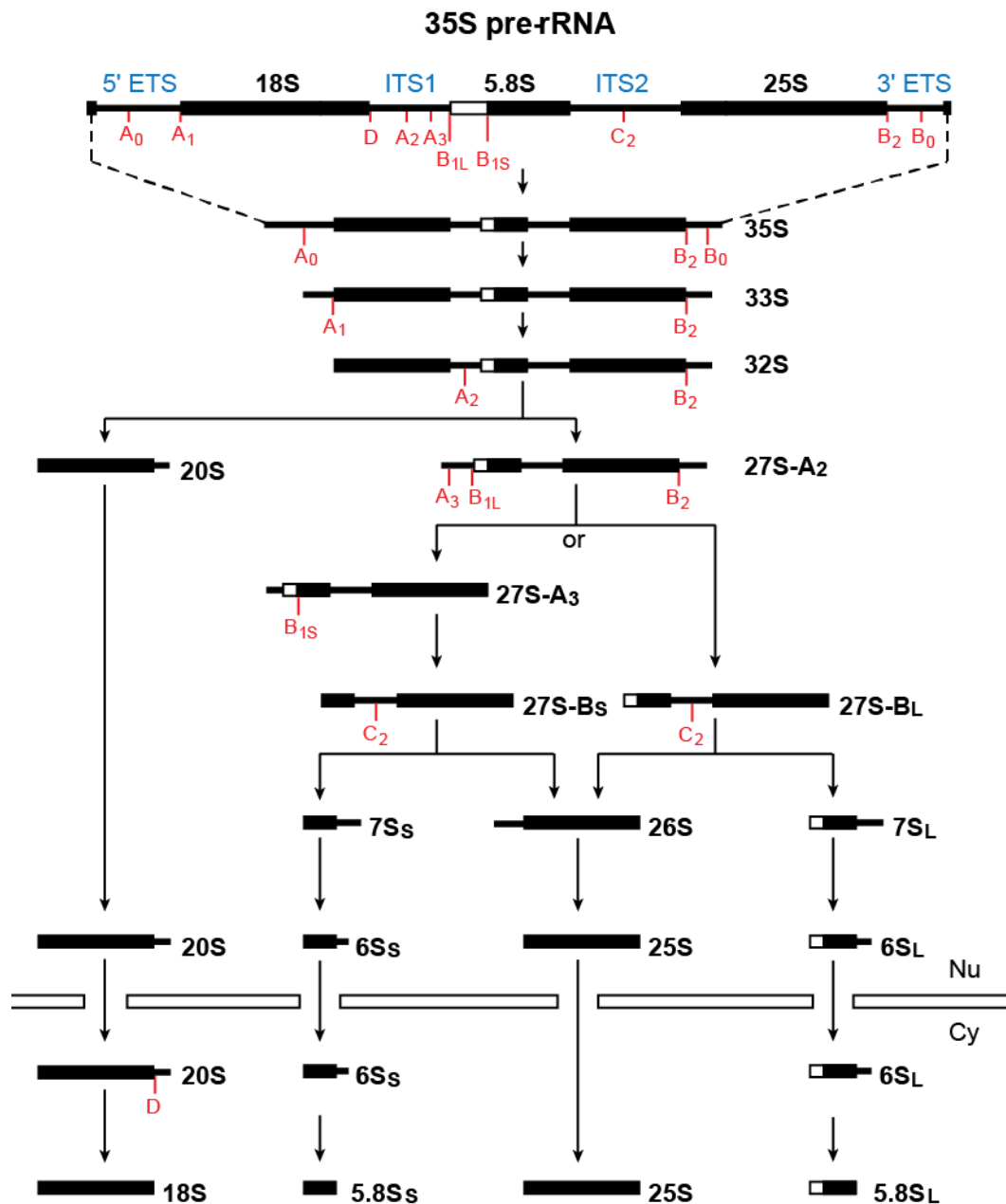
Figure 1.3: Pre-rRNA processing in the yeast *Saccharomyces cerevisiae.* Simplified schematic representations of pre-rRNA processing intermediates in yeast and the pathway by which they are generated are shown. Black lines represent transcribed sequences, with mature rRNA sequences indicated by thicker bars and spacer fragments that are removed by endonucleolytic cleavages and exonucleolytic processing shown as thinner lines. Spacer regions are named in blue, and mature rRNAs and processing intermediates are labelled in black. Pre-rRNA cleavage sites are indicated in red. Nu = nucleus; Cy = cytoplasm. Modified from Martin, 2014 (PhD thesis).

Elimination of the pre-rRNA transcribed spacer regions requires a complex series of endo- and exonucleolytic cleavages (Fig. 1.3; Henras *et al.*, 2015). For 18S maturation, endonucleolytic cleavages are carried out at sites A_0, A_1 and A_2, which all require the formation of the SSU processome (Phipps *et al.*, 2011). Central to this complex is the U3 snoRNA, which basepairs

with 5'ETS and 18S rRNA in order to chaperone pseudoknot formation, a structural prerequisite for endonucleolytic cleavages at sites A_0, A_1 and A_2 (Watkins and Bohnsack, 2012). A_1 and A_2 cleavages are suggested to be mediated by the PilT N-terminus (PIN) domain containing endonuclease Utp24 (Wells *et al.*, 2016), whereas the endonuclease responsible for cleavage at site A_0 still needs to be identified. After export to the cytoplasm, cleavage at site D by the endonuclease Nob1 defines the 3' end of 18S rRNA (Fatica *et al.*, 2003a). Interestingly, a proofreading mechanism for pre-40S complexes has been proposed that involves recruitment of 60S subunits and a translation-like cycle prior to Nob1 cleavage (Lebaron *et al.*, 2012; Strunk *et al.*, 2012).

Cleavage at A_2 separates the pathways of SSU and LSU biogenesis and can occur either co- or post-transcriptionally according to nutrient availability and/or cell cycle progression (Kos and Tollervey, 2010; Talkish *et al.*, 2016). Processing of LSU rRNAs after A_2-cleavage involves the coordinated 5' end formation of 5.8S rRNA and development of the mature 3' end of 25S rRNA. The endonuclease Rnt1 cleaves at B_0, an event which is thought to be coupled with transcription termination, to create an overhang that is trimmed by the 3'-5' exonuclease Rex1 (Kempers-Veenstra *et al.*, 1986; Nemeth *et al.*, 2013). For maturation of 5.8S rRNA, two alternative processing pathways exist leading to the formation of two alternative forms of the 5.8S rRNA that differ at their 5' end. On the one hand, an unknown endonuclease defines the 5' end of 5.8S rRNA by cleavage at B_{1L} on 27S-A_2, generating the 5' end of the minor form (5.8S$_L$; Faber *et al.*, 2006). On the other hand, after A_3-cleavage, catalysed by the RNase MRP (Torchet and Hermann-Le Denmat, 2000), two sequentially acting exonucleases, Rat1 and Rrp17, perform trimming to site B_{1S}, which results in the major form of 5.8S rRNA (5.8S$_S$; Henry *et al.*, 1994; Oeffinger *et al.*, 2009; Granneman *et al.*, 2011). Following the 5' end formation of 5.8S and 3' end formation of 25S rRNA, the transcript is processed endonucleolytically at site C_2 in ITS2 by the endonuclease Las1 (Allmang *et al.*, 1999; Gasse *et al.*, 2015). The 3'-5' exosome containing Rrp6 and the 3'-5' exonuclease Ngl2, trims the 7S precursor rRNA to generate the mature 3' end of 5.8S rRNA (Mitchell *et al.*, 1996; Briggs *et al.*, 1998; Allmang *et al.*, 1999). Besides 7S rRNA, C_2-cleavage results in a 26S rRNA, which is processed to produce the mature 5' end of the 25S rRNA by the 5'-3' exonucleolytic activity of Rat1 (Geerlings *et al.*, 2000).

1.2.3 rRNA modifications

Besides being processed, rRNAs undergo extensive modification, largely mediated by snoRNPs, which introduce 2'-*O*-methylations or catalyse the isomerisation of uridine to pseudouridine (reviewed in Watkins and Bohnsack, 2012; Sloan *et al.*, 2016). Modifications in rRNA are not evenly distributed, but cluster in important functional regions, such as the PTC, the decoding site or the site of subunit joining in the mature ribosome (Ben-Shem *et al.*, 2011;

Decatur and Fournier, 2002). Lack of individual modifications has been shown to increase sensitivity towards stress conditions or ribosome specific antibiotics, but in general the absence of single modifications does not impair cell viability under laboratory conditions (Esguerra *et al.*, 2008; Baudin-Baillieu *et al.*, 2009). However, the absence of certain groups of modifications disrupts ribosome biogenesis or function and compromises cell growth (King *et al.*, 2003; Liang *et al.*, 2007; Liang *et al.*, 2009). This implies that the landscape of modifications is important for efficient and accurate translation and additionally creates a source for regulation of ribosome function. In general, it is thought that 2'-*O*-methylation stabilises basepairing and promotes rRNA folding, whereas pseudouridylations maintain rRNA secondary structures and facilitate interactions between rRNA and RPs (Helm, 2006). 2'-*O*-methylations in rRNAs are introduced by box C/D snoRNPs, which are characterised by a snoRNA scaffold containing conserved sequence motifs, which form intramolecular basepair interactions (box C with box D, box C' with box D'). The snoRNA is associated with the common core proteins Nop56, Nop58 and Snu13, which additionally stabilise a certain RNA structure. Specific sequences between the C/D and C'/D' elements are complementary to the target regions of the rRNA and snoRNA-pre-rRNA basepairing allows 2'-*O*-methylation five nucleotides (nts) upstream of box D or D' by the enzyme component Nop1. This reaction requires S-adenosyl methionine (SAM), which serves as methyl group donor (Singh *et al.*, 2008; Lin *et al.*, 2011). Although it was shown that 10 nts of complementary sequence is sufficient for target site identification and efficient modification, box C/D snoRNAs often form longer stretches (up to 21 nts) of basepair interactions (van Nues *et al.*, 2011). This extensive interaction is proposed to facilitate snoRNA recruitment and to extend the residence time of snoRNAs, preventing premature folding of the pre-rRNA target sequences (Yang *et al.*, 2016). Box H/ACA snoRNPs are also characterised by their snoRNA component, which contains a box H and the ACA motif, and form a hairpin structure containing a pseudouridylation loop, which is stabilised by the box H/ACA core proteins Nhp2, Nop10 and Gar1. This loop forms short basepairing interactions (from 4 to 8 nts) with the pre-rRNA, exposing an unpaired uridine to the catalytically active site of the pseudouridine synthase Cbf5 for the isomerisation reaction (Lafontaine *et al.*, 1998). Some snoRNPs establish long-range interactions between distant sites within the primary sequence of rRNA and lack of these snoRNAs leads to defects in pre-rRNA processing (Morrissey and Tollervey, 1993; Enright *et al.*, 1996; Samarsky *et al.*, 1998; Martin *et al.*, 2014). In contrast to snoRNAs that guide modification, most snoRNAs required for pre-rRNA processing are essential. They are suggested to maintain an open rRNA conformation that exposes cleavage sites for endonucleolytic cleavage and to prevent premature formation of structural folds found in mature ribosomes. Generally, snoRNPs participating in pre-rRNA processing are devoid of modification activity, but exceptions include the U14 and snR10 snoRNAs that have maintained both functions. The vast majority of

snoRNA-guided rRNA modifications occur co-transcriptionally, indicating an early engagement of snoRNPs with the nascent transcript. If binding of snoRNAs happens stochastically or if it follows a defined hierarchy is still under debate. The high density of modifications in functionally important regions of the ribosome leads to overlapping pre-rRNA binding sites for several snoRNAs, suggesting a stepwise recruitment mechanism.

Besides snoRNP-derived modifications, eight different types of base modifications are present in rRNA, which are introduced by stand-alone enzymes. Interestingly, although the majority of these enzymes are essential, their catalytic activity is not always critical, indicating that these proteins also contribute to other aspects of ribosome assembly. How many of these enzymes identify their target residues still remains elusive, but some lines of evidence suggest recognition mechanisms involving RNA consensus sequences, secondary structures or multiple contacts with pre-rRNA and proteins within the context of assembling pre-ribosomes.

1.2.4 Ribosomal proteins

Of the 79 known yeast RPs, 64 are essential for growth under standard laboratory conditions, likely due to their functions in ribosome assembly and translation fidelity (Steffen *et al*., 2012). Due to gene duplications, 59 RPs have paralogs that only differ in few amino acids (Simoff *et al*., 2009). Although these paralogs are very similar, deletion and depletion experiments have shown variation of their phenotypes, indicating the existence of specialised ribosomes, which might be required for the translation of certain subsets of mRNAs. Prokaryotic and eukaryotic ribosomes share a conserved structural core, mostly devoid of RPs, containing the sites of ribosome function. Instead, RPs are mostly found in the periphery of ribosomes, where they thread across the surface and partially penetrate the rRNA core (Armache *et al*., 2010a; Ben-Shem *et al*., 2011; Rabl *et al*., 2011). After being translated in the cytoplasm, the vast majority of RPs need to be imported into the nucleus for assembly into pre-ribosomal complexes. Although they are very small in size and could passively diffuse through the phenylalanine-glycine (FG)-network of nuclear pore complexes, RPs contain nuclear localisation signals (NLS) and their import is facilitated by different ß-karyopherins (Rout *et al*., 1997). In order to prevent misfolding or aggregation of these basic proteins, there are examples of chaperones that bind to newly synthesised RPs and escort them to the nucleus to be incorporated into nascent pre-ribosomal particles (Koch *et al*., 2012; Pillet *et al*., 2015). High-resolution crystal structures of mature ribosomal subunits revealed the location of each RP on rRNA (Ben-Shem *et al*., 2011), but do not provide insight into the temporal aspect of RP assembly. It is suggested that most RPs assemble early into ribosomal precursors, where they play important roles in folding of the nascent rRNA transcript (Gamalinda *et al*., 2013, Ohmayer *et al*., 2013). In general, it is proposed that RPs form multiple interactions with the rRNA, some of which are formed early in the pathway and others that are formed later, which supports the idea of

progressive stabilisation of maturing ribosomes (Ferreira-Cerca *et al.*, 2007; Sahasranaman *et al.*, 2011; Ohmayer *et al.*, 2013). This loose tethering of early RPs creates binding sites for later RPs and ribosome biogenesis factors as well as keeping rRNA domains in close proximity. Furthermore, the binding of RPs to pre-rRNAs also triggers conformational changes that facilitate pre-rRNA processing (Ohmayer *et al.*, 2015). Similar to assembly of prokaryotic ribosomes, RPs in yeast SSU biogenesis are recruited sequentially with the formation of key structural features in 18S rRNA following a 5'-3' directionality (Ferreira-Cerca *et al.*, 2007; Woodson, 2008). Systematic examination of LSU RPs revealed differentiation into early, intermediate and late RPs, according to subcellular localisation of incorporation, depletion phenotypes in pre-rRNA processing and stoichiometric distributions of RPs in purified pre-ribosomal particles (Gamalinda *et al.*, 2014). Although much more complicated than SSU biogenesis, assembly of 60S subunits also occurs in a hierarchical fashion. Early binding events are required for formation of the convex solvent surface, followed by intermediate steps, where the polypeptide exit tunnel is formed, and late RPs assemble around the CP and PTC, functionally important regions of the ribosome (Gamalinda *et al.*, 2014).

1.2.5 *Trans*-acting factors and nuclear export

The biogenesis of eukaryotic ribosomes requires more than 200 non-ribosomal factors, (Fromont-Racine *et al.*, 2003). In addition to numerous structural/scaffold proteins, these include many enzymes, such as the previously described endo- and exonucleases and modification enzymes. These enzymes catalyse irreversible reactions thereby conferring directionality to the ribosome biogenesis pathway and providing a means for regulation and quality control (Strunk and Karbstein, 2009). Other enzymes that act in ribosome biogenesis are NTP-dependent RNA helicases, which play an important role in RNP structure modulation and will be described in more detail in section 1.3. Phosphorylation of RPs and ribosome biogenesis factors by kinases, observed in 40S and 60S maturation, are key regulatory steps in subunit assembly (Schäfer *et al.*, 2006; Ray *et al.*, 2008). Similarly, AAA-ATPases and GTPases, which are known regulators in many different cellular pathways, are implicated in the release of non-ribosomal factors and in mediating the incorporation of RPs and late-acting ribosome biogenesis factors (Karbstein *et al.*, 2005; Pertschy *et al.*, 2007).

In addition to these enzymatic components, an important group of ribosome biogenesis factors are those that facilitate the nuclear export of pre-ribosomal particles. Nuclear export of these large ribonucleoprotein complexes (> 2 MDa) is a major challenge, as they have to pass through the hydrophobic FG-meshwork of the nuclear pore complex (NPC). Nuclear export of pre-ribosomes is achieved by the binding of multiple export factors that interact with the FG-repeats to direct transport (Hurt *et al.*, 1999; Stage-Zimmermann *et al.*, 2000). The nuclear export signal (NES)-containing adaptor protein Nmd3 binds to pre-60S particles in order to

recruit the exportin Crm1 (Xpo1), which shuttles through the NPC in a Ran GTPase cycle-dependent manner (Gadal *et al.*, 2001). Additional factors including Arx1, Ecm1, Bud20 and Npl3 act as non-essential export factors that facilitate rapid export of pre-60S particles by directly binding FG-rich nucleoporins (Gerhardy *et al.*, 2014). Although Crm1 is also required for pre-40S export, export adaptor proteins still have to be identified. The ribosome biogenesis factors Ltv1, Dim2 and Rio2 all contain NES-sequences and are therefore likely candidates (Seiser *et al.*, 2006; Vanrobays *et al.*, 2008; Zemp *et al.*, 2009). The Mex67-Mtr2 hetero-dimer, which is known for its essential function in mRNA export, is required for the transport of both ribosomal subunits through the NPC in a Ran GTP-independent manner (Yao *et al.*, 2007; Faza *et al.*, 2012). In the cytoplasm, export factors are released and final maturation steps, such as pre-rRNA trimming and modification, dissociation of assembly factors and incorporation of remaining RPs, take place (Fatica *et al.*, 2003b).

The generation of export competent pre-ribosomes is an important quality control checkpoint in the ribosome biogenesis pathway (Matsuo *et al.*, 2014). For example, a hierarchical model of pre-60S biogenesis factor recruitment was suggested, which ultimately leads to the incorporation of Nog2 into pre-60S ribosomes. This GTPase acts as a placeholder for the essential export adaptor protein Nmd3 ensuring that pre-60S export can only occur after earlier maturation events have taken place (Talkish *et al.*, 2012; Matsuo *et al.*, 2014).

1.2.6 Structural dynamics of yeast pre-ribosomes

As described above, the assembly of the ribosomal subunits follows a strictly ordered series of events brought about by the sequential association and dissociation of numerous biogenesis factors. Functional analysis of individual biogenesis factors and steps in the pathway give insight into the complex remodelling events that occur during subunit assembly. However, a broader view of the major structural rearrangements that take place in ribosome biogenesis requires structural analysis of pre-ribosomal complexes. High-resolution structures of the mature yeast 40S and 60S subunits generated by cryo-electron microscopy (cryo-EM) provided the first detailed views of the molecular architecture of mature ribosomes (Ben-Shem *et al.*, 2011). However, these structures lack information regarding the binding sites of *trans*-acting ribosome biogenesis factors and the conformations of the pre-rRNAs. Excitingly, cryo-EM studies of late pre-40S particles uncovered the binding sites of several late-acting SSU biogenesis factors, such as Nob1, Dim1, Dim2 and Rio2. Furthermore, they revealed structural features of the beak region that are incompatible with binding of 60S subunits and translation initiation factors, suggesting that the presence of biogenesis factors in pre-40S complexes prevents premature translation after export of pre-40S particles to the cytoplasm (Strunk *et al.*, 2011). The kinase Hrr25 is suggested to be involved in the release of ribosome biogenesis factors Enp1 and Rsp3, which recruits Rps3 (uS3) for final maturation of the beak structure

(Schäfer *et al.*, 2006). More recently, the structure determination of the *Chaetomium thermophilum* 90S pre-ribosome provided information about early ribosome biogenesis steps on the level of nascent transcripts (Kornprobst *et al.*, 2016).
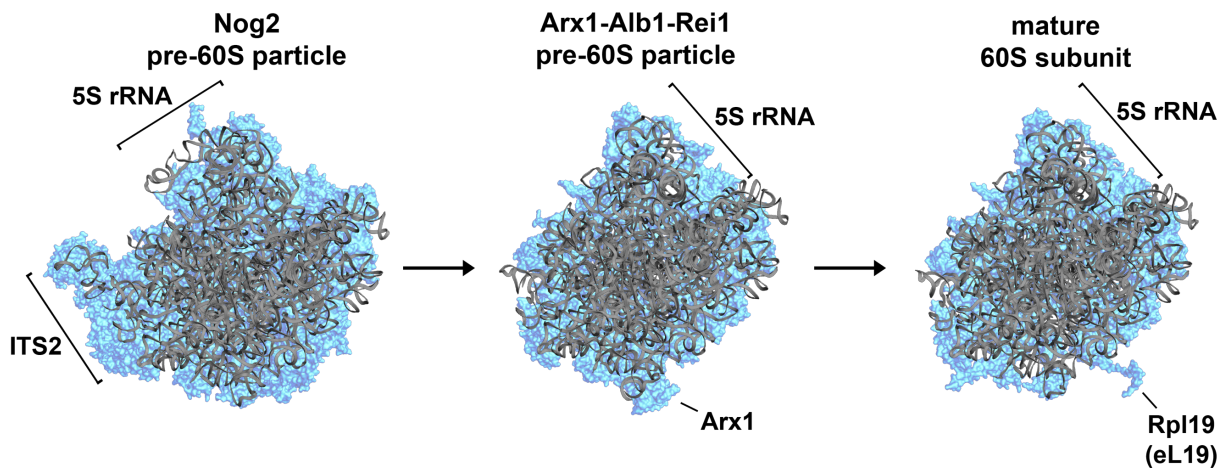
Figure 1.4: Structural dynamics of late pre-60S particles. Three sequential pre-60S particles are depicted: the Nog2-particle (Wu *et al.*, 2016; PDB-ID: 3JCT), the Arx1-Alb1-Rei1-particle (Greber *et al.*, 2016; PDB-ID: 5APN) and the mature 60S subunit (Ben-Shem *et al.*, 2011; PDB-ID: 4V88). The particles were aligned according to their 25S rRNA component, thereby highlighting the rotation of the 5S RNP, removal of the ITS2 sequence, release of Arx1 and incorporation of the ribosomal protein Rpl19. Ribosomal RNAs and ribosomal proteins are indicated in grey and blue respectively. Features that undergo major conformational changes are labelled.

Due to their large size and compositional complexity, pre-60S complexes undergo many structural transitions during their assembly. Several recent publications have reported cryo-EM structures of pre-60S particles, which were purified via different transiently binding ribosome biogenesis factors (Fig. 1.4). In contrast to earlier particles, the higher stability and reduced complexity of later pre-60S complexes have made the successful structure determination of Nog2-, Nmd3-, Arx1- and Rix1-derived late nuclear and early cytoplasmic particles possible (Bradatsch *et al.*, 2012; Barrio-Garcia *et al.*, 2016; Wu *et al.*, 2016; Ma *et al.*, 2017). Besides structural features, which are also found in mature subunits, these structures contain substantial additional mass, referred to as foot, knob and nose elements. These expansions represent associated ribosome biogenesis factors or unprocessed spacer elements as well as rRNA structures that are not yet folded to their final topology (Leidig *et al.*, 2014). Mass spectrometry analysis of the corresponding particles combined with available crystal structures or homology models of many pre-60S factors enabled the positions of numerous biogenesis factors to be assigned on different pre-60S complexes. In line with the proposal of a hierarchical recruitment and spatiotemporal binding of ribosomal proteins and biogenesis factors, the solvent side of the ribosome is largely devoid of ribosome biogenesis factors in pre-60S complexes. Instead, at these late steps in ribosome biogenesis, these can be mostly found in functionally important regions like the PTC, the CP or the intersubunit bridge. In the Nog2-derived pre-60S particle, portions of the ITS2 spacer sequence could be

resolved in contact with ITS2 binding factors, such as Nop53, which is required for the recruitment of Mtr4 and its associated exosome components for ITS2 removal (Fig. 1.4; Wu *et al.*, 2016). With the available series of crystal structures, a major unpredicted structural transition in the head region of pre-60S particles could be reconstructed. They revealed that the 5S RNP, a sub-complex of 5S rRNA, Rpl5 (uL18) and Rpl11 (uL5), is initially assembled in a pre-mature conformation. Following a stepwise mechanism, possibly triggered by ATP hydrolysis of the AAA-ATPase Rea1 and removal of a subset of ribosome biogenesis factors, the 5S RNP performs a 180 ° rotation to adopt its final topology (Fig.1.4; Leidig *et al.*, 2014). This rotation enforces conformational changes of proximal rRNA helices in 25S rRNA, which are key for the formation of the CP (Leidig *et al.*, 2014). Due to increasing flexibility of pre-rRNA and the dynamic changes of ribosome biogenesis factors, crystallisation of earlier particles upstream the ribosome biogenesis pathway remains a major challenge and alternative approaches may be required to gain insight into the binding sites of earlier ribosome biogenesis factors and the dynamics of these complexes.

1.3   RNA helicases in ribosome biogenesis

Due to their biochemical activities in remodelling RNA duplexes and RNP complexes, RNA helicases are key effectors and/or regulators of compositional and structural changes of pre-ribosomal complexes. Localisation assays, including cell fractionation, have revealed that numerous RNA helicases are present in the nucleolus, the initiation site of ribosome biogenesis. So far, 21 putative RNA helicases were suggested to directly participate in the process of ribosome biogenesis (see Table 1.1). Based on which pre-rRNA intermediates accumulate in response to depletion of each helicase and in which pre-ribosomal complexes each helicase has been identified in affinity purification experiments, eight were classified as SSU helicases (Dbp4, Dbp8, Dhr1, Dhr2, Rok1, Kre33, Fal1, Rrp3) and ten as LSU helicases (Dbp2, Dbp3, Dbp6, Dbp7, Dbp9, Dbp10, Drs1, Mak5, Spb4, Mtr4), while three were shown to be required for both pathways (Has1, Prp43 and Dbp5). Interestingly, with the exception of Dbp2, Dbp3 and Dbp7 all these proteins are essential for cell viability. With the exception of the Ski2-like helicase Mtr4, which contributes to processing of the 3' end of the 5.8S rRNA, all these helicases are DEAD- or DEAH-box proteins. The precise functions of many RNA helicases in ribosome biogenesis are not known but putative functions are unwinding of snoRNA-rRNA duplexes, rearrangement of rRNA secondary structures and remodelling events, such as the release of ribosome biogenesis factors in order to allow access of other ribosome biogenesis factors or RPs.

Table 1.1: RNA helicases involved in ribosome biogenesis. RNA helicases proposed to function in ribosome biogenesis are listed. The data presented in this table are supported by comprehensive mutational analyses of RNA helicases implicated in the maturation of small and large ribosomal subunits (Granneman *et al.*, 2006b; Bernstein *et al.*, 2006).

RNA helicase	Helicase family	Function in ribosome biogenesis	Essential	References
Fal1	DEAD	SSU	yes	Kressler *et al.*, 1997
Dbp4	DEAD	SSU; snoRNA release; SSU processome formation	yes	Kos and Tollervey, 2005; Turner *et al.*, 2009; Soltanieh *et al.*, 2015
Dbp8	DEAD	SSU	yes	Daugeron and Linder, 2001
Rok1	DEAD	SSU; snoRNA release	yes	Venema *et al.*, 1999; Bohnsack *et al.*, 2008; Martin *et al.*, 2014
Kre33	DEAD	SSU; snoRNA mediated acetylation	yes	Sharma *et al.*, 2015
Rrp3	DEAD	SSU	yes	O'Day *et al.*, 1996
Dhr1	DEAH	SSU; snoRNA release	yes	Colley *et al.*, 2000; Sardana *et al.*, 2015; Zhu *et al.*, 2016
Dhr2	DEAH	SSU	yes	Colley *et al.*, 2000; Choque *et al.*, 2011
Dbp2	DEAD	LSU; pre-rRNA processing (proposed)	no	Bond *et al.*, 2001
Dbp3	DEAD	LSU; pre-rRNA processing (proposed)	no	Weaver *et al.*, 1997
Dbp6	DEAD	LSU	yes	Kressler *et al.*, 1998, 1999; Daugeron *et al.*, 2001; de la Cruz *et al.*, 2004
Dbp7	DEAD	LSU	no	Daugeron and Linder, 1998
Dbp9	DEAD	LSU	yes	Daugeron *et al.*, 2001
Dbp10	DEAD	LSU	yes	Burger *et al.*, 2000
Drs1	DEAD	LSU	yes	Ripmaster *et al.*, 1992, 1993
Spb4	DEAD	LSU	yes	de la Cruz *et al.*, 1998; Garcia-Gomez *et al.*, 2011
Mak5	DEAD	LSU	yes	Zagulski *et al.*, 2003; Pratte *et al.*, 2013
Mtr4	Ski2-like	LSU; pre-rRNA processing	yes	de la Cruz *et al.*, 1998
Has1	DEAD	SSU/LSU; snoRNA release; pre-rRNA processing (proposed)	yes	Emery *et al.*, 2004; Liang and Fournier, 2006; Dembowski *et al.*, 2013
Dbp5	DEAD	SSU/LSU; export	yes	Neumann *et al.*, 2016
Prp43	DEAH	SSU/LSU; snoRNA release; snoRNA access; pre-rRNA processing	yes	Lebaron *et al.*, 2005; Combs *et al.*, 2006; Bohnsack *et al.*, 2009; Pertschy *et al.*, 2009; Chen *et al.*, 2014

The vast majority of snoRNPs are already recruited to pre-ribosomes co-transcriptionally and a function that has been described for several RNA helicases that act early in the pathway is the release of snoRNPs. Based on sucrose density gradient separation of ribosomal and non-ribosomal complexes and subsequent northern blotting, the DEAD-box proteins Has1 and Dbp4 were shown to be required for the release of the U14 snoRNA from pre-ribosomes (Kos and Tollervey, 2005; Liang and Fournier, 2006). Similarly, the DEAH-box protein Dhr1 was reported to facilitate the release of U3 from pre-rRNA (Sardana *et al.*, 2015). Furthermore, a combined approach of sucrose density centrifugation and quantitative polymerase chain reaction (qPCR-) analysis enabled monitoring of the levels of all snoRNAs on pre-ribosomes upon depletion of any one of the eight SSU RNA helicases (Bohnsack *et al.*, 2008). This revealed that the snR30 snoRNA significantly accumulates on pre-ribosomal complexes when Rok1 is depleted (Bohnsack *et al.*, 2008). The direct interaction of Rok1 with the snR30 snoRNA and the region of the 18S rRNA, which snR30 basepairs with, was confirmed by *in vivo* crosslinking approaches (Martin *et al.*, 2014). The detection of snR30-pre-rRNA hybrids bound by Rok1 would support a model of direct unwinding of the snR30-18S duplex by Rok1 (Martin *et al.*, 2014). However, Rok1 has also been shown to interact with and be regulated by the ribosome biogenesis factor Rrp5 (Young *et al.*, 2013) and it has been suggested that Rok1 releases Rrp5 leading to spontaneous dissociation of snR30 (Khoshnevis *et al.*, 2016). One of the best characterised RNA helicases in yeast, is the DEAH-box protein Prp43, which was originally identified as being required for the release of the intron-lariat and recycling of splicing factors in spliceosome disassembly (Arenas and Abelson, 1997) and which has also been shown to act in spliceosomal quality control by degrading aberrant spliceosomes (Fourmann *et al.*, 2013). In ribosome biogenesis, Prp43 was suggested to exhibit a similar function in recycling of snoRNPs and ribosome biogenesis factors during pre-rRNA processing (Leeds *et al.*, 2006). Using the UV crosslinking and analysis of cDNA (CRAC) approach, the binding sites of Prp43 on pre-ribosomal complexes could be identified (Bohnsack *et al.*, 2009). Based on this, Prp43 was found to be required for the release of a subset of snoRNPs that introduce modifications into domain II of the 25S rRNA (Bohnsack *et al.*, 2009). Interestingly, analysis of snoRNA levels on pre-ribosomes also lead to the suggestion that Prp43 promotes association of certain snoRNPs with pre-60S complexes. Additionally, the identification of a Prp43 binding site at the 3' end of the 18S rRNA (Bohnsack *et al.*, 2009) was in line with a proposed function of Prp43 in remodelling of cytoplasmic SSU particles to allow cleavage at site D at the 3' end of 18S rRNA by Nob1 (Pertschy *et al.*, 2009). Like Prp43, which is directed to its various sites of function by competing cofactor interactions (Heininger *et al.*, 2016), other RNA helicases are recruited to the pathway of ribosome biogenesis by the interaction with additional ribosome biogenesis factors. Dbp10 is recruited to the immature PTC by the GTPase Nug1, where nucleotide binding of Nug1 and the helicase activity of Dbp10 are proposed to be required for

PTC formation (Manikas *et al.*, 2016). The DEAD-box protein Dbp6 was shown to form an RNA-independent subcomplex with the ribosome biogenesis factors Npa1 (Urb1), Npa2 (Urb2), Nop8 and Rsa3, which is recruited to pre-60S particles, where it was proposed to interact with two additional RNA helicases, Dbp7 and Dbp9 (Rosado *et al.*, 2007). Genetic analysis and synthetic lethal screens lead to the proposal that the ribosome biogenesis factors Ebp2, Nop16 and Rpf1 together with the RP Rpl14 (eL14) may arrange a local pre-60S structure to efficiently recruit Mak5, where it might get activated by its pre-rRNA binding site or another not yet identified protein cofactor (Pratte *et al.*, 2013). RNA helicases were also shown to be required for efficient pre-rRNA processing. The DEAD-box protein Dbp3 was proposed to be involved in A_3 site processing in ITS2, because depletion experiments resemble the defects observed due to the inactivation of MRP, the RNase that mediates A_3-cleavage (Weaver *et al.*, 1997). More recently, the acetyltransferase Kre33 was shown to be required for the modification of two cytosines in 18S rRNA. Interestingly, the helicase activity of the DEAD-box module at the N-terminus of the protein is crucial for the modification reaction and it was proposed that the RecA-like domains facilitate annealing of the orphan box C/D snoRNAs snR4 and snR45 to its 18S rRNA target sequences. Similarly to the pseudouridylation pocket formation in box H/ACA snoRNPs, these snoRNAs expose their target site to the C-terminal acetyltransferase domain of Kre33 for efficient acetylation. This mechanism introduced a novel function of snoRNAs in directing RNA base modifications, which could be reasonable especially for several box C/D snoRNAs in higher eukaryotes, where no specific function could be assigned so far (Sharma *et al.*, 2015, 2017). Besides its function in mRNA export and translation termination, the DEAD-box protein Dbp5 was reported to be involved in the nuclear export of pre-ribosomal particles. Although including the same export factors, the proposed export mechanism was suggested to be mechanistically different compared to the export of mRNAs and not to rely on the ATPase cycle of the RNA helicase (Neumann *et al.*, 2016).

1.4   Aims and Objectives

ATP-dependent RNA helicases are enzymes that participate in several processes of RNA metabolism like transcription, translation, pre-mRNA splicing and ribosome biogenesis. The synthesis of ribosomes is a very dynamic and complex process that requires a plethora of *trans*-acting ribosome biogenesis factors that guide rRNA transcription, pre-rRNA processing, modification, structure formation and assembly of ribosomal proteins. Here, RNA helicases were suggested to mediate snoRNA release or remodelling of pre-rRNA structures, which dissociates ribosome biogenesis factors from pre-ribosomes or provides accessibility for ribosomal proteins and late ribosome biogenesis factors to be recruited into maturing particles. The role of RNA helicases in SSU biogenesis was investigated in much more detail compared to their LSU counterparts. Especially the functions of late-acting RNA helicases, which are suggested to be involved in rearrangements of structural important features of LSU, remained elusive, mostly due to the information lacking on their binding sites.

The objectives of this study were to identify the binding sites and characterise the interactions of RNA helicases Has1, Spb4 and Mak5 by UV crosslinking and analysis of cDNA (CRAC), in order to elucidate their functional relevance in late nuclear steps of LSU biogenesis.

This study therefore aimed to:

- Confirm depletion phenotypes of Has1, Spb4 and Mak5

- Identify the crosslinking sites of Has1, Spb4 and Mak5 on RNA

- Compare Has1 CRAC data with reported functions in the literature

- Characterise Spb4 and Mak5 *in vitro* and *in vivo*, including mutational analyses

- Analyse the role of Has1, Spb4 and Mak5 in mediating snoRNA levels

- Confirm Spb4 and Mak5 binding sites on pre-rRNA by DMS structure probing

- Study the function of Mak5 in LSU biogenesis

2 Materials and Methods

2.1 Chemicals

Chemicals used for experiments in this study were obtained from AppliChem GmbH (Darmstadt, Germany), Carl Roth GmbH + Co. KG (Karlsruhe, Germany), Roche (Penzberg, Germany), VWR International GmbH (Darmstadt, Germany), Sigma-Aldrich Chemie GmbH (Munich, Germany), Life Technologies (Darmstadt, Germany), Promega GmbH (Mannheim, Germany) and Merck Chemicals GmbH (Schwalbach, Germany). Enzymes were purchased from ThermoFisher Scientific (St. Leon-Roth, Germany) or New England Biolabs (Frankfurt am Main, Germany). Antibodies were supplied by Aviva Systems Biology (San Diego, USA), Covance Inc. (Munich, Germany), Life Technologies GmbH (Darmstadt, Germany), Roche (Penzberg, Germany), Jackson ImmunoResearch Europe Ltd. (Suffolk, UK) or Sigma-Aldrich (Mannheim, Germany). Kits that were used for standard RNA or DNA techniques were obtained from Machery-Nagel (Dueren, Germany) or Qiagen (Hilden, Germany). DNA and RNA oligonucleotides were ordered from Sigma-Aldrich (Mannheim, Germany) and IDT (Coralville, USA) respectively, ^{32}P-γ-ATP was delivered by Perkin-Elmer (Rodgau, Germany).

2.2 Molecular cloning

In order to perform molecular cloning, including DNA amplification, detection of amplified products, restriction by enzymes, ligation reactions and transformation of *Escherichia coli* (*E. coli*), the standard methods according to Sambrook were followed (Sambrook *et al.*, 1989). These methods were used, for example, to generate constructs for expression of tagged yeast proteins containing specified mutations.

2.2.1 DNA amplification and detection of products

The polymerase chain reaction (PCR) was used to amplify DNA sequences either from genomic DNA isolated from yeast cells or from plasmid DNA obtained from *E. coli* cells. Amplification was achieved using the catalytic activity of the *Pfu*T polymerase using a thermal cycling programme (Biometra), where an example of the standard reaction components and cycling conditions is given in Table 2.1. PCR products were precipitated by the addition of 1 Vol Milli-Q(MQ)-H_2O, 0.6 Vol 3 M sodium acetate pH 5.2 and 6 Vol of 100 % ethanol, and incubation at -20 °C for 16 h. After centrifugation (20,000 rcf, 4 °C, 30 min), the obtained DNA pellet was washed with 700 µl of 70 % ethanol and again, centrifuged using the above-mentioned conditions. For further steps in molecular cloning, the DNA was resupended in 16 µl of MQ-H_2O.

Table 2.1: Components and cycle conditions of a standard PCR reaction.

Component	Final concentration	Temperature	Time	Cycles
10 x *Pfu*T buffer	1 x	95 °C	5 min	1 x
2 mM dNTPs	120 µM	95 °C	30 sec	
Forward (FW) oligonucleotide	0.4 µM	52 °C	30 sec	39 x
		72 °C	1 min/kbp	
Reverse (RV) oligonucleotide	0.4 µM	72 °C	10 min	1 x
		4 °C	-	-
Template DNA	80 – 100 ng			
*Pfu*T polymerase	2.5 U			
MQ-H$_2$O	To 50 µl			

In order to visualise DNA, a 6 x DNA loading dye (0.2 % bromophenol blue, 0.2 % xylene cyanol, 60 % glycerol, 60 mM EDTA) was added to a 1 x final-concentration. According to the expected fragment length, samples were loaded onto a 1.2 % (w/v) or up to 3 % (w/v) agarose-gel containing SafeView (abm, 3 µl in 30 ml gel-mix) and separated at 120 V for 60 min in 1 x TAE buffer (40 mM Tris/HCl, 20 mM acetic acid, 1 mM EDTA). The separated DNA was then detected under UV light using an INTAS transilluminator.

Table 2.2: Oligonucleotides used for molecular cloning.

Name	Sequence (5' to 3')
FW Spb4 + 500 bp (*Pst*I)	ATATACTGCAGCCTGAAGTCTCTCTCTCCAACAAAATATGATGCGGC
RV Spb4 + 500 bp (*Sma*I)	TATATCCCGGGCTACTTCTTAACCTCTAATTACCAACGGGTC
FW Mak5 + 500 bp (*Pst*I)	TATATATCTGCAGACCTTTAATACTTAACCTGATAATTTTG
RV Mak5 + 500 bp (*Not*I)	TATATATGCGGCCGCAAGTCGTTTGCTATTGACAAAG
FW Spb4 (*Bam*HI)	ATATATGGATCCATGTCAAAGTCATTGGAATGG
RV Spb4 (*Nhe*I)	ATATATGCTAGCTAAGTCGTCAAAATTGCCTTG
FW Mak5 (*Bam*HI)	ATATATGGATCCATGGGTAAGAAAAGGGCTCC
RV Mak5 (*Nhe*I)	ATATATGCTAGCATTATTTCTCTTTTTCTTTTTCTTCAAAGTTTCTAAGG
FW Has1 (*Bam*HI)	ATATATGGATCCATGGCTACCCCGTCAAATAAACG
RV Has1 (*Nhe*I)	ATATATGCTAGCCTTATGAGTTTTACGTCTTTTGGTATTTGG

2.2.2 Restriction digestion and ligation of DNA

For cloning PCR products into target plasmids, restriction sites were introduced upstream and downstream within the oligonucleotide sequences used for amplification (see Table 2.2). Both the PCR product (insert DNA) and 2 µg of plasmid DNA were digested in a final volume of 20 µl using 10 U of the appropriate restriction enzyme(s) in 1 x enzyme buffer, according to manufacturer's recommendations, at 37 °C for 1 h. In order to dephosphorylate the plasmid DNA, 1 µl alkaline phosphatase (ThermoFisher Scientific) was added to the corresponding reaction mix and reactions were incubated for further 20 min at 37 °C. To purify the obtained DNA fragments, 4 µl 6 x DNA loading dye were added into the reaction mix, which was loaded

onto an agarose gel. DNA was separated, visualised on a UV table and fragments with the expected lengths were excised from the gel. DNA from the gel slices was purified using the NucleoSpin Gel and PCR Clean-Up kit (Machery-Nagel) following the manufacturer's instructions.

Subsequent ligation of the purified DNA fragments was achieved by setting up reactions containing a 5:1 molar ratio of insert:plasmid DNA, using 50 ng of plasmid, together with 1 µl of T4 DNA Ligase (ThermoFisher Scientific) and ATP-containing 1 x T4 DNA Ligase Buffer (ThermoFisher Scientific) in a total volume of 30 µl. The reaction mix was incubated at 16 °C overnight.

2.2.3 *E. coli* transformation and plasmid extraction

The ligation mix was used for transformation of *E. coli* strains TOP10 or DH5α, which were also used for amplification of plasmids. To do so, 50 µl of chemically competent cells were thawed on ice and incubated with either the ligation mix or 5 ng of plasmid DNA for 30 min on ice before applying a heat shock for 1 min at 42 °C. 700 µl of Luria Broth (LB) medium was added and cells were incubated at 37 °C for 20 – 30 min with gentle agitation in a thermoblock. After centrifugation (1,000 rcf, room temperature (RT), 3 min), cells were resuspended in 100 µl LB and spread on selective plates containing the relevant antibiotic. These plates were incubated overnight at 37 °C and resulting colonies were used to inoculate 4 ml LB + antibiotic, which was again incubated at 37 °C overnight while shaking. The enriched plasmid DNA was extracted using the NucleoSpin Plasmid kit (Machery-Nagel) according to the manufacturer's instructions.

The obtained plasmid DNA was sent to GATC Biotech for sequencing using oligonucleotide primers, where the sequenced regions covered the length of the PCR insert and the ligation sites, to check incorporation of the correct insert DNA into the plasmid backbone.

2.2.4 Site-directed mutagenesis

Exchanging single or multiple bases in existing plasmid DNA constructs, e.g. to swap amino acids in the encoded protein, was achieved by site-directed mutagenesis. Three PCR reactions, containing 5, 20 or 50 ng of plasmid DNA, together with 10 µl 5 x GC/HF buffer (ThermoFisher Scientific), 1.25 µl (10 µM) forward oligonucleotide and 1.25 µl (10 µM) reverse oligonucleotide (reverse complement of the forward oligonucleotide, both containing the desired nucleotide swap; Table 2.3), 0.4 mM dNTPs and 1 µl Phusion polymerase in a total volume of 50 µl, were set up. The reaction mix was heated at 95 °C for 30 sec before it was cycled 16 x through: 30 sec of 95 °C, 2 min of 55 °C and 68 °C for 1 min per kbp. After a final elongation step for 10 min at 68 °C, the reaction mix was cooled down to 4 °C. To remove

methylated template DNA, 1 µl of *Dpn*I (ThermoFisher Scientific) was added and the reactions were incubated for 2 h at 37 °C. Afterwards, the reaction mixes were pooled and the DNA was precipitated by the addition of 7.5 µl 3 M sodium acetate pH 5.2, 450 µl 100 % ethanol and incubation at -20 °C overnight. By centrifugation (20,000 rcf, 4 °C, 30 min), the DNA was pelleted, then the supernatant was removed and the pellet was washed with 500 µl 70 % ethanol. After repeating the centrifugation and removal of the supernatant, the DNA was dried and resuspended in 10 µl of MQ-H_2O. This DNA was then used to transform *E. coli* cells for amplification. After extraction of plasmid DNA, sequencing was used to check that the mutation had been introduced.

Table 2.3: Oligonucleotides used for site-directed mutagenesis.

Name	Sequence (5' to 3')
FW Spb4-DEAD	GCATGCAGTATGGTAGTTATGGATCAGGCAGACAGATTGTTGGATATGAG
RV Spb4-DEAD	CTCATATCCAACAATCTGTCTGCCTGATCCATAACTACCATACTGCATGC
FW Mak5-DEAD	CGAAAGTAAATACGCTAATCCTTGATCAGGCTGATAGGCTGTTACAAG
RV Mak5-DEAD	CTTGTAACAGCCTATCAGCCTGATCAAGGATTAGCGTATTTACTTTCG
FW Mak5-SAT	GGCAAACTTTGATCTTTGCGGCCGCCTTCTCCATCGACTTGTTTGATAAGC
RV Mak5-SAT	GCTTATCAAACAAGTCGATGGAGAAGGCGGCCGCAAAGATCAAAGTTTGCC

Table 2.4: Plasmids for recombinant expression and *in vivo* complementation.

ID	Name	Application	Source
pMB-031	pRS415 empty	Empty vector for protein expression in yeast	New England Biolabs
pMB-311	A21 Mak5	Recombinant expression in *E.coli*	Bohnsack lab
pMB-317	A21 Spb4	Recombinant expression in *E.coli*	Bohnsack lab
pMB-586	A21 Spb4 SAT	Recombinant expression in *E.coli*	Bohnsack lab
pMB-1245	pRS415 Spb4 WT	*In vivo* complementation (yeast)	This study
pMB-1319	pRS415 Mak5 WT	*In vivo* complementation (yeast)	This study
pMB-1323	pRS415 Mak5 DEAD	*In vivo* complementation (yeast)	This study
pMB-1341	A21 Mak5 DEAD	Recombinant expression in *E.coli*	This study
pMB-1343	A21 Mak5 SAT	Recombinant expression in *E.coli*	This study
pMB-1347	A21 Spb4 DEAD	Recombinant expression in *E.coli*	This study
pMB-1357	pRS415 Spb4 SAT	*In vivo* complementation (yeast)	This study
pMB-1358	pRS415 Mak5 SAT	*In vivo* complementation (yeast)	This study
pMB-1359	pRS415 Spb4 DEAD	*In vivo* complementation (yeast)	This study

2.3 Yeast cultivation

Routinely, yeast strains used in this study (see Table 2.5), which are derived from the BY4741 background (Brachmann *et al*., 1998), were cultured in YPD medium containing 1 % (w/v) yeast extract, 2 % (w/v) peptone and 2 % (w/v) glucose. If the DNA sequence in front of an

essential gene was exchanged for a galactose-dependent promoter sequence, cells were grown in YPG medium, where the carbon source was exchanged to 2 % galactose instead of 2 % glucose. For selection of cells using auxotrophic markers, synthetic dropout media lacking certain amino acids (ForMedium) were used.

Table 2.5: List of yeast strains used in this study.

ID	Name	Genotype	Source
YMB 006	BY4741a	MATa; hisΔ1; leu2Δ0; met15Δ0; ura3Δ0	Brachmann *et al.*, 1998
YMB 145	pTetO$_7$-Mak5	YMB 279; pTetO$_7$-3xHA-Mak5 (NatNT2)	Bohnsack lab
YMB 149	pTetO$_7$-Spb4	YMB 279; pTetO$_7$-3xHA-Spb4 (NatNT2)	Bohnsack lab
YMB 279	pTetO$_7$ parent	YMB 006; tTA::LYS2; tetR'::URA3; K.l.::LEU2	Alexander *et al.*, 2010
YMB 323	pTetO$_7$-Has1	YMB 279; pTetO$_7$-3xHA-Has1 (NatNT2)	Bohnsack lab
YMB 341	Ssf1-cTAP	YMB 006; Ssf1-TAP::HIS	Bohnsack lab
YMB 343	Arx1-cTAP	YMB 006; Arx1-TAP::HIS	Bohnsack lab
YMB 345	Nip7-cTAP	YMB 006; Nip7-TAP::HIS	Bohnsack lab
YMB 428	Has1-cHTP	YMB 006; Has1-HTP::URA3	Bohnsack lab
YMB 474	Mak5-cHTP	YMB 006; Mak5-HTP::URA3	Bohnsack lab
YMB 493	Spb4-cHTP	YMB 006; Spb4-HTP::URA3	Bohnsack lab
YMB 540	Npa1-cTAP	YMB 006; Npa1-TAP::URA3	Bohnsack lab
YMB 979	pTetO$_7$-Mak5 Nop2-cHTP	YMB 145; Nop2-HTP::HIS	This study
YMB 991	pTetO$_7$-Has1 Nop2-cHTP	YMB 323; Nop2-HTP::HIS	This study
YMB 998	pGal$_1$-Spb4 Nop2-cHTP	YMB 279; pGal$_1$-3xHA-Spb4 (KanMX); Nop2-HTP::HIS	This study
YMB 1097	pGalS-Prp43 Rpf2-cHTP	YMB 006; pGal$_S$-3xHA-Prp43 (NatNT2); Rpf2-HTP::HIS	This study
YMB 1139	Erb1-cHTP	YMB 006; Erb1-HTP::HIS	This study
YMB 1173	Rlp24-cHTP	YMB 006; Rlp24-HTP::HIS	This study
YMB 1453	pTetO$_7$-Mak5 Nop2-cHTP + EV	YMB 979; pMB-031::LEU2	This study
YMB 1455	pTetO$_7$-Mak5 Nop2-cHTP + Mak5-WT	YMB 979; pMB-1319::LEU2	This study
YMB 1457	pTetO$_7$-Mak5 Nop2-cHTP + Mak5-DEAD	YMB 979; pMB-1323::LEU2	This study
YMB 1459	pTetO$_7$-Mak5 Nop2-cHTP + Mak5-SAT	YMB 979; pMB-1358::LEU2	This study
YMB 1405	pGal$_1$-Spb4 Nop2-cHTP + EV	YMB 998; pMB-031::LEU2	This study
YMB 1407	pGal$_1$-Spb4 Nop2-cHTP + Spb4-WT	YMB 998: pMB-1245::LEU2	This study
YMB 1464	pGal$_1$-Spb4 Nop2-cHTP + Spb4-DEAD	YMB 998; pMB-1359::LEU2	This study
YMB 1466	pGal$_1$-Spb4 Nop2-cHTP + Spb4-SAT	YMB 998; pMB-1357::LEU2	This study

From glycerol stocks (yeast cells in medium containing 15 % glycerol, stored at -80 °C), cells were streaked out on appropriate plates and incubated at 30 °C for 2 d. Single colonies were

inoculated in 4 ml cultures, which were grown at 30 °C overnight while shaking. These starter cultures were either used directly or used to inoculate larger cultures that were maintained in exponential phase before harvesting by centrifugation at 2,000 rcf.

2.4   Yeast transformation

In order to generate yeast strains for genomic expression of tagged proteins or for expression of proteins from a regulatable promoter either genomically or from plasmids (Table 2.4), exogenous DNA had to be transferred into yeast strains. For homologous recombination, PCR cassettes were amplified from template plasmids using oligonucleotides listed in Table 2.6. For introducing N- or C-terminal epitopes as well as promoter or terminator sequences with its obligatory selection markers, plasmids from the BlueScript or the Longtine (Longtine *et al.*, 1998) collection were used (see Table 2.7).

Table 2.6: Oligonucleotides for amplification of PCR cassettes for homologous recombination.

Name	Sequence (5' to 3')	Application
FW Nop2-cHTP	GGGTGTCAATCCAAAAGCTAAAAGACCTTCTAACGAAAA ATCCATGGAGCACCATC	genomic tagging
RV Nop2-cHTP	GAGAAAACTATGCTAACATGATGCCACTACGTTTGTGGG TACGACTCACTATAGGGCG	genomic tagging
FW pGal$_1$-Spb4	GCCCATTGATTTGAGGTGTAGTAAGATAATATTAAAAGC TCAGCAGCAATAAAAACATCGAGCTCGTTTAAAC	promoter swap
RV pGal$_1$-Spb4	CCTTATCCAGGGAAGTAAAGAAAACCCGAGATTATCCCA TTCCAATGACTTTGACATGCACTGAGCAGCGTAATCTG	promoter swap

Table 2.7: Plasmid templates for amplification of cassettes used for homologous recombination.

ID	Name	Application	Source
pMB-439	pBS1539-HIS3-HTP	cHTP tagging (HIS)	Bohnsack lab
pMB-778	pFA6a-kanMX-pGal$_1$-3xHA	pGal$_1$ promoter transfer (KanMX)	Longtine *et al.*, 1998

PCR products were precipitated and resuspended in 12 µl of H$_2$O in order to be used according to the transformation protocol. For transforming yeast, cells of the parental strain were inoculated in 4 ml of permissive medium and grown overnight at 30 °C, with constant shaking. A 50 ml culture was then grown to mid-log phase and cells were harvested by centrifugation (2,000 rcf, 4 °C, 5 min). The cell pellet was washed with 10 ml of MQ-H$_2$O, pelleted again by centrifugation and resuspended in 1 ml of MQ-H$_2$O in order to transfer the cells to a 1.5 ml reaction tube. After pelleting the cells by centrifugation (2,000 rcf, 4 °C, 1 min), they were washed with 1.5 ml TE/LiAc buffer (10 mM Tris/HCl pH 7.4, 1 mM EDTA, 100 mM lithium acetate), centrifuged (2,000 rcf, 4 °C, 1 min) and resuspened in 200 µl TE/LiAc buffer.

For each transformation, 50 µl of cells together with 5 µl denatured salmon sperm DNA (Sigma-Aldrich, 10 mg/ml, pre-heated to 95 °C for 20 min then cooled on ice for 2 min) and 5 µg of plasmid DNA (or 12 µl of resupended PCR product) were mixed and 300 µl of PEG buffer (40 % PEG4000, 10 mM Tris/HCl pH 7.4, 100 mM lithium acetate) was directly added. This suspension was incubated at 30 °C and 750 rpm in an Eppendorf thermoblock for 30 min before a heat shock at 42 °C for 15 min was applied.

When using an auxotrophic marker, 800 µl of MQ-H_2O was added and the cell suspension was centrifuged (20,000 rcf, RT, 10 sec). The cell pellet was resuspended in 100 µl MQ-H_2O, plated onto selective plates and incubated for 2 d at 30 °C.

When using an antibiotic marker, instead of plating the resuspended cell pellet onto selective plates, they were plated onto permissive medium and incubated at 30 °C for 16 h before replica plating onto selective plates. In order to avoid mixed colonies from different genetic background, single colonies from selective plates were spread and selected twice.

2.5 Preparation of genomic DNA from yeast

For extracting genomic DNA from yeast cells, 1.5 ml of a yeast overnight culture was harvested by centrifugation (2,000 rcf, RT, 5 min). The cell pellet was resuspendend in 250 µl Lysis buffer (0.05 % Tween 20, 100 mM Tris/HCl pH 7.4, 1 mM EDTA, 1 % SDS). Together with 150 µl of glass beads, 250 µl phenol-chloroform-isoamylalcohol (PCI 25:24:1) were added and cells were lysed by vortexing at 4 °C. Centrifugation (20,000 rcf, 4 °C, 5 min) was used to separate the aqueous and organic phases, and the upper aqueous phase was transferred into a new reaction tube. It was supplemented with 20 µl 3 M sodium acetate pH 5.2 and 600 µl ethanol to precipitate the genomic DNA overnight at -20 °C. The precipitate was pelleted by centrifugation (20,000 rcf, 4 °C, 30 min). After washing the pellet with 500 µl 70 % ethanol and repeating the previous centrifugation step, the supernatant was removed, the DNA pellet was dried and resuspended in 50 µl MQ-H_2O. The integrity of genomic DNA could be tested on an agarose gel and after confirmation the DNA was used as template for polymerase chain reactions.

2.6 Protein extraction, SDS-PAGE, western blotting, Coomassie staining

For checking proteins from generated yeast strains or *E. coli* lysates after recombinant expression, denaturing sodium dodecyl sulfate polyacrylamide gel electrophoresis (SDS-PAGE) was used according to instructions from Laemmli (Laemmli, 1970). In order to extract proteins from yeast cells, 1.5 ml of an overnight culture was harvested (2,000 rcf, RT, 5 min). The cell pellet was resuspended in 100 µl MQ-H_2O and 50 µl glass beads were added. Cells

were disrupted by vortexing for 5 min at 4 °C. After addition of 1 ml 15 % trichloroacetic acid (TCA) and vortexing, the reaction was incubated on ice for 10 min. The suspension was vortexed once again and kept on ice for 10 sec to allow the glass beads to settle prior to transferring the supernatant into a fresh reaction tube. Centrifugation (20,000 rcf, 4 °C, 30 min) pelleted the precipitated proteins, which were washed with 1 ml acetone before another centrifugation step (20,000 rcf, 4 °C, 30 min). After removal of the supernatant, the protein pellet was dried and resuspended in 30 µl 1 x SDS-buffer (60 mM Tris/HCl pH 6.8, 2 % SDS, 0.01 % bromophenol blue, 1.25 % ß-mercaptoethanol).

Protein samples were incubated for 5 min at 95 °C before they were used for SDS-PAGE, which separates denatured proteins according to their molecular weight. Gels contained a 4 % stacking gel for focusing of proteins and a 10 – 15 % resolving gel, using different concentrations of polyacrylamide for larger (>100 kDa) and smaller proteins (<50 kDa) respectively. Using a BioRad system, the process of electrophoresis was done at 25 mA for a gel of 0.75 mm thickness for 1 h. Afterwards, proteins were visualised by incubation of the gel with Coomassie Blue (0.1 % Coomassie Blue (w/v), 40 % methanol (v/v), 10 % acetic acid (v/v)) for 1 h while shaking. Destaining was carried by washing with Destain Solution (40 % methanol (v/v), 10 % acetic acid (v/v)) at least for 16 h.

Table 2.8: Antibodies used in this study.

Name	Source	Fold dilution
Anti-HA	Covance Inc.	1:1,000
Anti-PAP	Sigma-Aldrich Chemie GmbH	1:5,000
Anti-Pgk1	Life Technologies GmbH	1:7,500
Anti-GFP	Roche	1:1,000
Anti-Rpl15	Aviva Systems Biology	1:1,000
Goat-anti-mouse	Jackson ImmunoResearch Europe Ltd.	1:10,000
Goat-anti-rabbit	Jackson ImmunoResearch Europe Ltd.	1:10,000

To detect specific or epitope-tagged proteins, Western blot analysis was performed after proteins were separated by SDS-PAGE. Transfer of proteins from polyacrylamide gel onto nitrocellulose membranes (GE Healthcare) was achieved by wet blotting in Western Blot buffer (25 mM Tris, 192 mM glycin, 0.05 % SDS, 20 % methanol) at 100 V for 1 h using the BioRad system. To avoid unspecific binding of antibodies to the membrane, it was incubated with Blocking Solution (5 % milk in phosphate buffered saline containing Tween (PBS-T, 137 mM NaCl, 2.7 mM KCl, 10 mM Na_2HPO_4, 1.8 mM KH_2PO_4, 1 % Tween2000 (v/v)) for 1 h at RT with gentle agitation. Before use, primary antibodies (see Table 2.8) were diluted in Blocking Solution according to manufacturer's instructions. Membranes were incubated with the primary antibody overnight at 4 °C and afterwards, were washed three times with PBS-T for 10 min.

For binding of a secondary antibody (see Table 2.8), membranes were incubated with appropriate dilutions of the antibody in Blocking Solution at RT for 1 h before they were washed again three times with PBS-T for 10 min. Since the secondary antibodies used are conjugated to horseradish peroxidase (HRP), the specific proteins were detected by enhanced chemiluminescence using substrate solutions (ECL, Millipore) when exposed to X-ray films.

2.7   Serial dilution growth assay

For testing growth of yeast strains in permissive or non-permissive medium, cultures were grown in exponential phase and cells corresponding to 1 ml of OD_{600} = 1 were harvested (2,500 rcf, RT, 5 min). The cell pellet was washed with 1 ml of the following medium (permissive or non-permissive) and centrifuged once again (2,500 rcf, RT, 5 min). Following three serial 1:10 dilutions, 5 µl of each cell suspension were spotted on plates with different conditions. Plates were incubated for 3 d at 30 °C and growth of cell spots could be recorded.

2.8   Depletion of essential proteins and growth analysis

As the deletion of essential genes leads to non-viable strains, we made use of different depletion systems, where an artificial promoter is inserted in front of our gene of interest allowing regulation of gene expression by addition of a chemical or by changing the carbon source. On one hand, we used a $pTetO_7$-3xHA-promoter that allows repression of gene expression by addition of the non-hydrolysable tetracycline variant doxycycline by activating the genomically encoded Tet repressor. On the other hand, a $pGal_1$-3xHA-promoter was inserted, enabling gene expression to be blocked by changing the carbon source from galactose to glucose. In order to prevent secondary effects after repression of protein expression, an appropriate depletion time, where the decreasing protein level becomes limiting for growth, was estimated. For this reason, yeast cultures were grown under permissive conditions to mid-log phase before the depletion was initiated either by addition of doxycycline to a final concentration of 10 µg/ml (20 µg/ml in synthetic medium) or by changing the carbon source by harvesting (2,000 rcf, RT, 5 min), washing the cells with medium containing the new carbon source (2,000 rcf, RT, 5 min) and resuspending them in new medium for further growth. Every 2 h the OD_{600} was measured and samples corresponding to 1 ml of OD_{600} = 1 (1 ml of OD_{600} = 5 in synthetic medium) were taken. The resulting growth curves under permissive and non-permissive conditions were compared to each other and also compared with the protein levels that were determined by TCA precipitation of proteins from the taken cell samples and immunoblotting using an antibody against the N-terminal HA-epitope. We determined the depletion time as the time where the growth curves under permissive and non-permissive conditions diverge and the protein was no longer detectable.

2.9   Yeast RNA isolation

Yeast cells were grown in 30 ml cultures to mid-log phase and harvested by centrifugation (2,000 rcf, 4 °C, 5 min) in a 15 ml falcon-tube. Cell pellets were resuspended in 300 µl GTC mix (2 M guanidine thiocyanate, 25 mM Tris/HCl pH 8.0, 5 mM EDTA pH 8.0, 1 % (v/v) N-lauroylsarcosine, 150 mM ß-mercaptoethanol) and 300 µl Roti-Aqua-Phenol (Roth). After adding 600 µl of glass beads, cells were disrupted by vortexing for 5 min at 4 °C. An additional 3 ml of GTC and 3 ml of phenol were added and the suspension was vortexed before incubation at 65 °C for 5 min. Following incubation at 4 °C for 5 min, 1.6 ml sodium acetate-mix (100 mM sodium acetate, 1 mM EDTA pH 8.0, 10 mM Tris/HCl pH 8.0) and 3 ml chloroform were added and the suspension was vortexed. The aqueous and organic phases were separated by centrifugation (2,000 rcf, 4 °C, 30 min), and the upper, aqueous phase (approx. 5 ml) was transferred into a new 15 ml falcon-tube. This was mixed with PCI in a 1:1 ratio. Again, phases were separated by centrifugation (2,000 rcf, 4 °C, 5 min) and the aqueous phase (approx. 4.5 ml) was mixed with chloroform in a 1:1 ratio by inverting. After separating the phases (see previous centrifugation), the aqueous phase was transferred into another 15 ml falcon-tube and 11 ml of 100 % ethanol, together with 1 µl of glycogen were added. The reactions were thoroughly mixed by inverting and stored overnight at -20 °C.

Precipitated RNA was pelleted by centrifugation (2,000 rcf, 4 °C, 30 min) and the supernatant was removed. The remaining pellet was washed with 2 ml of 70 % ethanol and the suspension was centrifuged (2,000 rcf, 4 °C, 30 min). After the supernatant was removed, the RNA pellet was dried and resuspended in 30 µl of MQ-H_2O at 50 °C and 100 rcf.

2.10   Polyacrylamide- and agarose gels for RNA + northern blotting

For separation of small RNAs, RNA samples were supplemented with 2 x formamide loading dye (80 % formamide, 10 mM EDTA pH 8.0, 1 mg/ml xylene cyanol FF, 1 mg/ml bromophenol blue), denatured at 95 °C for 5 min and loaded onto denaturing (7 M urea) 10 % polyacrylamide gels in 1 x TBE (89 mM Tris/HCl, 89 mM boric acid, 2 mM EDTA). RNA samples were generally separated at 30 W for 1.5 h or depending on required separation. Afterwards, the RNA was transferred, in 0.5 x TBE at 60 V and 4 °C for 2 h, onto a Hybond N membrane (GE Healthcare) using the Trans Blot Cell system (BioRad). The RNA was crosslinked to the membrane by the UV Stratalinker 2400 (Stratagene) applying UV light of 0.12 J/cm^2 twice.

Larger RNA molecules like rRNA precursors were separated on 1.2 % agarose gels in 1 x BPTE (10 mM Pipes, 30 mM Bis-Tris, 1 mM EDTA pH 8.0). 6 µg of RNA were mixed with 4 Vol Glyoxal loading dye (20 % (v/v) glyoxal, 61 % DMSO (v/v), 5 % glycerol, 0.1 % ethidium bromide (v/v) in 1 x BPTE) and heated at 55 °C for 1 h before loading. Gels were run at 60 V for 16 h. Afterwards, gels were washed for 20 min in 100 mM NaOH for fragmentation of RNA,

followed by two washes in a quenching Tris/NaCl buffer (0.5 M Tris/HCl pH 6.4, 1.5 M NaCl) for 15 min each and a final wash step in 6 x SSC buffer (150 mM NaCl, 15 mM sodium citrate) for another 20 min. The RNA was then transferred onto a Hybond N membrane using the vacuum blotting system VacuGene XL (GE Healthcare), where vacuum was applied at 300 mbar for 3 h. Finally, transferred RNA was crosslinked to the membrane by exposure to UV light of 0.12 J/cm^2 twice.

By methylene blue staining (10 min in 0.03 % methylene blue (w/v), 0.3 M sodium acetate pH 5.2), the most abundant RNAs on the membrane could be visualised. For detection of specific, lower abundance RNAs, membranes were hybridised with radioactively-labelled antisense DNA-oligonucleotides. For labelling, 2 µl 10 mM oligonucleotide were incubated with 2 µl ^{32}P-γ-ATP (Perkin-Elmer), 2 µl T4 polynucleotide kinase buffer (Fermentas) and 1 µl T4 polynucleotide kinase (PNK, Fermentas) in a 20 µl reaction at 37 °C for 30 min. After the phosphorylation, the reaction mix was diluted in 40 ml SES1 buffer (0.5 M sodium phosphate pH 7.2, 7 % SDS, 1 mM EDTA pH 8.0). Membranes to be incubated with radiolabelled oligonucleotides (see Table 2.9) were pre-incubated with SES1 buffer at 37 °C for 30 min before hybridisation with the probe overnight at 37 °C. After washes with 6 x SSC and 2 x SSC containing 0.1 % SDS at 37 °C for 30 min each, the membranes were dried and exposed to a phosphorimager screen. Detection of radioactive signals was carried out using a Typhoon FLA 9500 phosphorimager (GE Healthcare).

Table 2.9: Oligonucleotides used for northern blotting.

Name	Sequence (5' to 3')	Application
004	CGGTTTTAATTGTCCTA	Northern probe ITS1
020	TGAGAAGGAAATGACGCT	Northern probe ITS2
scR1	ATCCCGGCCGCCTCCATCAC	Northern probe

2.11 Recombinant protein expression in *E. coli*

In order to purify a protein of interest, it was recombinantly expressed from a multi-copy plasmid under the control of an isopropyl-beta-D-thiogalactopyranoside (IPTG) inducible promoter in the *E. coli* strain BL 21 Codon Plus. The plasmid used (A21) enables expression of an N-terminally His$_{10}$-ZZ-tagged fusion protein, allowing specific enrichment, via the His$_{10}$-tag, on Ni^{2+} beads (Roche). After transforming the plasmid into the bacterial strain and selection by antibiotic markers (see section 2.2.3), a single colony was used to inoculate a 20 ml culture of LB medium containing 100 µg/ml ampicillin (Amp) and 12.5 µg/ml chloramphenicol (Chl), which was then grown at 37 °C while shaking overnight. This overnight culture was then used to inoculate 1 L of LB + Amp + Chl, which was grown at 37 °C while shaking to an OD$_{600}$ = 0.5. The culture was cooled by incubation for at least 30 min at 4 °C

before recombinant protein expression was induced by addition of IPTG to a final concentration of 1 mM and the cells were grown overnight at 18 °C.

After adding 1 mM PMSF to the culture, it was centrifuged (4,000 rcf, 4 °C, 20 min) to pellet the cells. The cells were then washed with 20 ml 1 x PBS and transferred to a 50 ml falcon-tube. After another step of centrifugation (2,000 rcf, 4 °C, 5 min), cells were resuspended in 20 ml of Lysis buffer (50 mM Tris/HCl pH 7, 500 mM NaCl, 1 mM $MgCl_2$, 10 mM imidazole, 1 mM PMSF, 10 % glycerol). The cell suspension was sonicated (4 x 30 sec, 45 % amplitude, 0.7 sec in, 0.3 sec off) on ice. The lysate was then cleared of cell debris by centrifugation (20,000 rcf, 4 °C, 20 min) in a JA30.50 rotor (Beckman-Coulter). To precipitate protein-associated nucleic acids, polyethyleneimine (PEI) was added to a final concentration of 0.05 % and the lysate was incubated, rotating at 4 °C for 15 min. Precipitates were pelleted by centrifugation (33,000 rcf, 4 °C, 30 min) and the supernatant was mixed with Ni-NTA beads (1 ml slurry), which had been pre-equilibrated in Wash buffer I (50 mM Tris/HCl pH 7, 500 mM NaCl, 1 mM $MgCl_2$, 30 mM imidazole, 10 % glycerol), for incubation at 4 °C while rotating for 1 h. The lysate-beads-suspension was transferred to a gravity-flow column and the beads were washed with 10 ml of Wash buffer I, followed by a high-salt wash with 10 ml Wash buffer II (50 mM Tris/HCl pH 7, 1 M NaCl, 1 mM $MgCl_2$, 30 mM imidazole, 10 % glycerol) and another wash with 10 ml of Wash buffer I. For elution, the beads were incubated with 3 ml of Elution buffer (50 mM Tris/HCl pH 7, 500 mM NaCl, 1 mM $MgCl_2$, 10 % glycerol, 300 mM imidazole) for 5 min and fractions of 1 ml were collected. This procedure was repeated three times over and 1 µl of each elution fraction was spotted onto a nitrocellulose membrane. Protein was visualised by amidoblack staining (0.1 % (w/v) in 50 % ethanol) and fractions containing the highest protein content were pooled for dialysis. In order to prevent precipitation of the protein during dialysis, glycerol to an end-concentration of 20 % was added and the protein was dialysed against Dialysis buffer (50 mM Tris/HCl pH 7, 120 mM NaCl, 2 mM $MgCl_2$, 20 % glycerol) overnight at 4 °C through a 30 kDa cutoff dialyse membrane (Spectrum Laboratories), which had previously been equilibrated in 5 mM EDTA.

A final centrifugation step (20,000 rcf, 4 °C, 30 min) separated the soluble supernatant from any precipitates that occurred during the dialysis procedure. The protein concentration was estimated by Bradford assay and, if necessary, the protein was concentrated using concentrator columns (Corning).

2.12 Steady state ATPase activity of recombinant proteins

To study the steady state ATPase activity of recombinantly expressed and purified RNA helicases, we used an indirect NADH-coupled ATPase assay (Kiianitsa *et al.*, 2003). Reactions containing 2 µM protein and increasing amounts of RNA (0 – 4 µM), 45 mM Tris/HCl pH 7.4, 25 mM NaCl, 2 mM $MgCl_2$, 4 mM ATP, 1 mM phosphoenolpyruvate (PEP, Sigma-Aldrich),

20 U/ml pyruvate kinase/ lactic dehydrogenase (Sigma-Aldrich) and 300 µM ß-nicotinamide adenine dinucleotide (NADH) were set up. The hydrolysis of ATP causes increasing ADP levels leading to the conversion of phosphoenol pyruvate (PEP) to pyruvate by the available pyruvate kinase. The pyruvate afterwards was converted to lactate by the enzyme lactate dehydrogenase. This step is coupled to the oxidation of NADH to NAD^+, which could be measured by the decrease of absorption at 340 nm (A_{340}), the absorbance maximum of NADH. Measurements were done at 30 °C using a BioTEK Synergy HT microplate spectrophotometer.

The ATP hydrolysis rate of proteins was estimated using the following equation, where K_{path} is the molar absorption coefficient for a given optical pathlength, specified by the fill volume of 150 µl per well and background NADH decomposition.

$$\text{ATPase rate} \left[\frac{\text{ATP}}{\text{min}}\right] = \frac{\frac{\text{dA340}}{\text{dt}} \left[\frac{\text{OD}}{\text{min}}\right]}{\text{Kpath} * \text{moles ATP}}$$

2.13   UV crosslinking and analysis of cDNA (CRAC)

The UV crosslinking and analysis of cDNA (CRAC) technique is a method to detect protein-RNA interaction sites as described in Bohnsack *et al.* (2012) and Granneman *et al*. (2009) (see Fig. 2.1). The CRAC method was performed with the help of Maike Ruprecht and Philipp Hackert.

Two alternative approaches for covalent crosslinking of proteins to their associated RNAs were used: applying UV light of 254 nm to actively growing yeast cells in culture (*in culturo*; UV-CRAC) or applying light of 365 nm to pelleted cells that were resuspended in a small volume and spread onto a petri dish (*in vivo*; PAR-CRAC). In order to perform *in culturo* UV crosslinking a custom-built crosslinker (iTRIC: *in culturo* temperature regulated interaction crosslinker) was used that allowed 254 nm UV irradiation of cells with 1.6 J/cm^2 while the culture (1 l in mid-log phase) was actively cooled down, so that a constant temperature of approx. 22 °C was maintained. After centrifugation (4,600 rcf, 4 °C, 5 min), the irradiated cells were washed with 20 ml 1 x PBS, transferred in a 50 ml falcon tube and pelleted again (4,600 rcf, 4 °C, 5 min). photoactivatable ribonucleoside-enhanced (PAR-) CRAC is based on the incorporation of 4-thiouridine (4SU) that can be crosslinked to adjacent amino acids by irradiation at 365 nm. For PAR-CRAC, cells of 1 l culture were grown in the presence of 4-thiouracil, which is converted to 4SU by yeast, for 4 h before harvesting in mid-log phase (6,000 rcf, 4 °C, 10 min). After washing with 1 x PBS and resuspending in 1 Vol 1 x PBS, the cell suspension was spread onto a petri dish, which was placed on ice in a Stratalinker 2400 (Stratagene). Cells were then irradiated with 2 x 600 mJ/cm^2 and transferred to a 50 ml falcon tube. Remaining cells in the petri dish were taken up by washing twice with 10 ml of 1 x PBS and transfer to the falcon containing cells pelleted by centrifugation (4,600 rcf, 4 °C, 5 min).
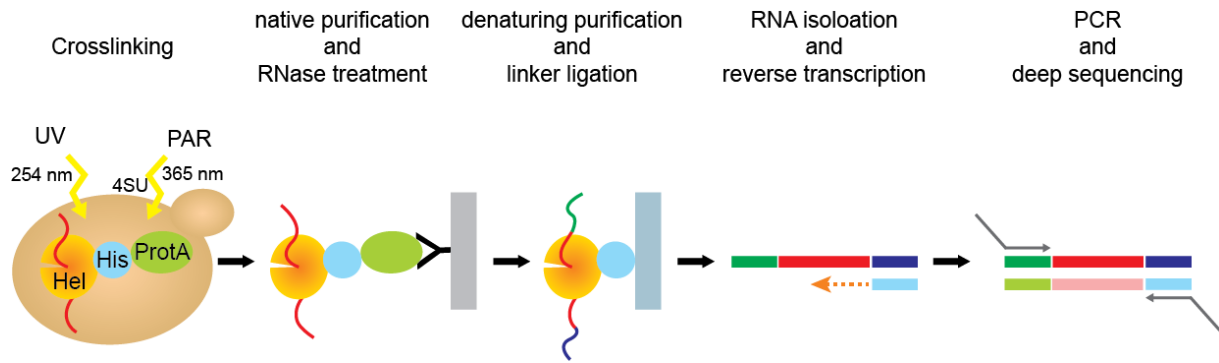
Figure 2.1: UV <u>c</u>rosslinking and <u>a</u>nalysis of <u>c</u>DNA (CRAC). Schematic representation of the (PAR-) CRAC protocol. Yeast cells expressing an RNA helicase (Hel) with a C-terminal His$_6$(His)-TEV cleavage site-ProteinA(ProtA)-tag were grown in the presence of 4-thiouracil, which is converted to 4-thiouridine (4SU) by yeast and incorporated into nascent RNAs, then irradiated at 365 nm (PAR-CRAC), or directly irradiated at 254 nm (*in culturo* UV-CRAC). A purification under native conditions via IgG-sepharose is followed by trimming of RNA sequence not bound, and therefore protected by the protein of interest. A second denaturing purification step via a Ni-NTA matrix is then followed by ligation of linkers. After extraction of the RNA, it is used as a template for reverse transcription and a PCR amplification step, generating a library of cDNA, which can be analysed by Illumina deep sequencing. Modified from Haag *et al.*, 2017.

After cell lysis, both crosslinking methods follow the same protocol, where initially the cell pellet was resuspended in 1 Vol (approx. 2 ml) of TMN150 buffer (50 mM Tris/HCl pH 7.8, 150 mM NaCl, 1.5 mM MgCl$_2$, 0.1 % NP-40, 5 mM ß-mercaptoethanol) containing a protease inhibitor (+ PI; 1 tablet cOmplete Mini protease inhibitor mix in 25 ml TMN150, Roche). Addition of 4 ml of zirconia beads (Thistle Scientific) allowed disruption of cells by vortexing on ice for five minutes. 1.5 Vol (approx. 3 ml) of TMN150+PI buffer were added before the suspension was centrifuged (2,000 rcf, 4 °C, 20 min) and the supernatant was transferred to 1.5 ml reaction tubes. The remaining insoluble cell components were pelleted by high speed centrifugation (20,000 rcf, 4 °C, 20 min). The cleared lysate was incubated with IgG-sepharose (500 µl slurry; GE Healthcare), which had been pre-equilibrated in TMN150, for 2 h at 4 °C with gentle agitation.

The beads were then washed with 10 ml TMN150 (100 rcf, 4 °C, 20 sec), twice with 10 ml TMN1,000 (50 mM Tris/HCl pH 7.8, 1 M NaCl, 1.5 mM MgCl$_2$, 0.1 % NP-40, 5 mM ß-mercaptoethanol) (100 rcf, 4 °C, 20 sec) and twice with 10 ml TMN150 (100 rcf, 4 °C, 20 sec). With 600 µl TMN150 buffer, the beads were transferred to a new 1.5 ml reaction tube, where 10 µl of GST-TEV (glutathione-S-transferase - tobacco etch virus) protease were added to the suspension for incubation overnight at 4 °C.

The supernatant was transferred to a fresh 1.5 ml reaction tube and 0.1 U RNace-IT (Agilent Technologies) was added and samples were incubated for 30 sec at 37 °C. The reaction mix was then transferred into a stopping reagent (6 M guanidinium-HCl, 300 mM NaCl and 10 mM imidazole pH 8.0). For purification of protein-RNA complexes under denaturing conditions, 100 µl of Ni-NTA matrix slurry (Qiagen) was first equilibrated with WB1 buffer (50 mM Tris/HCl pH 7.8, 300 mM NaCl, 10 mM imidazole, 6 M guanidinium-HCl, 0.1 % NP-40, 5 mM ß-

mercaptoethanol) (500 rcf, 4 °C, 20 sec) before incubation with the RNase-treated cell extract for 2 h at 4 °C with gentle agitation. Afterwards, the beads were washed two times with 750 µl WB1, followed by three washing steps with 1 x PNK buffer (50 mM Tris/HCl pH 7.8, 10 mM MgCl$_2$, 0.5 % NP-40, 5 mM ß-mercaptoethanol) (500 rcf, 4 °C, 20 sec). With the last wash, the beads were transferred to a Mobicol spin column (BioRad; 35 nm pore size). Treatment with alkaline phosphatase removes phosphates at 5' and 3' ends that occur as products after cleavage by RNace-IT. For this reason, remaining buffer was removed by centrifugation (500 rcf, 4 °C, 20 sec) and the beads were resuspended in a TSAP-mix (1 x PNK, 8 U thermo sensitive alkaline phosphatase (TSAP; Promega), 80 U RNasin (Promega)) for incubation at 37 °C for 30 min. The beads were then washed once with 400 µl WB1, followed by three washes with 1 x PNK buffer (500 rcf, 4 °C, 20 sec) with centrifugation (500 rcf, 4 °C, 20 sec) between washing steps. For on-bead ligation of a linker to the 3' end of the RNA, a DNA oligonucleotide was used that contained an activated adenosine (App) at the 5' end as well as a blocked 3' end (ddC) to enable a ligation reaction without addition of ATP and prevented inter-linker ligations (see Table 2.10). The beads were resuspended in 80 µl of 3' linker mix (1 x PNK buffer, 1.25 µM CRAC 3' linker, 10 % PEG8000 (Sigma-Aldrich), 60 U RNasin, 800 U T4 RNA ligase II mutant (Epicentre)) and incubated overnight at 16 °C.

The supernatant of the reaction mix was removed by centrifugation (500 rcf, 4 °C, 20 sec) and then the beads were washed once with 400 µl WB1 and three times with 400 µl 1 x PNK. The 5' ends of co-precipitated RNAs were radioactively phosphorylated to enable detection of the protein-RNA complexes by autoradiography in later steps and was achieved by incubating the beads with 80 µl of PNK mix (1 x PNK, 80 U T4 PNK (New England Biolabs), 60 U RNasin, 40 µCi ^{32}P-γ-ATP) for 40 min at 37 °C. After addition of 1.25 µM Li-ATP (Roche), the reaction was incubated for further 20 min at 37 °C. The beads were again washed with 400 µl WB1 and three times with 400 µl 1 x PNK buffer, centrifuging 500 rcf, 4 °C, 20 sec) in between each washing step. For ligation to the 5' linker, the beads were resuspended in 80 µl of 5' linker-mix (1 x PNK, 1.25 µM CRAC 5' linker, 1 mM ATP (Roche), 60 U RNasin, 40 U T4 single-strand RNA ligase I (New England Biolabs)) and incubated at 16 °C overnight. The CRAC 5' linker is a DNA-RNA hybrid, which contained an inverted ddT at the 5' end that blocks multimerisation of the oligonucleotide, and additionally five nucleotides of randomised sequence that allows bioinformatic identification of PCR artefacts after sequencing (see Table 2.10). Following the ligation reaction, the beads were washed three times with 400 µl WB2 buffer (50 mM Tris/HCl pH 7.8, 50 mM NaCl, 10 mM imidazole pH 8, 0.1 % NP-40, 5 mM ß-mercaptoethanol) before 200 µl of Elution buffer (50 mM Tris/HCl pH 7.8, 50 mM NaCl, 150 mM imidazole pH 8, 0.1 % NP-40, 5 mM ß-mercaptoethanol) were added for 5 min. The eluate was collected by centrifugation into a fresh tube and this elution step was repeated once, giving a final elution volume of 400 µl. The eluate was supplemented with 2 µg of bovine serum albumin (BSA),

20 µg of glycogen and trichloroacetic acid (TCA) was added to a final concentration of 20 %. Samples were vortexed and incubated on ice for 30 min before protein-RNA precipitates were pelleted by centrifugation (20,000 rcf, 4 °C, 30 min). The pellet was washed with 500 µl of 100 % acetone (20,000 rcf, 4 °C, 20 min) and air-dried for at least 5 min before resuspension in 30 µl of 1 x NuPAGE buffer, containing 50 mM DTT (Invitrogen).

The resulting protein-RNA-complexes were resolved on a 4 – 12 % Bis-Tris NuPAGE gradient gel (Invitrogen) by electrophoresis for 1.5 h at 100 V. Complexes were transferred onto a Hybond C nitrocellulose membrane (GE Healthcare) for 2 h at 80 V and 4 °C and subsequently visualised by exposure of the membrane to an x-ray Hyperscreen (GE Healthcare) for up to 16 h at -80 °C. Membrane areas containing radioactive signal, corresponding to the expected protein-RNA-complex size, were excised and subjected to proteinase K digestion to elute the bound RNA. For this, 400 µl WB2 (containing 1 % SDS, 5 mM EDTA) and 6.5 µl commercial proteinase K (Roche) was added and the reaction mix was incubated overnight at 55 °C. For RNA precipitation, 50 µl 3 M sodium acetate pH 5.2 and 500 µl PCI were added, the reaction tube was inverted and phases separated by centrifugation (20,000 rcf, 4 °C, 5 min). The aqueous phase was transferred to a fresh 1.5 ml reaction tube, supplemented with 1 ml of 100 % ethanol and 20 µg of glycogen, and incubated overnight at -20 °C.

Table 2.10: Oligonucleotides used during application of the CRAC method. The CRAC 5' linker contains an inverted dideoxythymine at the 5' end to prevent formation of concatemers, as well as five random nucleotides (N5) at the 3' end, which allows collapsing of PCR amplified cDNAs. The CRAC 3' linker ends with a dideoxycytosine at 3' and is preadenylated at the 5' end to enable ligation reactions in the absence of ATP. In order to be able to multiplex different CRAC samples in a single lane for deep sequencing, four FW CRAC oligonucleotides are listed, which differ in six internal alternative sequences (underlined).

Name	Sequence (5' to 3')
CRAC 5' linker	InvddGTTCAGAGTTCTACAGTCCGACGATCNNNNNAGC
CRAC 3' linker	rAppTGGAATTCTCGGGTGCCAAGGddC
CRAC RT	GCCTTGGCACCCGAGAATTCCA
RPI5	CAAGCAGAAGACGGCATACGAGAT<u>CACTGT</u>GTGACTGGAGTTCCTTGGCACCCGAGAATTCCA
RPI6	CAAGCAGAAGACGGCATACGAGAT<u>ATTGGC</u>GTGACTGGAGTTCCTTGGCACCCGAGAATTCCA
RPI12	CAAGCAGAAGACGGCATACGAGAT<u>TACAAG</u>GTGACTGGAGTTCCTTGGCACCCGAGAATTCCA
RPI19	CAAGCAGAAGACGGCATACGAGAT<u>TTTCAC</u>GTGACTGGAGTTCCTTGGCACCCGAGAATTCCA
RP1	AATGATACGGCGACCACCGAGATCTACACGTTCAGAGTTCTACAGTCCGA

Precipitated RNA was pelleted by centrifugation (20,000 rcf, 4 °C, 30 min), washed with 500 µl 70 % ethanol, pelleted again by centrifugation (20,000 rcf, 4 °C, 30 min) and air-dried. The RNA pellet was then resuspended in 13 µl of RT-mix, containing 1 µl CRAC RT oligonucleotide (sequence is a reverse complement sequence to the 3' linker sequence; Table 2.10) and 2 µl of 5 mM dNTP Mix (Roche). To anneal the primer to the RNA template, the mixture was heated at 80 °C for 3 min and subsequently incubated on ice for 5 min. 6 µl of Extension buffer (4 µl

5 x first-strand buffer (Invitrogen), 1 µl 100 mM DTT, 1 µl 40 U/µl RNasin) were added and incubated at 50 °C for 3 min. 1 µl SuperScript III reverse transcriptase (Invitrogen) was then added to initiate the transcription reaction, which was allowed to proceed for 1 h at 50 °C. The reaction was terminated by incubating the reaction mix at 65 °C for 15 min and the template RNA was digested by the addition of 2 µl of RNase H (New England Biolabs) and incubation for another 30 min at 37 °C.

1 µl of cDNA was subjected to amplification by PCR using 0.2 µM oligonucleotides binding in the 5' and 3' linker regions (Table 2.10), 1 x LA Taq buffer + MgCl$_2$, 2.5 U LA TakaRa Taq polymerase (Takara Bio Inc.) and 125 µM dNTPs. PCR products from three individual 50 µl reaction mixes were pooled and supplemented with 30 µl 3 M sodium acetate pH 5.2, followed by a PCI treatment as described previously (section 2.9.) and precipitation overnight in 3 Vol 100 % ethanol at -20 °C.

Precipitated DNA was pelleted by centrifugation (20,000 rcf, 4 °C, 30 min), washed with 500 µl 70 % ethanol and after another round of centrifugation (20,000 rcf, 4 °C, 20 min), the DNA was air-dried and resuspended in 20 µl Gel pilot Loading Dye (Qiagen). Products were separated on a 3 % Metaphore agarose gel (Lonza) in 1 x TBE and fragments with lengths between 150 and 400 bps were excised and eluted from the gel using the Qiagen MINIelute kit. The DNA concentration of the eluates was estimated using the Qubit quantification system (Invitrogen) and cDNA libraries were sent for single-end deep sequencing (Illumina).

2.14 Bioinformatic analysis of sequencing data

A sequence read obtained by Illumina deep sequencing of a CRAC sample consists of 50 nucleotides, including a random barcode at the 5' end to identify reads amplified from the same template RNAs, followed by AGC, then the sequence of the purified RNA and, potentially, nucleotides of the 3' linker. For data analysis, software packages from the pyCRAC software suite (Webb *et al.*, 2014) and self-written python 2.7 scripts available in the Bohnsack group or developed in the context of this work were used. In a first step, the barcode sequences were identified by pyBarcodeFilter and sequences containing identical barcode sequences were regarded as PCR artefacts and collapsed to a single read by pyDuplicateRemover. Remaining reads were quality checked using the quality score assigned to each individual nucleotide during the sequencing reaction. Using Flexbar 2.7, reads were trimmed such that the overall read reaches a certain quality threshold. This software also removed remaining 3' linker nucleotides and all reads that were subsequently shorter than 18 nucleotides were discarded from further analysis.

After fulfilling the above-mentioned criteria, the sequence reads were mapped onto the yeast genome (Saccharomyces_cerevisiae.EF2.59.1.0). During the PAR-CRAC protocol, specific T

to C mutations are introduced at sites of protein-RNA crosslinking. Therefore, the Bowtie 1.1.2 software was used for alignment of sequence reads with the genome as this allows single mismatches to be selected for and a self-written python 2.7 script was used to extract reads containing T to C mutations. For *in culturo* UV-CRAC, the Bowtie 2.2.6 aligner was used to align sequence reads with zero, one or more mismatches to the genome, allowing for deletions and substitutions in the sequence reads. Further scripts from the pyCRAC package (pyReadCounters, pyPileup, pyReadAligner) and self-written python 2.7 scripts created "hit tables" showing read distributions between different RNAs or overviews reflecting the quality of the sequencing data.

In order to visualise the read distribution of RNA helicase CRAC data on ribosomal RNA, using python 2.7 scripts, the data was plotted over the primary sequence of *RDN37*, the gene locus of ribosomal RNA. Furthermore, the data was also mapped onto the secondary structures of the ribosomal RNAs (Petrov *et al.*, 2014a; http://apollo.chemistry.gatech.edu/RibosomeGallery) as well as onto available 3D structure of yeast pre-60S particles (Wu *et al.*, 2016; PDB entry: 3JCT) or mature yeast ribosomal subunits (Ben-Shem *et al.*, 2011; PDB entry: 4V88).

Identification of chimeric reads consisting of two distinct RNA sequences bound to the protein of interest was done using the Hyb-pipeline (Travis *et al.*, 2014). This analysis is analogous to the CLASH analysis (Crosslinking, ligation and sequencing of hybrids) developed in the Kudla lab. In brief, the CRAC data was first filtered using parameters like barcode and adapter removal, quality control and short read length as described above, before the remaining reads were mapped onto the yeast genome and reads containing two different RNA sequences, which are separated by more than four nucleotides, were selected. The pipeline also included a clustering of resulting hybrids, which allowed mapping of frequently occurring snoRNA-rRNA hybrids on the rRNA secondary structure.

2.15   Purification of pre-ribosomal complexes

To purify pre-LSU particles, yeast strains genomically expressing C-terminally TAP- or HTP-tagged *trans*-acting ribosome biogenesis factors were used. These factors served as bait proteins for affinity chromatography under native conditions using IgG-sepharose. 500 ml of mid-log phase yeast cells were harvested (6,000 rcf, 4 °C, 10 min), washed with 20 ml 1 x PBS (2,000 rcf, 4 °C, 5 min) and resuspended in 1 Vol TMN150+PI buffer. Cells were disrupted by grinding in liquid nitrogen and, after samples were thawed on ice, the lysate was cleared by centrifugation (20,000 rcf, 4 °C, 30 min). 400 µl of IgG-sepharose slurry were equilibrated in TMN150 buffer (100 rcf, 4 °C, 20 sec), the cleared lysate was added and incubated with the beads for 3 h at 4 °C with gentle agitation. Four washes with 2 ml TMN150 buffer (100 rcf, 4 °C, 20 sec) were performed to provide specificity to the immunoprecipitation. RNA that co-

purified with the bait proteins was eluted from beads using the RNA extraction protocol (section 2.9) and was analysed by northern blotting (section 2.10). To verify the presence of particular proteins in the pre-ribosomal complexes, the IgG-beads were resuspended in 600 µl TMN150 buffer and 5 µl of GST-TEV protease was added for incubation overnight at 4 °C while rotating. The reaction mix was then transferred to a Mobicol spin column (BioRad, 35 nm pore size), and the supernatant was retrieved from the beads. The supernatant was transferred to 100 µl glutathione sepharose slurry (GE Healthcare), which has been pre-equilibrated in TMN150 buffer, and incubated at 4 °C for 1 h with gentle agitation. Once more, the Mobicol spin columns were used to separate the supernatant from GST beads. Proteins in the supernatant were subjected to TCA precipitation as previously described (section 2.15) and were separated by SDS-PAGE followed by western blotting using epitope- or protein-specific antibodies.

2.16   DMS structure probing

The method of structure probing using the chemical dimethyl sulfate (DMS) was adapted from Swiatkowska *et al*. (2012). In general, it is a used to identify structural alterations of RNAs in the absence or presence of as associated protein or its catalytically inactive mutant. In each case, 500 ml of yeast culture was grown under permissive or non-permissive conditions to reach an OD_{600} of approx. 0.8 in the determined depletion time. In addition to the genomically integrated repressible promoter in front of the RNA helicases (Has1, Spb4 and Mak5), the yeast strains used in this experiment expressed a C-terminal HTP-tagged version of Nop2 from its genomic locus. Nop2 is a *trans*-acting ribosome biogenesis factor that acts at a similar stage of pre-60S maturation as the investigated RNA helicases and allows purification of pre-ribosomal complexes containing these helicases. In order to purify pre-ribosomes, cell lysates were subjected to pull-downs using IgG-sepharose like previously described (section 2.15), but with the difference that instead of elution, beads carrying immobilized pre-ribosomal complexes were subjected to three washes with 2 ml of TMN150 buffer (100 rcf, 4 °C, 20 sec). The last washing step was used to split the beads in half and into fresh 15 ml falcon tubes. Both sets of beads were resuspended in 1 ml of TMN150 before 0.5 % DMS (final concentration) was added to one sample for 2 min at RT while shaking. The methylation reaction was quenched by the addition of 1 ml quenching solution containing 0.5 M ß-mercaptoethanol and 1.5 M sodium acetate pH 5.2. After centrifugation (100 rcf, 4 °C, 1 min), the supernatant was removed and co-precipitated RNA was extracted by the previously described RNA extraction protocol (section 2.9).

Primer extension was used to detected methylated nucleotides and this for, DNA oligonucleotides (Table 2.11) were radiolabelled with ^{32}P-γ-ATP by incubation of 2 µl 10 mM oligonucleotide, 2 µl ^{32}P-γ-ATP (Perkin-Elmer), 2 µl T4 PNK buffer A and 1 µl T4 PNK (both Fermentas) in a 20 µl reaction at 37 °C for 45 min. After the phosphorylation reaction, 80 µl

MQ-H_2O were added to dilute the labelled primer. Annealing was achieved by mixing 1 µl radiolabelled oligonucleotide with 500 ng of co-purified RNA (for sequencing ladder 2 µg of total RNA) in a total volume of 8 µl. Reactions were incubated at 85 °C for 3 min and then cooled down slowly to 50 °C in the thermoblock. Extension was carried out by addition of 4.5 µl Extension buffer (2.5 µl 5 x first-strand buffer, 0.4 µl 0.1 M DTT (Invitrogen), 0.3 µl RiboLock (ThermoFisher Scientific), 0.3 µl SuperScript III reverse transcriptase, 0.5 mM dNTPs, 0.5 µl MQ-H_2O) and incubation at 50 °C for 50 min. In order to create a sequencing ladder, four primer extension reactions were set up and supplemented with 1 µl 2 mM ddCTP, ddATP, ddTTP or ddGTP respectively. An incubation step at 85 °C for 5 min inactivated the polymerase and stopped the extension reaction. After cooling the samples on ice, the cDNA was precipitated overnight by adding H_2O to a final volume of 50 µl as well as 2.5 µl 3 M sodium acetate, 1 µl glycogen and 150 µl 100 % ethanol. Samples were the incubated at -20 °C overnight.

Table 2.11: Oligonucleotides used for structure probing experiments.

Name	Sequence (5' to 3')	Application
25S_1171	GAGCGTGTATTCCGGCACC	Structure probing - Mak5
25S_1979	GCAGTCCACAAGCACGCCCGC	Structure probing - Spb4
25S_3377	CAAATCAGACAACAAAGGC	Structure probing - Spb4

Centrifugation (20,000 rcf, 4 °C, 30 min) pelleted the precipitated nucleic acids, and the pellet was washed with 200 µl 70 % ethanol, followed by another centrifugation (20,000 rcf, 4 °C, 20 min). Following the removal of the supernatant, the pellet was air-dried carefully and resuspended in 10 µl formamide loading dye at 50 °C shaking at 750 rpm in an Eppendorf thermoblock. Prior to loading onto a denaturing (7 M urea), 10 % polyacrylamide sequencing gel in 1 x TBE, samples were heated at 95 °C for 5 min. Products were separated for 2 h at 60 W, then the gel was dried on a gel-drier for 3 h and exposed to an phosphorimager screen. Radioactive signals were then detected using the Typhoon FLA 9500 phosphorimager.

2.17   Sucrose density gradients

To separate (pre-)ribosomal complexes according to their sedimentation coefficient, yeast cell lysate was subjected to sucrose density gradient centrifugation. 100 ml of mid-log phase yeast cells were pelleted (2,000 rcf, RT, 10 min) and resuspended in 1.5 Vol Extract buffer (50 mM Tris/HCl pH 7.4, 100 mM NaCl, 5 mM $MgCl_2$, 1 mM DTT). Cells were disrupted in liquid nitrogen using a pestle and mortar. After the powder was thawed on ice, the sample was transferred to a 1.5 ml reaction tube, which centrifuged (20,000 rcf, 4 °C, 30 min) to clear the lysate. The cleared lysate was transferred into a fresh reaction tube and stored on ice until loading onto gradients.

6 ml of Extract buffer containing 45 % sucrose was layered below 6 ml of Extract buffer with 10 % sucrose in a 12 ml Sw40Ti gradient tube. To generate a 10 – 45 % sucrose gradient the GradientMaster system (Biocomp) and the "short sucrose 10 – 45 %" setting (rotation time: 1 min 25 sec, angle: 82.0 °, speed: 19) programme was used. The gradient was incubated at 4 °C for 1 h before 300 µl from the top of the gradient were removed and the same volume of cleared lysate was carefully loaded onto the top of the gradient. A 10 % (= 30 µl) sample of cleared lysate were retained to serve as an input control.

Centrifugation of the gradient was carried out for 16 h at 23,500 rpm and 4 °C (Beckman L7-80 centrifuge) using a Sw40Ti rotor. After centrifugation, 23 fractions of approx. 530 µl volume each were taken using a fraction collector (BioRad). The fraction collector measures the RNA concentration at 254 nm, enabling a profile of the collected fractions to be generated.

2.18 Quantitative PCR for analysing snoRNA levels on pre-ribosomes

To monitor snoRNA levels of pre-ribosomal complexes upon depletion of a particular helicase, a method combining sucrose density centrifugation and quantitative PCR (qPCR) was used (see Fig. 2.2). This method was performed as described in Bohnsack *et al.*, 2008, with the help of Roman Martin. Depletion of the RNA helicases Has1, Spb4 or Mak5 was achieved using yeast strains in which they were expressed under the control of a tetracycline repressible promoter and as a control, a yeast strain was used, which harbors only the tetracycline repressor gene. Cells were grown to mid-log phase in the estimated depletion time, harvested by centrifugation (6,000 rcf, 4 °C, 10 min) and resuspended in 1 Vol of Lysis buffer (50 mM Tris/HCl pH 7.5, 100 mM NaCl, 5 mM $MgCl_2$, 1 mM DTT, 5 mM vanadyl ribonucleoside complexes (VRC; New England Biolabs), 1 tablet cOmplete Mini protease inhibitor mix (Roche) per 10 ml buffer). Disruption of cells was accomplished by grinding in liquid nitrogen. After the sample was thawed on ice, the lysate was cleared by centrifugation (20,000 rcf, 4 °C, 12 min) and the supernatant was loaded on a 10 – 45 % sucrose gradient as previously described in section 2.17.

After RNA extraction from all collected gradient fractions (section 2.9), fractions which contained free (low sedimentation coefficient) or pre-ribosome bound (high sedimentation coefficient) snoRNAs were pooled. For polyadenylation, 5 – 10 µg total RNA were incubated with 8 U poly(A) polymerase (Life Technologies), 2.5 mM $MnCl_2$ and 5 mM (free snoRNAs) or 2.5 mM (pre-ribosome bound snoRNAs) ATP (Roche) for 2 h at 37 °C. Using the MirVana miRNA isolation kit (Life Technologies) polyadenylated RNAs were purified and eluted in a volume of 40 µl of H_2O. Subsequently, reverse transcription was initiated by annealing 12.5 µg (free snoRNAs) or 7.5 µg (pre-ribosome bound snoRNAs) of poly-dT oligonucleotide to the eluted RNA samples by heating at 65 °C for 10 min and then incubating for 5 min on ice).

Extension Mix (2.5 µl RNasin, 1,000 U Superscript III reverse transcriptase, 1 x first-strand buffer, 1 mM dNTPs, 5 mM DTT) was added in a total volume of 100 µl, and samples were incubated at 50 °C for 1 h. The extension reaction was stopped by heat inactivation at 70 °C for 15 min. The template RNA was afterwards degraded by incubation with 25 U RNase H and 10 U RNase A (New England Biolabs) for 2 h at 37 °C. 20 min at 65 °C denatured the degrading enzymes and the resulting cDNA was purified using the QIAquick PCR purification kit (Qiagen).
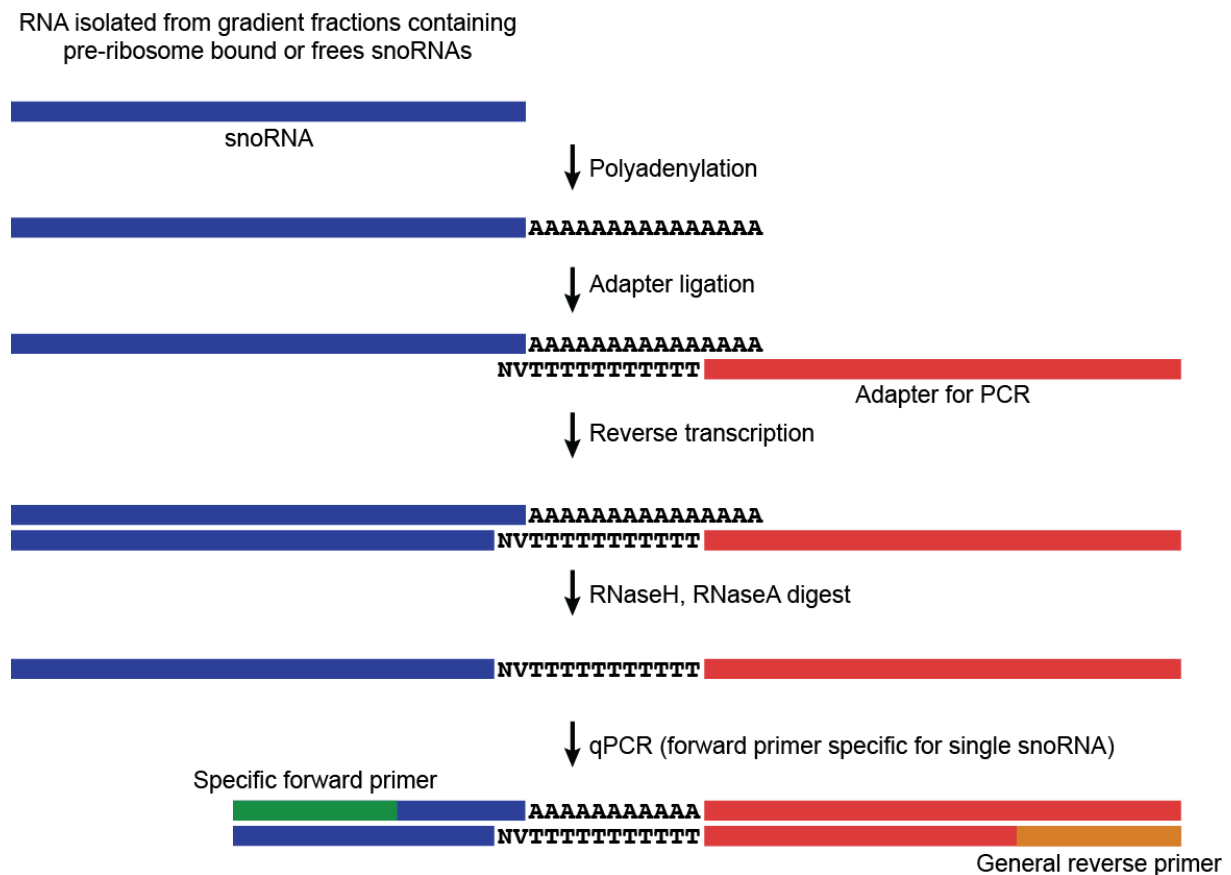
Figure 2.2: Schematic representation of the qPCR approach to quantify snoRNA levels. SnoRNAs that are either pre-ribosome bound or in the free pool of snoRNAs are first separated by sucrose density centrifugation. After isolation of RNAs from corresponding gradient fractions, they are polyadenylated in order to allow adapter ligation and subsequent reverse transcription from an oligo-d(T) primer. Template RNA is digested and the remaining cDNA provides template material for quantitative PCR using a snoRNA-specific forward and a general reverse oligonucleotide. Modified from Bohnsack *et al.*, 2008.

A common reverse, and a snoRNA-specific forward, oligonucleotide (see Bohnsack et al., 2008) allowed determination of the relative level of 75 known yeast snoRNAs in parallel using qPCR, which was performed in a Mx3000P qPCR machine (Agilent Technologies). Data analysis was performed according to Bohnsack *et al.*, 2008, following the ddCt-method using self-written python 2.7 scripts. Individual cycle threshold (Ct) values for each snoRNA were normalized to the median of all 75 Ct values of surveyed snoRNAs and to the Ct value of the control sample. This enable the ratio of pre-ribosome bound:free snoRNA to be calculated.

3 Results

3.1 Depletion of Has1, Spb4 or Mak5 leads to pre-rRNA processing defects

In yeast, there are 21 RNA helicases proposed so far to be involved in ribosome biogenesis. Ten of them act in the maturation of the large ribosomal subunit, eight in small subunit biogenesis and three are involved in the maturation of both subunits. Along the pathway of ribosome biogenesis, *trans*-acting factors, such as RNA helicases, are proposed to accomplish irreversible steps promoting directionality of this process and preventing kinetic trapping of pre-mature particles. Has1, Mak5 and Spb4 are three RNA helicases that are suggested to function at relatively late nuclear steps in the maturation of large ribosomal subunits. Has1 was reported to be localised in the nucleolus, where the DEAD-box protein carries out essential functions in both SSU and LSU biogenesis, concomitant with delayed pre-rRNA processing detected by pulse-chase experiments and sedimentation of Has1 with high-molecular-weight complexes in sucrose gradients (Emery *et al*., 2004). The DEAD-box protein Spb4 was shown to be essential for cell viability (Sachs and Davis, 1990) and was initially identified as a suppressor of the thermosensitive phenotype of a polyA-binding protein mutant (suppressor of polyA-binding protein; Sachs and Davis, 1989). Cold-sensitive mutations in *SPB4* revealed decreased levels of LSU and reduced synthesis of 25S rRNA, which indicated an involvement of the protein in LSU biogenesis (Sachs and Davis, 1989, 1990). The *MAK5* gene was identified as one of thirty *MAK* genes (maintenance of killer) that were reported to be required for propagation of the dsRNA virus M1 (Ohtake and Wickner, 1995). However, the Mak5 protein, containing the classical DEAD-box helicase motifs as well, was shown to be an essential nucleolar protein. Depletion of Mak5 caused reduction of LSUs, half-mer polysome formation and a delay in 25S as well as 5.8S rRNA production, indicating its role in LSU biogenesis (Zagulski *et al*., 2003).

Deletion/depletion experiments are a method that can be used to investigate the requirement of proteins for particular cellular processes, such as the maturation of ribosomal subunits. Analysis of pre-rRNA processing by northern blotting allows the accumulation or reduction of pre-rRNA intermediates to be detected, which can be used to monitor defects in subunit assembly. Because these three RNA helicases, which all belong to the family of DEAD-box proteins, are essential proteins, the generation of deletion strains was not possible. In order to analyse defects in ribosome biogenesis caused by the lack of any of these proteins, depletion cassettes were genomically integrated upstream the desired open reading frames. Besides the selection marker, this cassette contained a repressible promoter. *HAS1* and *MAK5* were placed under a tetracycline-repressible promoter (pTetO$_7$), which necessitated the presence of a plasmid-encoded repressor (TetR). In contrast, *SPB4* was placed under the control of a

pGal$_1$ promoter, which could be repressed by the exchange of carbon source from galactose to glucose. Additionally, the cassette encoded a 3xHA-tag expressed at the amino-terminal end of the protein, making it possible to detect the helicase by western blotting.

The optimum time that yeast strains should be grown under restrictive conditions needed to be determined for each protein as the stability of mRNAs varies, as does the half-life of different proteins. Furthermore, if cells are grown too long in the absence of essential proteins, secondary effects can be observed. The time taken for Has1, Mak5 and Spb4 to become limiting was first determined by investigating growth; upon repression, the decreased protein levels over time lead to cell death and growth retardation, which can be monitored by measuring the optical density of yeast cultures at 600 nm (OD$_{600}$). The OD$_{600}$ of exponential phase cultures was measured before initiation of repression and then over a time-course, where the obtained values were compared to untreated control samples. The time point at which the growth rates of depletion and control cultures diverged, was estimated as the depletion time. For Has1, the depletion time was 7 h, whereas Mak5 and Spb4 showed longer depletion times with 10 h and 12 h respectively. To demonstrate the specific reduction of the desired protein(s) at this time, cells were harvested and extracted proteins were subjected to a western blot using antibodies against the HA-tag and the cytoplasmic protein Pgk1, as a loading control. This showed that the levels of each of the RNA helicases was specifically reduced in the non-permissive medium at the estimated depletion time, demonstrating the loss of each of these proteins in cultures under repressive conditions (Fig. 3.1).
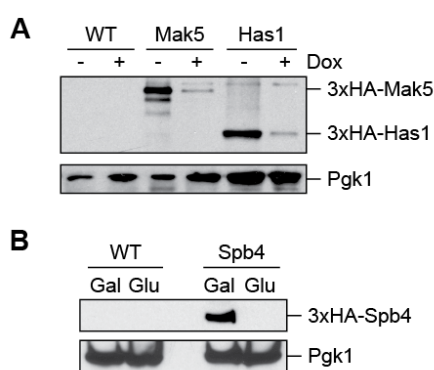
Figure 3.1: Establishment of depletion conditions for Mak5, Has1 and Spb4. Yeast strains were generated in which the genes coding for the RNA helicases Has1, Mak5 or Spb4 were under the control of a repressible promoter, which additionally introduced a 3xHA-epitope at the N-terminus of each protein. **(A)** Transcription of *MAK5* (pTetO$_7$-*MAK5*) and *HAS1* (pTetO$_7$-*HAS1*) was repressed by the addition of 10 µg/ml doxycycline (Dox) for 10 and 7 h respectively. After reaching the depletion time, proteins were extracted from normalised amounts of cells. Extracted proteins were subjected to western blotting using antibodies against the HA-epitopes or endogenous Pgk1. **(B)** Yeast cultures expressing Spb4 from a pGal$_1$-promoter (pGal$_1$-*SPB4*) were grown for 12 h in galactose (Gal) or glucose (Glu) containing medium for checking protein depletion and protein samples were analysed by western blotting as in (A).

Having established an appropriate depletion time for Has1, Spb4 and Mak5, defects in ribosome biogenesis could be visualised by the detection of mature rRNA and pre-rRNA processing intermediates within yeast cultures, when the protein of interest was limiting. To achieve this, exponentially growing cells of each of the yeast strains were grown in permissive and non-permissive conditions and total RNA was extracted after the culture had reached its depletion time. These RNAs were subjected to denaturing agarose gel electrophoresis in order to separate RNA according to its length, and this was followed by northern blotting. Mature

rRNAs were visualised by methylene blue staining, whereas radioactively labelled probes hybridising to the ITS1 or ITS2 regions of the pre-rRNAs (Fig. 3.2A) enabled changes in the levels of pre-rRNA intermediates between depletion and control samples to be detected.
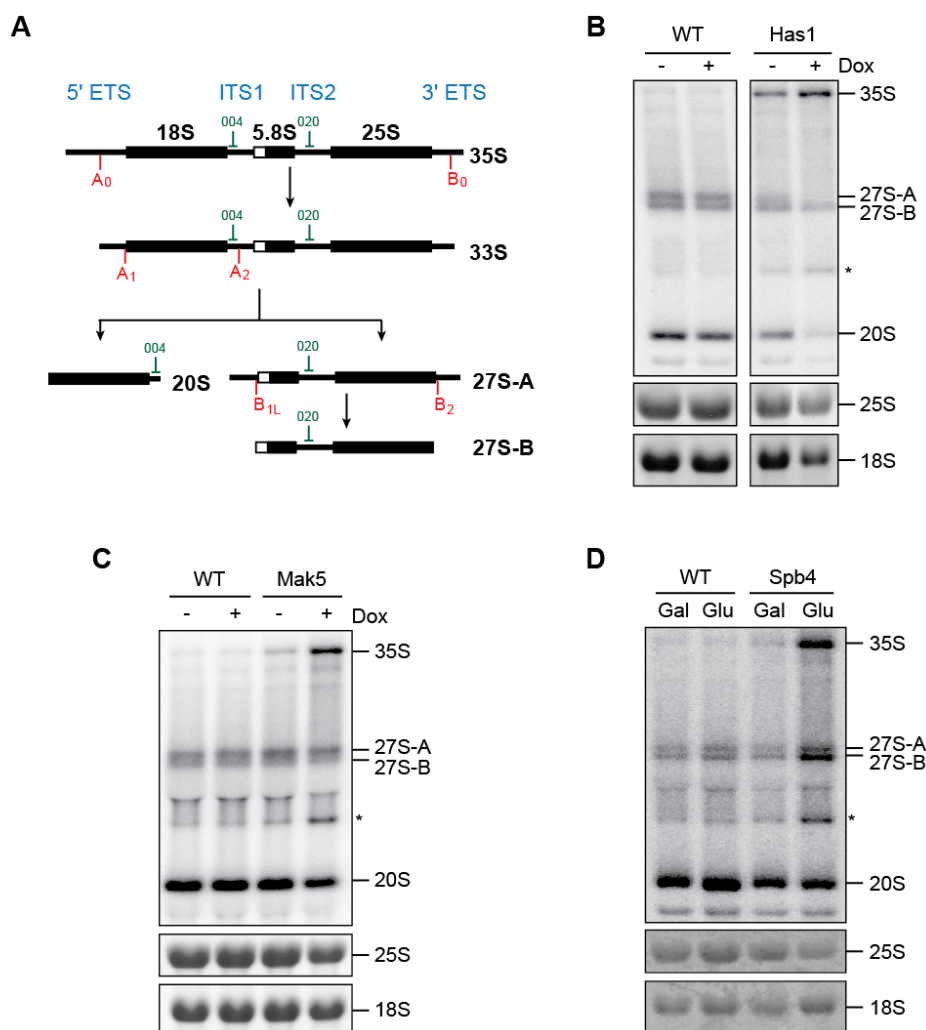
Figure 3.2: Depletion of Has1, Spb4 or Mak5 causes defects in pre-rRNA processing. (A) Simplified pre-rRNA processing scheme with generally occurring processing intermediates, including spacer regions (blue) and mature rRNAs (black). Binding sites of radioactively labelled probes are shown in green. Sites of relevant endonucleolytic cleavage events are shown in red. **(B-D)** The pTetO$_7$-Has1 **(B)** and pTetO$_7$-Mak5 **(C)** and pGal$_1$-Spb4 **(D)** yeast strains were grown in exponential phase under permissive (-Dox or Gal) and restrictive (+ Dox or Glu) conditions for the appropriate depletion time for each protein. Total RNA was extracted and subjected to denaturing agarose gel electrophoresis for subsequent northern blotting. After transfer of RNAs to a nylon membrane, mature rRNAs were visualised by methylene blue staining. Pre-rRNA processing intermediates were detected using radioactively labelled probes against sequences in ITS1 (004) and ITS2 (020). Asterisks mark an aberrant 23S pre-rRNA species.

Upon depletion of any of the three RNA helicases, the mature 25S rRNA levels decreased, but to variable extents depending on which of the three investigated proteins was lacking (Fig. 3.2B-D). The strongest effect was observed for Has1, where depletion of the protein caused a strong reduction of both the 25S and 18S rRNAs as well as concomitant accumulation of the initial 35S pre-rRNA and decreases in the levels of the 27S-A and 20S pre-rRNAs (Fig. 3.2B). These observations are in line with the requirement of Has1 for the maturation pathways of

both ribosomal subunits and suggests that Has1 is required for the processing of the 35S pre-rRNA to early downstream intermediates for both the SSU and LSU. Depletion of Spb4 resulted in a decrease of 25S, but not 18S rRNA, consistent with a role in LSU biogenesis. Furthermore, accumulation of 27S rRNA precursors, especially 27S-B, was observed as well as a visible increase of the 35S pre-rRNA levels (Fig. 3.2C). This suggests that Spb4 acts in the later stages of LSU assembly when the 27S pre-rRNAs are processed, with the accumulation of the 35S pre-rRNA likely caused by a feedback mechanism. This result is in line with previous pulse-chase labelling experiments (de la Cruz *et al*., 1998) and pull-down analyses, which suggested that although Spb4 may bind to early 90S pre-ribosomal particles, it dissociates late from pre-60S complexes after processing of 27S-B pre-rRNA (Garcia-Gomez *et al*., 2011). Similarly, the depletion of Mak5 caused a reduction in the level of the mature 25S rRNA, accumulation of the 35S pre-rRNA and a decrease in the level of the 27S-B intermediate (Fig. 3.2D). In summary, for all three investigated RNA helicases their requirement for biogenesis of the large ribosomal subunit could be confirmed by the observation of pre-rRNA processing defects in the absence of each of the proteins. However, the changes in the levels of pre-rRNA observed upon depletion of each of the helicases, suggests that they are required at slightly different stages of LSU biogenesis, with Has1 likely acting earliest and Spb4 latest.

3.2 The RNA helicases Has1, Spb4 and Mak5 crosslink at distinct sites in the rRNA sequences

Functional characterisation of ribosome biogenesis factors like RNA helicases is often impeded by a lack of information about their binding sites on pre-ribosomal complexes, as this provides evidence on the targets of their remodelling activity. For this reason, after demonstrating the requirement of Has1, Mak5 and Spb4 for the biogenesis of ribosomal subunits, these proteins were subjected to <u>c</u>rosslinking and <u>a</u>nalysis of <u>c</u>DNA (CRAC) in order to identify their RNA binding sites (see Bohnsack *et al*., 2012). This approach is based on the introduction of covalent bonds between the protein of interest and its associated RNAs by applying high-energy light. For this, yeast strains were generated expressing either Has1, Mak5 or Spb4 with a tri-partite tag (His$_6$-TEV protease cleavage site-Protein A; HTP), fused to the carboxyl-terminal end of each RNA helicases so that the proteins could be purified with their bound RNAs stepwise under native and denaturing conditions. Two alternative variants of the CRAC methodology were applied (UV-CRAC and PAR-CRAC), which mainly differ in the crosslinking approach used. For UV-CRAC, *in culturo* crosslinking using UV radiation at 254 nm was applied to actively growing yeast cells. In order to perform PAR-CRAC, yeast cells were grown for several hours in the presence of 4-thiouracil, which is converted to the nucleoside analogue 4-thiouridine (4SU) so that this could be incorporated into nascent RNA transcripts before harvesting the cells. Resuspended cells were subsequently spread onto a

petri dish and *in vivo* irradiated on ice using light at 365 nm. Afterwards, samples from both methods were handled in the same way, starting with a native purification of helicase-RNA complexes via the ProteinA-tag using IgG-sepharose. Following specific proteolytic TEV cleavage of protein-RNA complexes, RNA not directly bound by the helicase was trimmed by mild RNase treatment, resulting in a protein footprint on the RNA. Denaturing purification of complexes by Ni-NTA chromatography then ensured that only covalently bound RNAs were subjected to subsequent adapter ligation and cDNA library preparation. After 3' linker ligation, co-purified RNAs were 5' end labelled using ^{32}P, a 5' linker was ligated and protein-RNA complexes were separated by polyacrylamide gel electrophoresis and transferred to a nitrocellulose membrane.

Autoradiography revealed RNAs specifically crosslinked to all three RNA helicases in the PAR-CRAC approach, whereas RNAs were only detected as bound to Spb4 in the UV-CRAC samples. The areas of the membrane containing specific signals, and the corresponding regions from the lane containing the WT samples, were excised. Following protein digestion and RNA isolation, the adapters were used for reverse transcription and PCR to generate a cDNA library, which was subjected to Illumina deep sequencing.

The obtained sequence reads, which correspond to RNA molecules co-purified with the RNA helicase, were checked bioinformatically according to several parameters, such as read quality and read length after adapter removal. Afterwards, the remaining reads were aligned to the yeast genome. For UV-CRAC experiments, none or only a single mismatch (deletion or substitution) was allowed during the mapping. Such mutations often arise from errors during elongation of the polymerase at crosslinking sites. At these sites, residual amino acids were still attached to the RNA after protein digestion and caused polymerase skipping or misincorporation of nucleotides. In contrast, reads of PAR-CRAC were obliged to contain a specific thymine to cytosine conversion, because, due to the increased hydrogen-bonding capacity of 4SU compared to uracil, this is complemented by guanine instead of an adenine during reverse transcription. Alignment of reads to annotated yeast genomic features allowed identification of the transcripts classes bound by each of the proteins (Fig. 3.3).

In comparison to control samples, which were WT yeast cells that were devoid of an HTP-tag, all investigated RNA helicases showed an enrichment of sequences that map to rRNA, which is in line with their role in ribosome biogenesis (Fig. 3.3). To determine where these proteins crosslinked within the rRNA sequences, we focused on the sequence reads that were mapped onto *RDN37*, the gene locus of a single rDNA repeat. In order to directly compare the different CRAC experiments, the determined number of reads at each nucleotide was normalised to the total number of mapped reads per million. For visualisation, the resulting values were plotted on the primary sequence of *RDN37* corresponding to the 35S primary transcript containing the mature 18S, 5.8S and 25S rRNAs (Fig. 3.4).
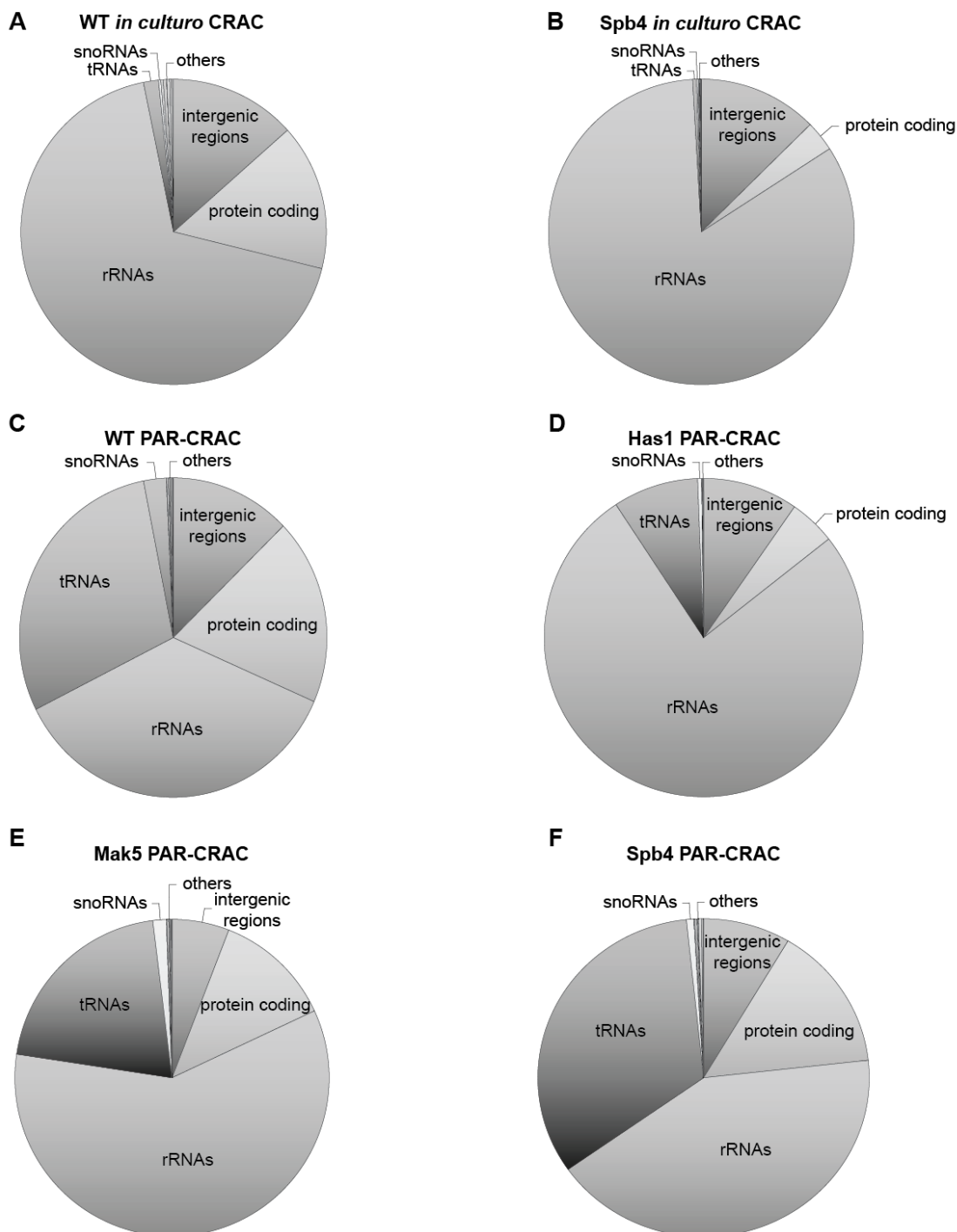
Figure 3.3: Crosslinking and analysis of cDNA (CRAC) revealed crosslinking of Has1, Spb4 and Mak5 to rRNAs. (A-F) Wild-type (WT) yeast cells or cells expressing HTP-tagged RNA helicases Has1, Spb4 or Mak5 were crosslinked *in culturo* (A, B) or by the PAR-CRAC approach (C-F). After purification of protein-RNA complexes and trimming of protruding RNA sequences, adapters were ligated, which were used for generating a cDNA library for Illumina deep sequencing. Obtained sequence reads were analysed bioinformatically, including quality control of the sequencing reaction, adapter removal and disregarding short reads. Remaining sequences were aligned to the annotated yeast genome and the distribution of reads corresponding to different classes of RNAs are shown. The category "Others" includes small nuclear RNAs, pseudogenes, mitochondrial-encoded RNAs and long non-coding RNAs. **(A)** WT control *in culturo* CRAC (UV). **(B)** Spb4 *in culturo* CRAC. **(C)** WT PAR-CRAC. **(D)** Has1 PAR-CRAC. **(E)** Mak5 PAR-CRAC. **(F)** Spb4 PAR-CRAC. Crosslinking experiments were performed with Maike Ruprecht and Philipp Hackert.
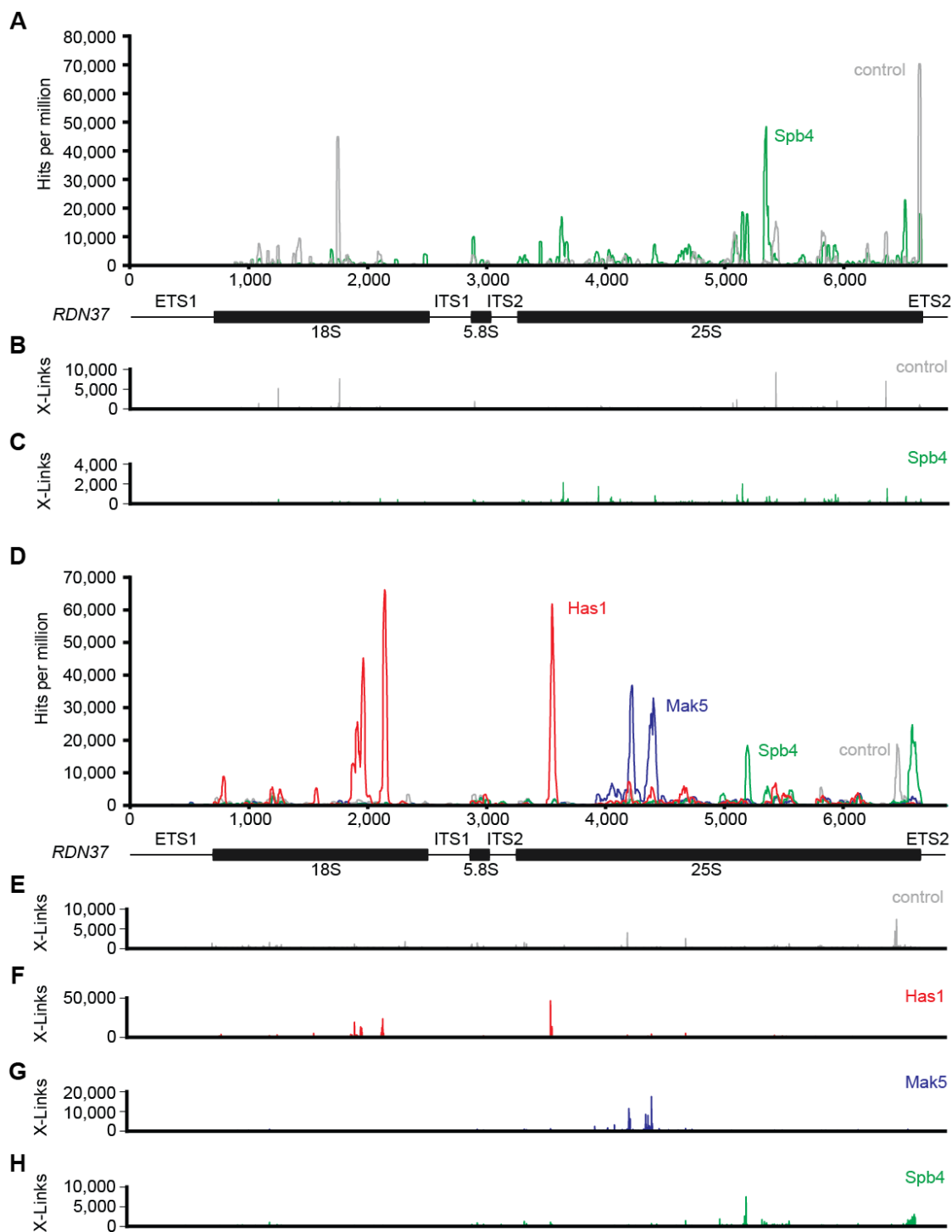
Figure 3.4: RNA helicases crosslink at distinct sites within ribosomal RNA. Within the gene locus of *RDN37*, representing rRNA on genomic level, the number of hits was determined according to the total number of sequences that overlap with each nucleotide. In order to compare different experiments, this number was normalised to the total number of mapped reads per million. Peaks represent a high number of reads corresponding to those nucleotides and resemble crosslinking sites. The relative position of mature rRNAs within *RDN37* are indicated. **(A)** Read distribution of WT control (grey) and Spb4 (green) *in culturo* CRAC (UV) within *RDN37*. **(B)** Deletions or substitutions within mapped reads of WT *in culturo* CRAC. **(C)** Deletions or substitutions within mapped reads of Spb4 *in culturo* CRAC. **(D)** Read distribution of WT control (grey), Has1 (red), Mak5 (blue) and Spb4 (green) PAR-CRAC within *RDN37*. **(E)** T to C substitutions within mapped reads of WT PAR-CRAC. **(F)** T to C substitutions within mapped reads of Has1 PAR-CRAC. **(G)** T to C substitutions within mapped reads of Mak5 PAR-CRAC. **(H)** T to C substitutions within mapped reads of Spb4 PAR-CRAC.

For the UV-CRAC (*in culturo*), in comparison to the WT control, the Spb4 sample revealed large numbers of reads mapping to two specific regions within 25S rRNA (peaks) suggesting that these sequences are bound by Spb4 *in vivo* (Fig. 3.4A). The high rate of mutations within the observed peaks strongly suggested that these are real protein binding sites, because they indicate direct contacts between protein and RNA (Fig. 3.4B/C). The PAR-CRAC data revealed peaks corresponding to crosslinking sites for all three RNA helicases, which were distinct from each other and, most importantly, distinct from the WT control (Fig. 3.4D-H).

Interestingly, the peak distribution between SSU und LSU RNAs was in line with the observed pre-rRNA processing defects and the proposed requirement of each of these proteins for LSU and/or SSU biogenesis. Therefore, Has1 crosslinked within both the 18S and 25S rRNA sequences, whereas Mak5 and Spb4 crosslinked only to 25S rRNA sequences (Fig. 3.4A/D). In the case of Spb4, the crosslinking pattern observed in the PAR-CRAC experiment resembled the peaks detected using *in culturo* UV crosslinking, further supporting these as genuine protein binding sites. For consistency, only the further analysis of the PAR-CRAC data of the three RNA helicases will be presented in the following sections.

3.3   Has1 has multiple functions in ribosome biogenesis

Amongst the three investigated RNA helicases, Has1 is the best characterised protein and it was shown already to be an RNA-dependent ATPase *in vitro* and to unwind DNA as well as RNA duplexes in an ATP-dependent manner (Rocak *et al*., 2005). Depletion of Has1 causes reduced dissociation of snoRNPs from pre-ribosomes, which was most prominent for the U14 snoRNP, and a role for Has1 in U14 release was further emphasised by mutational analyses showing accumulation of U14 on pre-rRNA in ATP deficient mutants of Has1 (Liang and Fournier, 2006). The U14 snoRNA is known to have dual functions in small subunit biogenesis, being required for pre-rRNA processing and also for a 2'-*O*-methylation reaction in 18S rRNA (Liang and Fournier, 1995; Dunbar and Baserga, 1998). In line with this, U14 has two known basepairing sites in the 18S rRNA: one at its modification site (18S-Cm414) and the other on the opposite strand of helices 5 and 6, where it is involved in forming long-range interactions. However, whether Has1 has a direct role in release of U14 has remained elusive, because of the lacking information about the binding sites of the helicase on the pre-rRNA.

Mapping of Has1 PAR-CRAC data onto the primary sequence of 35S pre-rRNA already revealed putative binding sites on both ribosomal subunits. In order to get insight into the functional relevance of these sites, we first focused on the SSU and the number of normalised hits were mapped onto the available secondary structure (2D) of 18S rRNA following a colour gradient representing the peak height of the mapping on the primary sequence. SSU 2D mapping highlighted two Has1 crosslinking sites in the 18S rRNA within helices 30 - 35 of the 3' major domain and in helices 6 and 6a of the 5' domain (Fig. 3.5). Notably, the Has1

crosslinking site in the 5' domain of 18S rRNA overlapped with one of the known basepairing sites of the C/D box snoRNA U14.
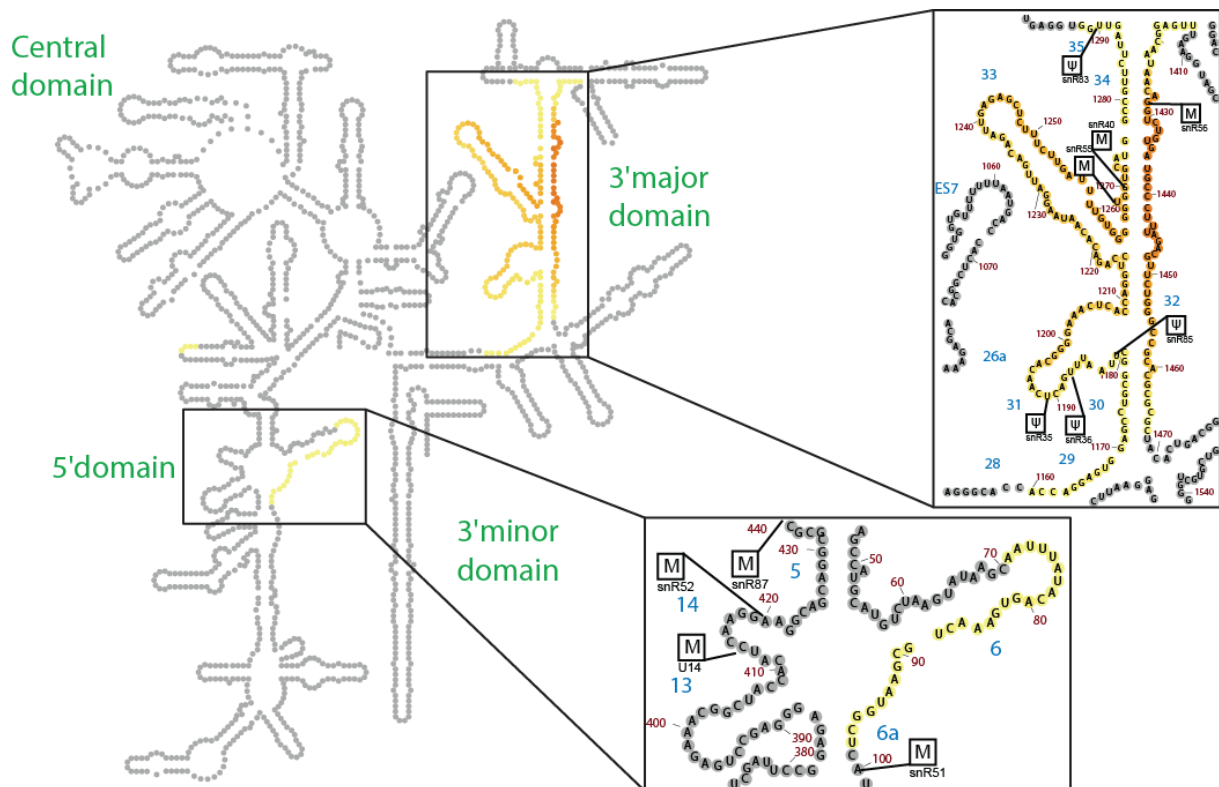

Figure 3.5: Has1 crosslinks at two sites within 18S rRNA. Has1 PAR-CRAC data depicted as colour-coded hit representation above a 10 % threshold from yellow (low value) to red (highest value) in correlation to all hits across *RDN37*. Mapping onto the secondary structure of mature SSU is shown (Petrov *et al*., 2014a). Secondary structure elements of 18S rRNA are indicated in green. Boxed M or Ψ represent 2'-*O*-methylations or pseudouridylations respectively, and the corresponding snoRNAs are given below.

Interestingly, CRAC analysis enables the transcriptome-wide detection of RNA interactions and closer inspection of the hit distribution between individual snoRNAs indicated a significant enrichment of sequences mapping to the U14 snoRNA in the Has1 dataset compared to the WT control (Fig. 3.6A). This demonstrates that Has1 also directly associates with the U14 snoRNA. Furthermore, mapping of the crosslinking sites of Has1 on the U14 sequence revealed that Has1 binds to the B domain of U14 (Fig. 3.6B), which is responsible for forming basepairing interactions with the 18S rRNA (Fig. 3.6C).

During the ligation reactions of the CRAC procedure, chimeric reads consisting of two non-consecutive sequences can be produced. After RNase treatment, free 5' and 3' ends of individual RNA strands crosslinked to the helicase can be in close proximity and are therefore ligated. Alternatively, template switching of the reverse transcriptase during final cDNA synthesis can be another source of producing chimeric reads (Houseley and Tollervey, 2010). In order to detect these hybrids, sequence reads obtained from the Has1 PAR-CRAC experiment were subjected to bioinformatics CLASH (crosslinking, ligation and analysis of sequence hybrids) analysis (Kudla *et al*., 2011).

Interestingly, a significant number of sequence hybrids detected within the Has1 PAR-CRAC data, were chimeric reads of U14 and 18S rRNA sequences, indicating simultaneous binding of Has1 to U14 and 18S rRNA, likely while they are basepaired. Mapping the 18S rRNA fraction of identified chimeric reads onto the secondary structure of 18S rRNA (Fig. 3.6D) showed that CLASH hybrids detected corresponded to the crosslinking site observed for Has1 (Fig. 3.5) and the known binding sites of U14 (Fig. 3.6C). Taken together, these findings strongly support the model that Has1 is directly involved in the release of U14 from pre-40S particles.
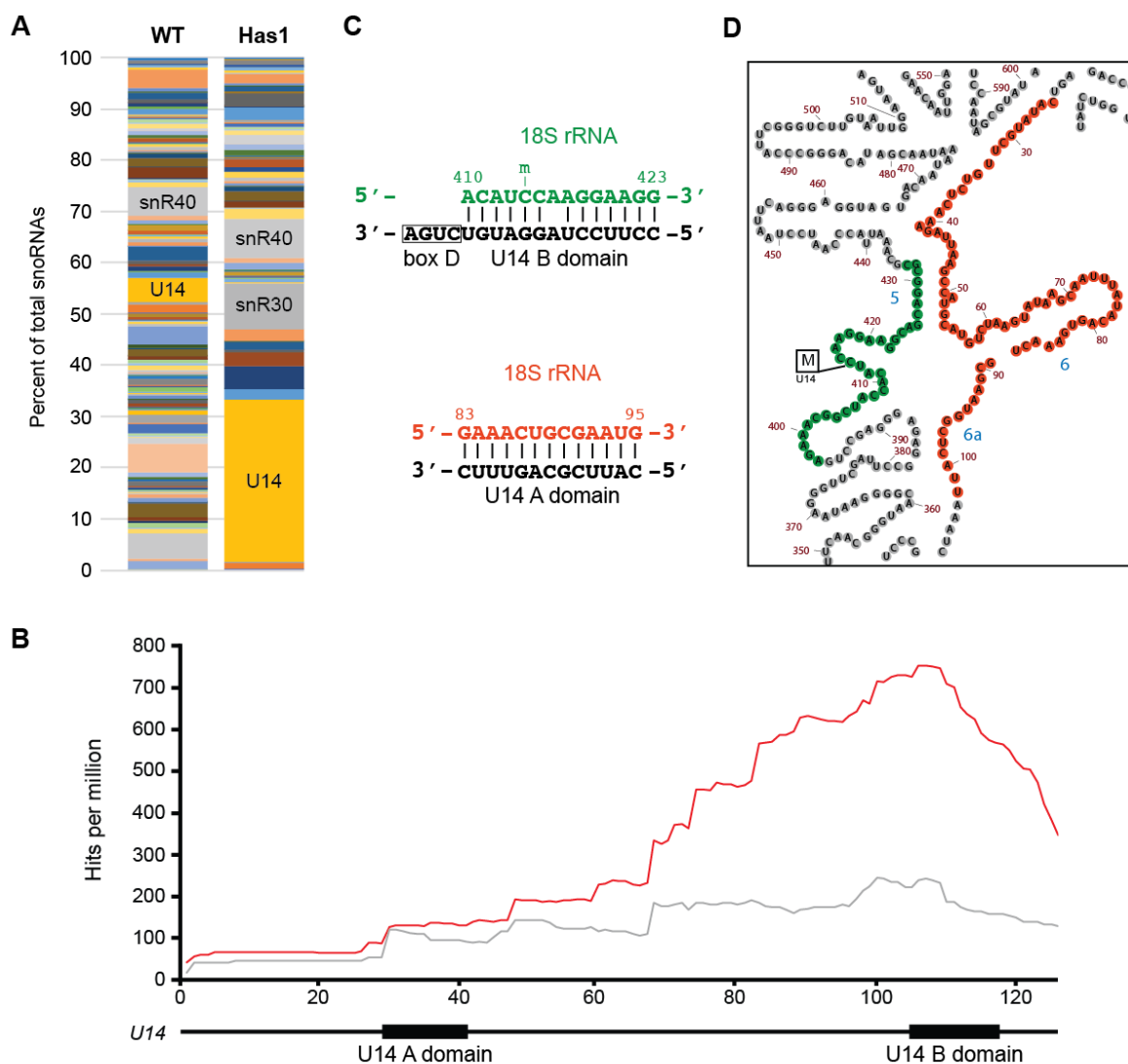
Figure 3.6: Has1 crosslinks to U14 sequences involved in basepairing with the 18S rRNA. (A) Relative distribution of obtained Has1 PAR-CRAC (Has1) sequence reads that map to snoRNAs reads in comparison to the WT PAR-CRAC control (WT). **(B)** Read distribution of WT control (grey) and Has1 (red) PAR-CRAC within *U14*. **(C)** Basepairing interactions between the U14 snoRNA (black) and the 18S rRNA (green and red). **(D)** CLASH hybrids identified within PAR-CRAC sequence reads. Indicated by coloured nucleotides are 18S rRNA sequences that were found in chimeric reads together with sequences of the U14 snoRNA. Colours correspond to sequences shown in (C).

Notably, in the 1D mapping of the Has1 PAR-CRAC data, another crosslinking site in the 3' major domain of the 18S rRNA was observed. This appeared distinct from the 3' minor domain where the known basepairing sites of the U14 snoRNA are. However, as RNA has the potential to form features of higher structural order, to see if Has1 binding to this site may be linked to its role in U14 release, the Has1 PAR-CRAC data was also mapped onto the tertiary (3D) structure of the mature small ribosomal subunit (Fig. 3.7). This also showed distinct crosslinking sites for Has1, where one site directly overlaps with the known U14 basepairing site, but the other is spatially distant. Since the structure of the early pre-40S complexes, which Has1 is thought to associate with, is probably very different to the mature SSU structure, this Has1 binding site could still reflect a role for Has1 in mediating U14 release, if these sites within the 18S rRNA are in closer proximity in a pre-40S particle. Alternatively, this crosslinking site could be linked to a so far unknown function of Has1 in the maturation of the small ribosomal subunit.
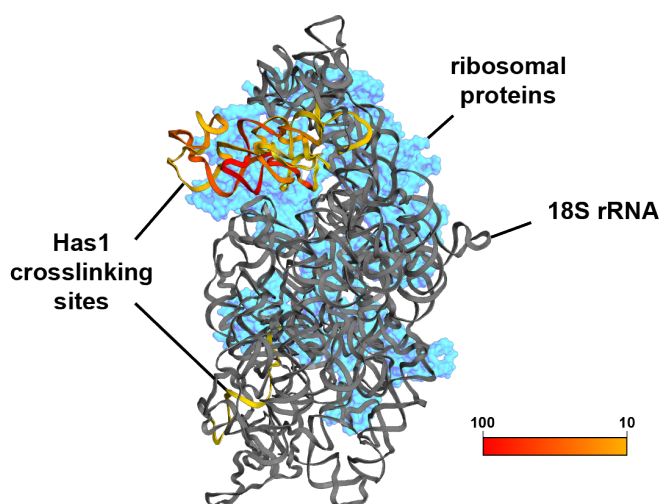
Figure 3.7: Has1 crosslinks at two sites within the small ribosomal subunit. Has1 PAR-CRAC data was mapped onto the 3D structure of mature SSU (Ben-Shem *et al*., 2011; PDB-ID: 4V88). Ribosomal RNA and ribosomal proteins are indicated in grey and blue respectively. Colour-code reflects peak height above a 10 % threshold from yellow (low value) to red (highest value).

In order to elucidate the function of Has1 in the biogenesis of the large ribosomal subunit, the obtained Has1 PAR-CRAC data was also mapped onto the mature LSU secondary structure (Fig. 3.8). Here, a single putative binding site in domain I of 25S rRNA was found to efficiently crosslink to Has1. Remarkably, this site was reported to be a binding site of another *trans*-acting factor Erb1, which is recruited to the pre-ribosome in an ATP-independent manner as part of a cluster of several "A_3-factors" required for ITS2 processing (Granneman *et al*., 2011; Dembowski *et al*., 2013). Furthermore, it was shown that in the absence of Has1, Erb1 and other A_3-factors accumulate on pre-ribosomal particles (Dembowski *et al*., 2013). Together with the newly identified crosslinking site of Has1 in domain I of the 25S rRNA, these findings suggest that Has1 is directly involved in the release of Erb1 during pre-60S biogenesis.

Figure 3.8: Has1 shares an overlapping binding site with the *trans*-acting ribosome biogenesis factor Erb1.
Has1 PAR-CRAC data depicted as colour-coded hit representation above a 10 % threshold from yellow (low value) to red (highest value) in correlation to all hits across *RDN37*. Mapping onto the secondary structure of mature LSU is shown (Petrov *et al*., 2014a). Secondary structure elements of 25S rRNA are indicated by green numbers. 5S and 5.8S rRNA are labelled in brown. The green line represents the reported binding site of Erb1 (Granneman *et al*., 2011).
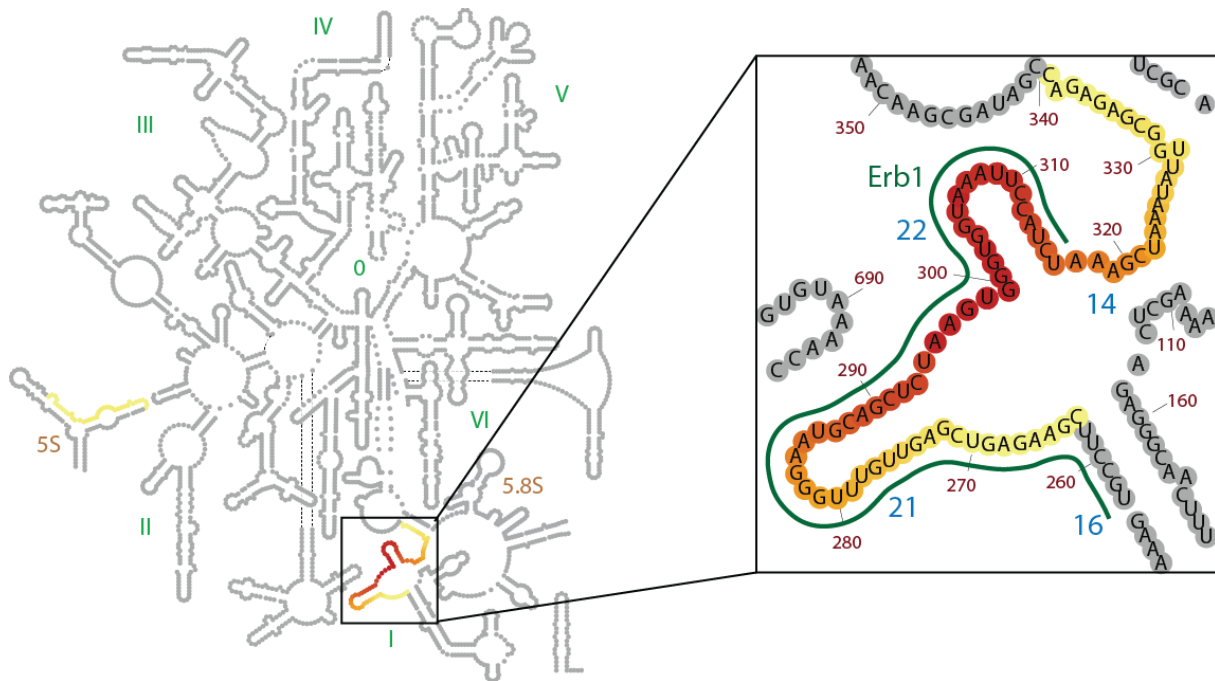
3.4 *In vitro* characterisation of the putative RNA helicases Spb4 and Mak5

While ATPase and unwinding activity has been previously shown for Has1, although Spb4 and Mak5 contain a helicase core domain, the activity of these putative enzymes had not been demonstrated so far. Therefore, before addressing in-depth functional characterisation of these proteins, it was important to determine whether they have catalytic activity, which was addressed using *in vitro* biochemical approaches. Due to their conserved sequence motifs, Spb4 and Mak5 resemble classical DEAD-box RNA helicases, which conventionally exhibit RNA-dependent ATPase activity. To test whether Spb4 and Mak5 have such activity, yeast *SPB4* and *MAK5* were cloned into a plasmid, which contained an IPTG-inducible promoter for expression of proteins with a His-ZZ-tag fused to the N-terminus. These plasmids were transformed into *E. coli* cells for recombinant expression and subsequently, proteins were purified via their His-tags. The obtained eluates and protein samples taken throughout the purification procedure were separated by SDS-PAGE and analysed by Coomassie-staining (Fig. 3.9). This revealed that the final preparations contained high concentrations of Spb4 and Mak5 without major contamination of unspecific *E. coli* proteins. In order to allow any ATPase activity observed to be attributed to Spb4 or Mak5, the *SPB4-* and *MAK5*-containing A21 plasmids were subjected to site-directed mutagenesis, to modify sequences encoding for motif

II (DEAD) and III (SAT). These two motifs are known to be involved in ATP hydrolysis and the coupling of ATP hydrolysis with helicase activity respectively. To achieve disruption of the Spb4 DEAD motif, glutamate 173 (E334 in Mak5) was substituted by a glutamine. Similarly, serine 203 (S378 in Mak5) and threonine 205 (T379 in Mak5) of the SAT motif were exchanged for alanine. These protein mutants, Spb4$_{DEAD/SAT}$ and Mak5$_{DEAD/SAT}$, were recombinantly expressed, purified and analysed as well by Coomassie-stained SDS-PAGE (Fig. 3.9), which revealed pure products available for subsequent analyses.
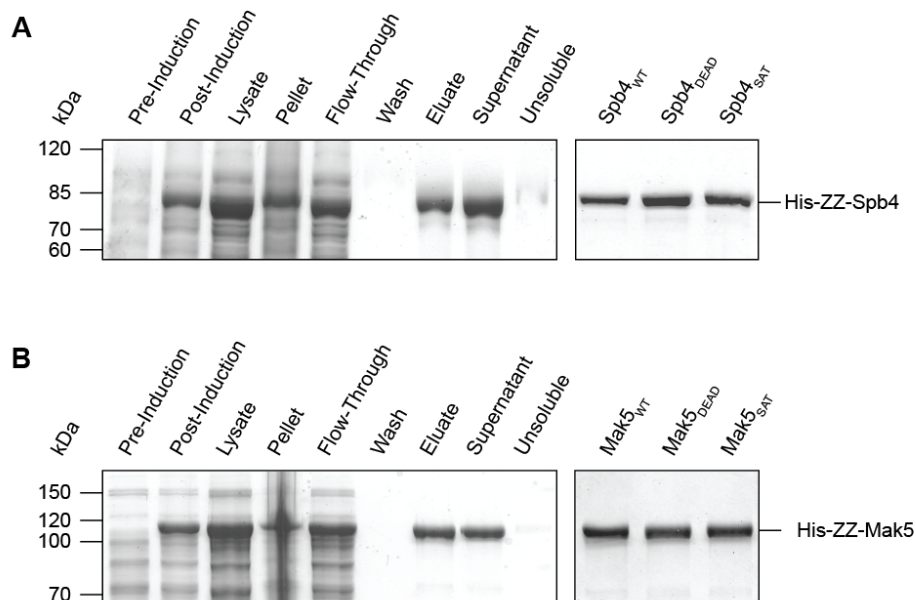
Figure 3.9: Recombinant expression and affinity purification of Spb4 and Mak5. His-ZZ-Spb4$_{WT/DEAD/SAT}$ and His-ZZ-Mak5$_{WT/DEAD/SAT}$ were expressed in *E. coli* and subjected to Ni-NTA chromatography. **(A)** Protein samples from indicated steps during expression and purification of Spb4$_{WT}$ (left) as well as purification products of all Spb4 variants (right) were separated by SDS-PAGE, and proteins were visualised by Coomassie-staining. **(B)** Protein samples from indicated steps during expression and purification of Mak5$_{WT}$ (left) as well as purification products of all Mak5 variants (right) were separated by SDS-PAGE, and proteins were visualised by Coomassie-staining.

Using an NADH-coupled ATPase assay allowed the *in vitro* activity of the purified WT proteins and their mutant versions to be tested. Here, in the presence of ATP, 2 µM of protein were incubated with an increasing amount of RNA (0 – 4 µM), which was supplemented with phosphoenol pyruvate, NADH as well as an enzymatic mix of pyruvate kinase and lactic dehydrogenase under physiological salt conditions. Increasing ADP levels, which are due to ATP hydrolysis, allow conversion of phosphoenol pyruvate to pyruvate with the help of added pyruvate kinase. The following reaction step, where pyruvate is converted to lactate by the lactate dehydrogenase, is coupled to the oxidation of NADH to NAD$^+$. The assay measured the reduction of absorption at 340 nm at 30 °C as the consequence of NADH oxidation, which responded indirectly to the protein mediated hydrolysis of ATP (Kiianitsa *et al*., 2003).

Figure 3.10: Mutations in conserved RNA helicase motifs compromises the RNA-dependent ATPase activity of Spb4 and Mak5. Recombinantly expressed and purified Spb4 and Mak5 variants were subjected to NADH-coupled ATPase assays. 2 μM of protein were incubated with increasing amounts of RNA (0 – 4 μM RNA) and the rate of ATP hydrolysis was estimated by measuring NADH oxidation resulting in loss of absorption at 340 nm. **(A)** Comparative analysis of Spb4 variants. **(B)** Comparative analysis of Mak5 analysis.
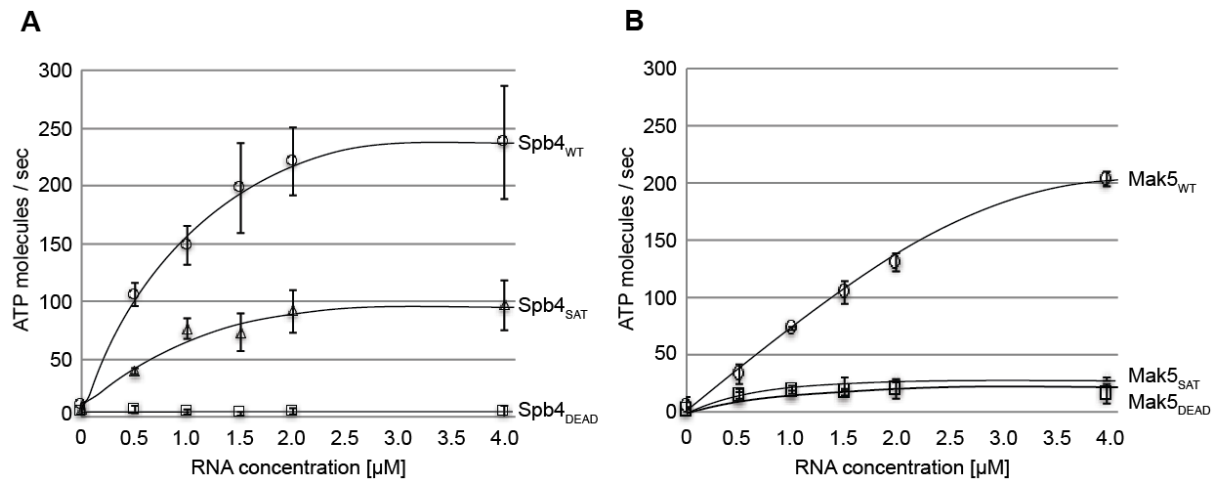
Spb4 and Mak5 WT proteins exhibited increasing ATPase activities in the presence of increasing amounts of RNA, confirming their activities as RNA-dependent ATPases (Fig. 3.10). This ability was completely diminished in the $Spb4_{DEAD}$ mutant and significantly compromised in the $Mak5_{DEAD}$ mutant, demonstrating that the observed ATP hydrolysis is specifically due to the presence of the putative helicases. In contrast, the $Spb4_{SAT}$ mutant showed reduced ATPase activity, but was still able to slowly hydrolyse ATP (Fig 3.10A), whereas the $Mak5_{SAT}$ mutant hardly showed any ATPase activity (Fig. 3.10B).

3.5 The catalytic activity of Spb4 and Mak5 is required for their functions in LSU biogenesis

Having demonstrated that Spb4 and Mak5 possess ATPase activities *in vitro*, the next step was to address the question of whether this activity is required for their functions in biogenesis of the large ribosome subunit. For this reason, complementation systems were constructed, which allowed depletion of the endogenous protein while expressing a plasmid-encoded WT or mutant protein from its endogenous promoter. Here, *SPB4* and *MAK5* were cloned, with 500 bp up- and downstream of their coding sequences, into a low-copy plasmid (pRS415). After site-directed mutagenesis in order to produce constructs for expression of the DEAD and SAT mutants characterised by the *in vitro* assays, the plasmids were transformed into their corresponding depletion strains (see Fig. 3.1 and 3.2).

Growing these cells into mid-log phase and spotting a serial dilution onto plates with permissive and non-permissive medium, allowed monitoring of growth behaviour of cells containing the introduced plasmids in the presence or absence of endogenous proteins.
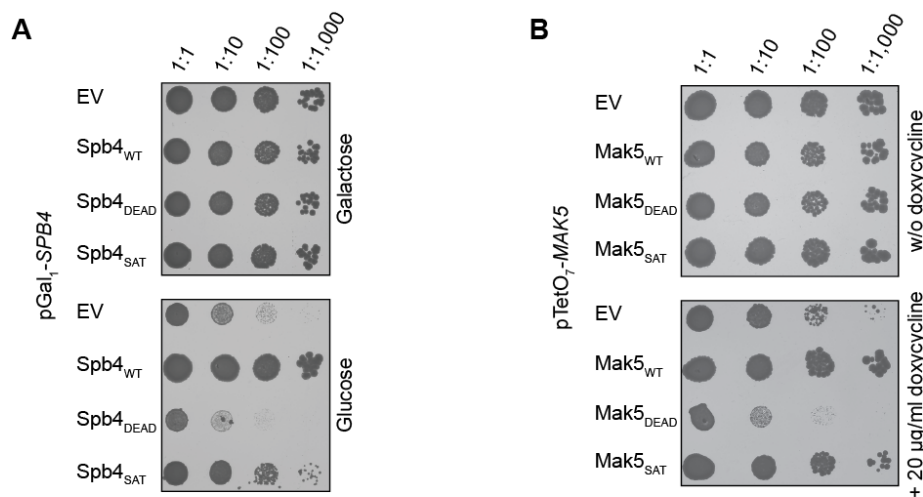
Figure 3.11: The catalytic activity of Spb4 and Mak5 is required for cell growth. Endogenous RNA helicases were depleted under non-permissive conditions, which was complemented by an empty vector (EV) or by the expression of indicated plasmid encoded proteins. Cells were grown under permissive conditions to mid-log phase and spotted onto plates in a series of 1:10 dilutions. Growth was recorded after 3 d of growth at 30 °C. **(A)** Spb4 depletion strain (pGal$_1$-*SPB4*) with complementation plasmids was spotted onto galactose- or glucose-containing plates. **(B)** Mak5 depletion strain (pTetO$_7$-*MAK5*) with complementation plasmids was spotted onto plates, which contained 20 µg/ml doxycycline or which were devoid of doxycycline.

Investigation of growth after 3 d of incubation at 30 °C indicated a strong correlation between cell growth and ATPase activity, which was nearly identical for both RNA helicases, Spb4 and Mak5 (Fig. 3.11A/B). Growth under permissive conditions, where the endogenous RNA helicases were continuously expressed, did not show any growth defects. In contrast, when the endogenous proteins were depleted, complementation with the empty vector (EV) revealed growth defects. Expression of the WT proteins were able to complement this phenotype, such that cell growth was comparable to growth under permissive conditions. In contrast, cells expressing RNA helicase DEAD mutants under non-permissive conditions showed strong growth defects. These defects were more significant than the phenotypes observed upon complementation with the EV, suggesting that these mutations could have a dominant negative effect. Growth of the yeast strains expressing the Spb4$_{SAT}$ or Mak5$_{SAT}$ mutants under non-permissive conditions, showed reduced growth compared to the cells complemented with plasmids expressing WT protein (Fig. 3.11A/B). The growth defects observed were not as strong as those seen when the helicases carrying mutations in the DEAD motif were expressed. This correlates with the compromised, rather than abolished, ATPase activity seen in the previous *in vitro* assay for Spb4 and suggests that the DEAD motif is more important than the SAT motif for the function of Mak5 *in vivo*. Together, these results demonstrate that the ATPase activity of both Mak5 and Spb4 is important for their cellular functions.

Next, investigation of pre-rRNA processing using the complementation systems allowed to determine if the catalytic activity of Spb4 and/or Mak5 or the presence of the proteins is required for their functions in ribosome biogenesis. To analyse this, the complementation

strains were grown to mid-log phase in permissive medium before they were shifted to non-permissive medium for the appropriate depletion time of each RNA helicase. After harvesting of cells and RNA extraction, total RNA was subjected to denaturing agarose gel electrophoresis and subsequent northern blotting. Mature rRNAs (18S and 25S rRNA) were visualised by methylene blue staining and pre-rRNA processing intermediates were detected using radioactively labelled probes hybridising to the ITS1 and ITS2 sequences (Fig. 3.12).

In the case of Spb4, the pre-rRNA processing defects (accumulation of the 35S and 27S pre-rRNAs) seen for protein depletion without complementation (Fig. 3.2B), were reproduced by depletion of endogenous Spb4 while adding back EV (Fig. 3.12A). However, these defects could be rescued by expression of $Spb4_{WT}$ from the complementation plasmid, confirming that these defects arise due to a lack of Spb4. In contrast, expression of either catalytically deficient mutant ($Spb4_{DEAD}$ or $Spb4_{SAT}$) showed strong pre-rRNA processing defects, which were slightly more pronounced for $Spb4_{DEAD}$.
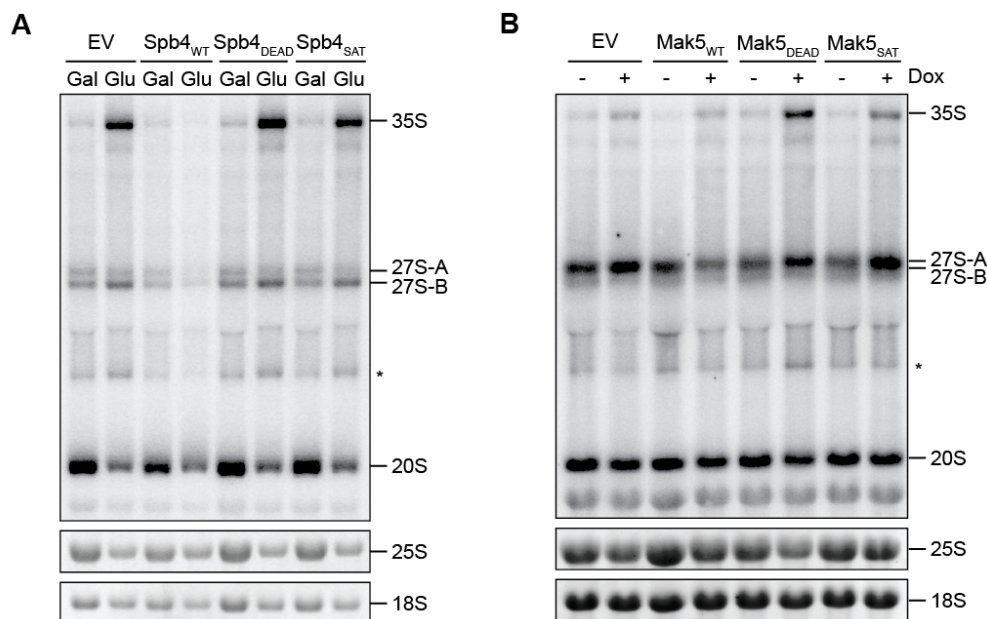
Figure 3.12: The catalytic activity of Spb4 and Mak5 is required for processing of pre-ribosomal RNA. Northern blot analysis in order to visualise pre-rRNA processing using the complementation systems. Genomic Spb4 and Mak5 were depleted by growth in non-permissive medium for the appropriate depletion time, which was complemented by the indicated plasmid encoded protein variants. Total RNA was extracted and 6 µg were subjected to denaturing agarose gel electrophoresis and subsequent northern blotting. Mature rRNAs (18S and 25S rRNA) were visualised by methylene blue staining, while pre-rRNA precursors were detected by autoradiography. The aberrant 23S pre-rRNA intermediate is indicated by an asterisk. **(A)** The Spb4 depletion strain containing EV, $Spb4_{WT}$, $Spb4_{DEAD}$ or the $Spb4_{SAT}$ complementation plasmid was grown in galactose (Gal) or glucose (Glu) for 12 h. **(B)** The Mak5 depletion strain containing EV, $Mak5_{WT}$, $Mak5_{DEAD}$ or the $Mak5_{SAT}$ complementation plasmid was grown in medium supplemented with 20 µg/ml doxycycline (+Dox) or in medium that was devoid of doxycycline (-Dox) for 10 h.

Depletion of Mak5 in the presence of EV only lead to a small processing defect (Fig. 3.12B), which was more intense in the previously shown depletion experiment in the absence of a complementation plasmid (Fig. 3.2D). As expected, adding back $Mak5_{WT}$ did not change the

levels of mature and pre-rRNAs. However, complementing the depletion of genomic Mak5 with Mak5$_{DEAD}$ showed a significant accumulation of pre-rRNA intermediates, which could also be detected for Mak5$_{SAT}$, although to a much lesser extent. In conclusion, for both proteins, Spb4 and Mak5, their catalytic activity is not only required for cell viability, but more precisely for processing of pre-rRNA in the context of ribosome biogenesis.

3.6 The RNA helicases Spb4 and Mak5 are not implicated in snoRNA recruitment or release from pre-ribosomal complexes

By basepairing to pre-rRNAs, snoRNAs direct 2'-*O*-methylation or pseudouridylation reactions on the pre-rRNA, which are mediated by the associated enzymes (Watkins and Bohnsack, 2012). However, another reported function for snoRNAs is to assist in RNA folding and establish long-range interactions to bring more distant rRNA sequences in closer proximity (Liang and Fournier, 1995; Martin *et al.*, 2014). Several RNA helicases have been shown to be required for the release of specific snoRNAs from pre-ribosomal complexes after they have carried out their modification and/or RNA folding functions (see for example Kos *et al.*, 2005; Liang and Fournier, 2006; Bohnsack *et al.*, 2008; Sardana *et al.*, 2015). Moreover, Prp43 was suggested to be involved in facilitating the association of two snoRNAs with pre-ribosomal particles, most likely by remodelling their binding sites, making them available for snoRNA basepairing (Bohnsack *et al.*, 2009).

It would be possible that the roles of Spb4 or Mak5 in LSU biogenesis are to regulate the interaction of specific snoRNAs with pre-ribosomal complexes. This could particularly be the case for Mak5 as its crosslinking site on the 25S rRNA is in close proximity to several known rRNA modifications. To investigate this, whole cell extracts from WT yeast or cells depleted of either Has1, Spb4 or Mak5 were subjected to sucrose density gradient centrifugation to separate (pre-)ribosomal complexes from non-ribosome-associated proteins. Here, Has1 served as a positive control, because it was already shown that the U14 snoRNA accumulates on pre-ribosomal particles upon depletion of U14 (Liang and Fournier, 2006). Fractions containing "free" snoRNAs and pre-ribosome-bound snoRNAs were pooled, then RNAs were extracted, reverse transcribed and analysed by qPCR to determine the levels of all 75 snoRNAs in each of these two pools. The relative distribution of snoRNAs (pre-ribosome bound versus free snoRNAs) were normalised to the values of control (WT) samples, which were processed and analysed in parallel. According to this normalisation, a value of 1 corresponded to no difference in snoRNA distribution between RNA helicase depletion and WT conditions, a value of 2.1 or below 0.48 (corresponding to the 95 % confidence limit) was regarded as accumulation or deficiency of snoRNAs on pre-ribosomes upon depletion of the helicase.
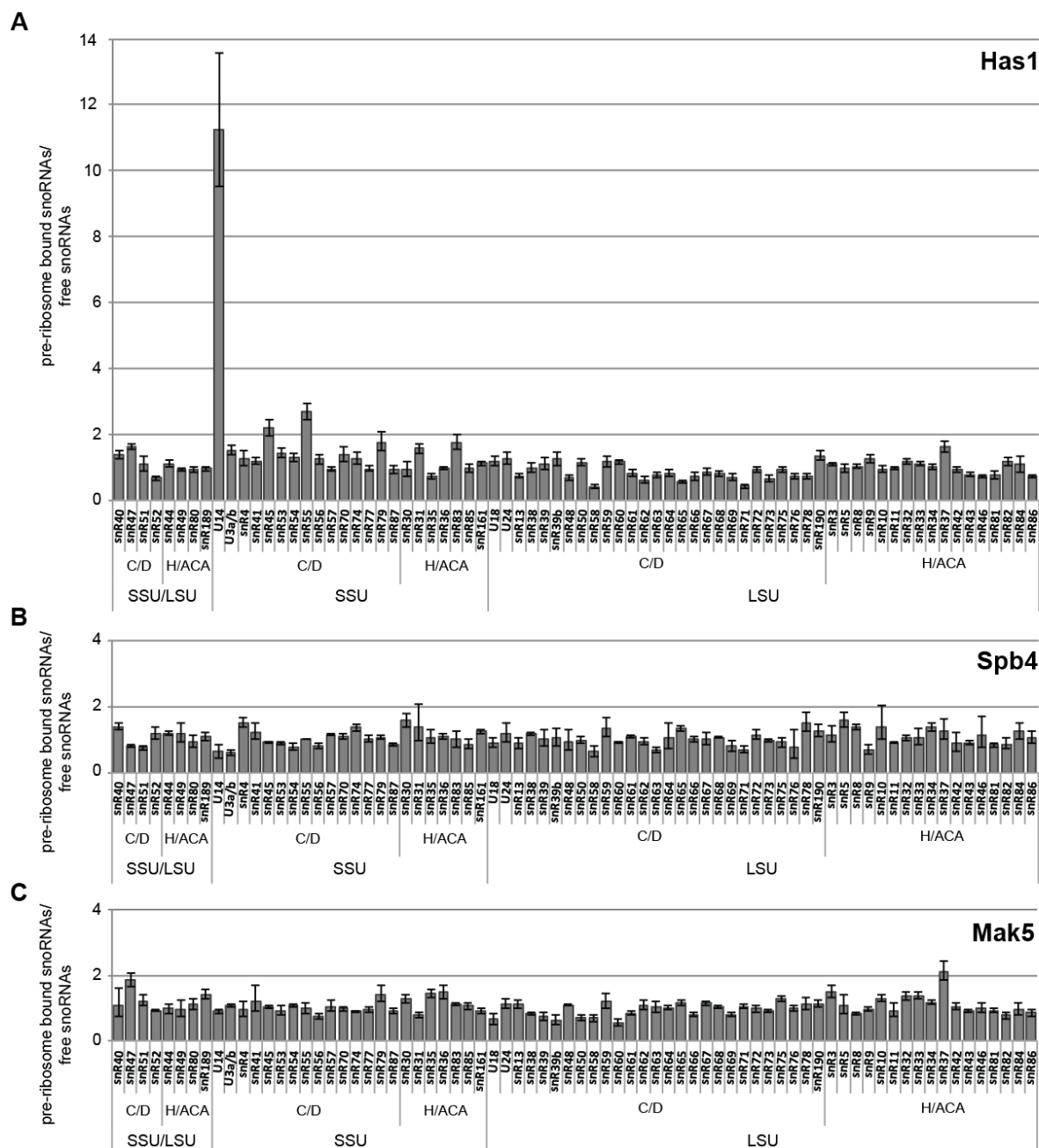
Figure 3.13: Spb4 and Mak5 are not involved in mediating snoRNA release or access. Has1 **(A)**, Spb4 **(B)** and Mak5 **(C)** depletion strains were cultivated for their appropriate depletion times under non-permissive conditions before cells were harvested and lysed. Soluble cell components were subjected to sucrose density centrifugation. Fractions containing free snoRNAs and fractions containing pre-ribosomal bound snoRNAs were pooled and RNA was extracted. Reverse transcription provided templates for determination of the relative levels of all 75 snoRNAs by qPCR analysis. Relative distributions of bound versus free snoRNAs in the absence of RNA helicases were normalised to WT control levels. The average values of three independent experiments are shown as bars with the corresponding error bars reflecting the standard deviation. SnoRNAs are grouped according to their classification as C/D box or H/ACA box snoRNA and their rRNA target. These experiments were performed by Roman Martin and Markus Bohnsack.

A clear accumulation of U14 on pre-ribosomes with a value of 11.22 could be observed upon depletion of the RNA helicase Has1 (Fig. 3.13A). This result confirmed the previously described investigations. Notably, there was no other snoRNA, which was significantly affected by depleting Has1. Upon depletion of neither Spb4 nor Mak5, there was a significant

accumulation or deficiency of any snoRNA detectable. This suggests that neither of these RNA helicases regulates the interactions of snoRNAs with pre-ribosomes, and indicates that instead, these two proteins have other functions in the process of ribosome biogenesis.

3.7 Spb4 binds to two regions of the 25S rRNA sequence, which may be a helicase binding platform and an rRNA region that is remodelled

Recently, investigations addressing the assembly of so called "B-factors", which are required for processing of the 27S-B pre-rRNA intermediate, revealed that Spb4 is required for the efficient recruitment of the GTPase Nog2, a factor implicated in C_2 cleavage and a known placeholder for the export adaptor Nmd3 (Saveanu *et al.*, 2001; Talkish *et al.*, 2012; Matsuo *et al.*, 2014). However, elucidation of the precise role of Spb4 in Nog2 recruitment and whether Spb4 has additional functions in LSU biogenesis has been hampered by the lack of information on its binding site.

Mapping of the obtained Spb4 PAR-CRAC data onto the primary sequence of *RDN37* showed two peaks within the 25S rRNA sequence corresponding to sequences that were enriched with Spb4 (Fig. 3.4D). Akin to Has1 analysis, in order to get a closer view onto the physiological relevance of these peaks, the Spb4 PAR-CRAC data was mapped onto the secondary structure of mature LSU rRNAs (Fig. 3.14).
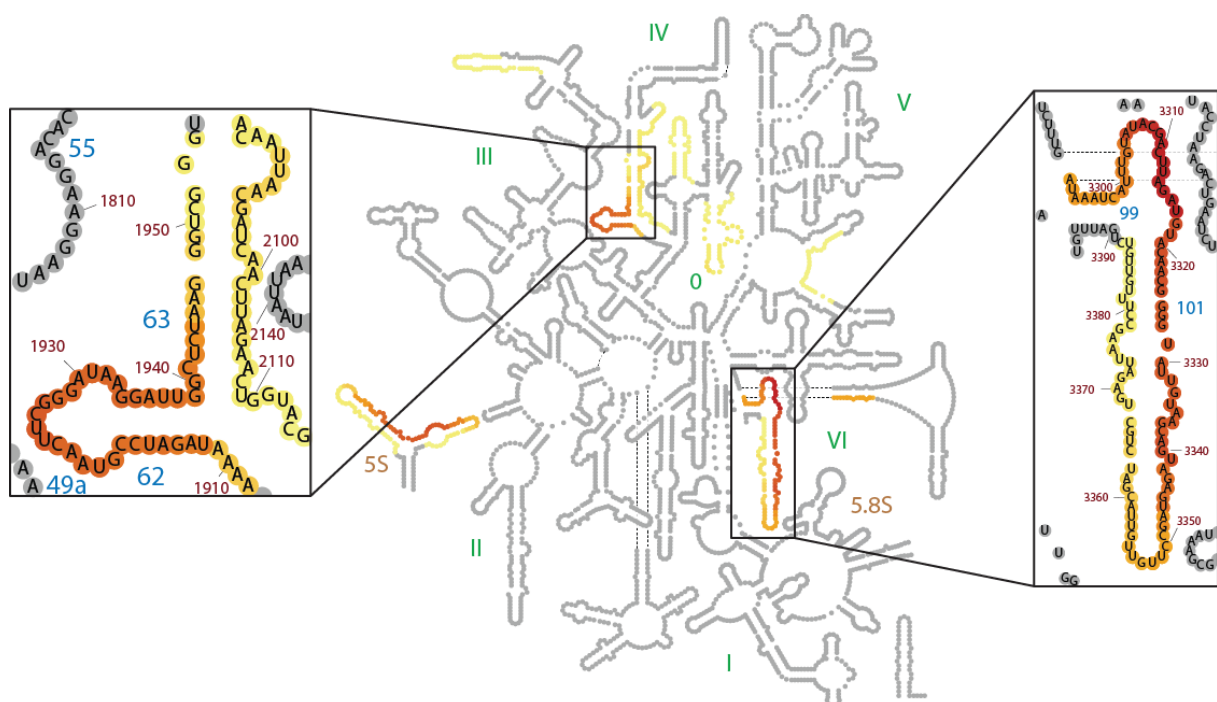
Figure 3.14: Spb4 crosslinks at two distinct sites within the 25S rRNA secondary structure. Spb4 PAR-CRAC data depicted as colour-coded hit representation above a 10 % threshold from yellow (low value) to red (highest value) in correlation to all hits across *RDN37*. Mapping onto the secondary structure of mature LSU is shown (Petrov *et al.*, 2014a). Secondary structure elements of 25S rRNA are indicated in green. 5S and 5.8S rRNA are labelled in brown.

This showed that a significant proportion of Spb4 crosslinked to the very 3' end of 25S rRNA, in helices 99 - 101 of domain VI. The other Spb4 crosslinking site was located in domain IV at helices 62 and 63 at the base of a protruding eukaryotic specific expansion segment (ES27). Although an enrichment of reads mapping to the 5S rRNA was observed, this was not considered significant because this pattern was also detected in WT control samples. Mapping the Spb4 PAR-CRAC data onto the 3D structure of the pre-LSU Nog2-particle (Wu *et al.*, 2016; PDB-ID: 3JCT) showed that although the two Spb4 crosslinking sites are on the same face of the pre-ribosome and in relatively close proximity to each other, they are still somewhat spatially separated (Fig. 3.15A). It is possible that the observed crosslinking sites reflect binding of a single Spb4 molecule and because the Nog2-particle is downstream of the Spb4 functional particle in the context of ribosome biogenesis, these two sites might be even closer in the pre-ribosomal particle that Spb4 associates with. Interestingly, the identified Spb4 crosslinking site was in close proximity to the GTPase Nog2 (Fig. 3.15B). It has recently been suggested that Spb4 is required for the recruitment of Nog2 (Talkish *et al.*, 2012) and these data suggest that Spb4 may play a direct role in this process.
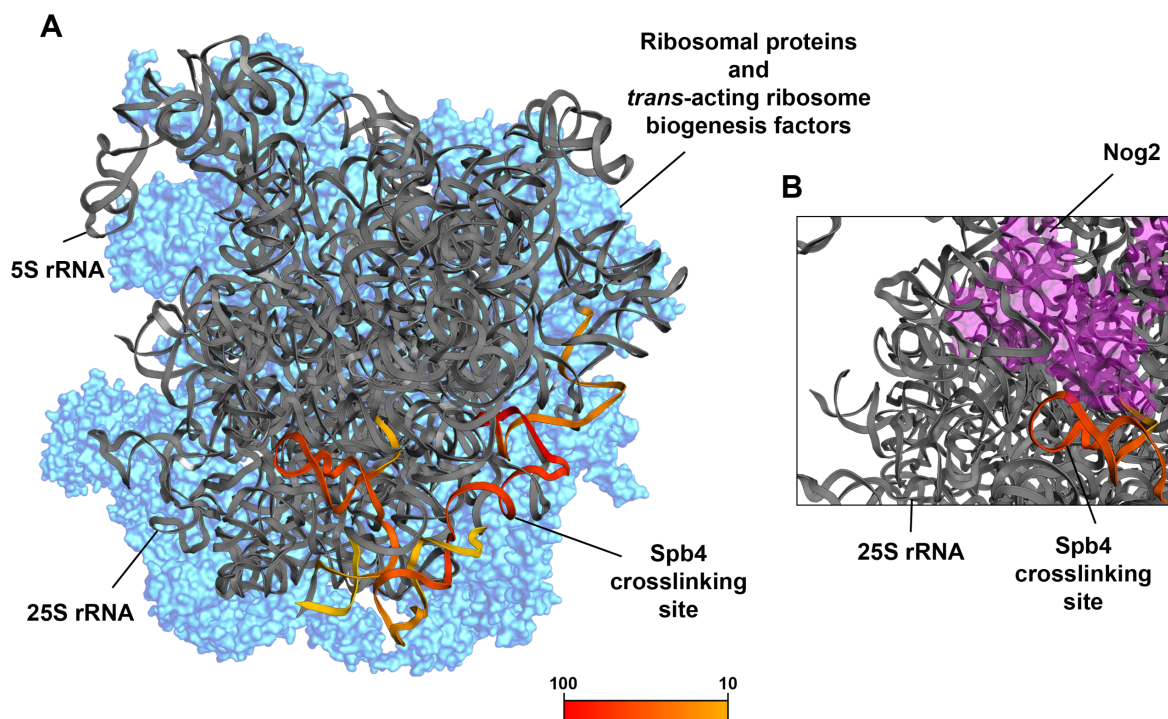
Figure 3.15: Spb4 crosslinks at two distinct sites within the Nog2 pre-60S particle. (A) Spb4 PAR-CRAC data was mapped onto the 3D structure of the pre-LSU Nog2-particle (Wu *et al.*, 2016; PDB-ID: 3JCT). Colour-code reflects peak height above a 10 % threshold from yellow (low value) to red (highest value). **(B)** Magnified view shows the GTPase Nog2 (magenta) in close proximity to the Spb4 crosslinking site.

The identification of crosslinking sites of Spb4 on the 25S rRNA sequence by PAR-CRAC strongly suggests that these regions are bound by the helicase, however, an independent experiment was applied in order to confirm the presence of Spb4 at these sites in pre-ribosomal

complexes. *Ex vivo* dimethyl sulfate (DMS) structure probing was employed, as this approach enables the presence of proteins bound to RNAs to be detected as well as RNA structural changes caused by the action of a protein, such as an RNA helicase (Wells *et al.*, 2000). The reactive chemical donates methyl groups, preferentially to hydrogen-bond accepting ring nitrogens of adenines and cytosines, and this is prevented if the nucleotide forms basepairing interactions or is bound by a protein. The modification pattern of an RNA molecule can be monitored by diagnostic primer extension analysis using a radioactively labelled oligonucleotide, because once installed, these methyl groups cause stops in the elongation reaction during reverse transcription. Comparison of the modification pattern of RNAs from RNA helicase-depleted and non-depleted samples as well as RNAs from DMS-treated and non-treated control samples allows structural transitions caused by depletion of the protein to be monitored. As Spb4 functions in pre-ribosomal particles, but binds to the 25S rRNA sequence, which is also present in mature ribosomes, purification of ribosome biogenesis intermediates was necessary for structure probing analyses. Otherwise, the majority of the observed signals would be derived from the much more abundant, mature 25S rRNA and differences in the modification pattern caused by lack of Spb4 would be undetectable. To enable purification of pre-ribosomal complexes that contain Spb4 under normal conditions, the methyltransferase Nop2, which was reported to associate with pre-60S particles in an intermediate step and to be released before ribosomal export to the cytoplasm (Hong *et al.*, 1997; Talkish *et al.*, 2012), was genomically HTP-tagged. To verify that Spb4 was present in pre-60S complexes purified via Nop2-HTP and to determine, which pre-rRNA species were present in these particles, pull-down assays were performed (Fig. 3.16). A yeast strain expressing Nop2-HTP and 3xHA-tagged Spb4 was grown in exponential phase and after harvesting and cell lysis, Nop2-containing complexes were retrieved on IgG-sepharose. Both proteins and RNAs were extracted from the eluates and analysis of the protein by western blotting using an HA-antibody revealed the presence of Spb4 co-purified with Nop2, demonstrating its presence in the isolated pre-ribosomal particles (Fig. 3.16A). Northern blot analysis of the RNAs co-purified with Nop2-HTP demonstrated the enrichment of the 27S-A/B pre-rRNAs in the eluates (Fig. 3.16C). As these are the pre-rRNA intermediates that accumulate when Spb4 is depleted, this suggests that pre-60S complexes isolated via Nop2 are appropriate for DMS structure probing experiments to analyse the function of Spb4. For subsequent functional analysis of Mak5, the presence of this helicase in the Nop2-HTP particle was also confirmed by western blotting (Fig. 3.16B).

To perform structure probing experiments, the Spb4 depletion strain in which Nop2 was HTP-tagged, was grown under permissive and non-permissive conditions before cells were harvested, disrupted and lysates were subjected to native purification using IgG-sepharose. When purified pre-60S particles were still attached to the beads, DMS was either added or, as

a control, were left untreated. The chemical reaction was quenched and RNA was subsequently extracted providing template material for primer extension analyses. As Spb4 PAR-CRAC revealed two sites of interaction between the helicase and the 25S rRNA sequence, both sites were addressed individually, using specific oligonucleotides for the primer extensions. First, an oligonucleotide was used that annealed downstream of the observed crosslinking site at the 3' end of 25S rRNA and the primer extension products were separated by denaturing PAGE alongside a sequencing ladder generated using the same oligonucleotides to enable identification of the nucleotides at which extension reactions had stalled (Fig. 3.17A/B). Comparing the modification pattern of DMS treated samples in the presence or absence of Spb4, the nucleotide A3336 showed increased sensitivity towards DMS in the absence of Spb4, indicating exposure of this nucleotide when Spb4 is absent from the purified pre-60S particles. In close proximity of A3336, several nucleotides showed an altered modification pattern upon depletion of Spb4, whereas other more distant nucleotides seemed to be unaffected. This result independently confirmed the crosslinking site at the 3' end of 25S rRNA, obtained by PAR-CRAC analysis, to be a *bona-fide* Spb4 binding site.
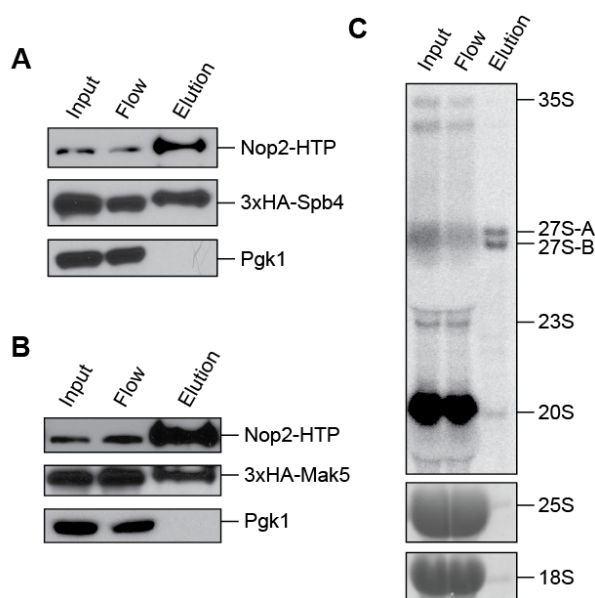
Figure 3.16: Nop2-HTP co-immunoprecipitates Spb4, Mak5 and 27S pre-rRNAs. (A) A yeast culture containing genomically HTP-tagged Nop2 and 3xHA-Spb4 was grow to mid-log phase. Cell lysate was subjected to pull-down analysis using IgG-sepharose. 0.2 % of taken Input and Flow samples, together with 20 % of the elution fraction were analysed by SDS-PAGE and western blotting using anti-ProteinA, anti-HA and anti-Pgk1 (control) antibodies. **(B)** Yeast cells expressing Nop2-HTP and 3xHA-Mak5 were grown to mid-log phase and analysed by western blotting as in (A). **(C)** Yeast cells expressing Nop2-HTP only were grown to mid-log phase. Cell lysate was subjected to pull-down analysis using IgG-sepharose. 2.5 % of taken Input and Flow samples, together with 50 % of the elution fraction were subjected to agarose gel electrophoresis and subsequent northern blotting. Mature rRNAs (25S and 18S rRNA) were visualised by methylene blue staining, whereas pre-rRNA intermediates were detected by radiography using radioactively labelled probes hybridising to sequences in ITS1 (004) and ITS2 (020).

In order to analyse the second putative Spb4 binding site, an oligonucleotide was used for primer extensions that annealed to the 25S rRNA sequence downstream of helix 63 (Fig. 3.17C/D). Analogous to the first Spb4 site, several nucleotides within the Spb4 crosslinking site showed altered sensitivity towards DMS in the absence of the protein (A1907, C1926, A1933). These changes therefore confirmed the association of Spb4 also with the region around helix 63. Since the observed changes in this region included both nucleotides that

became more and less accessible for DMS modification when Spb4 was depleted, this raises the possibility that this region is actively remodelled by the helicase activity of Spb4.
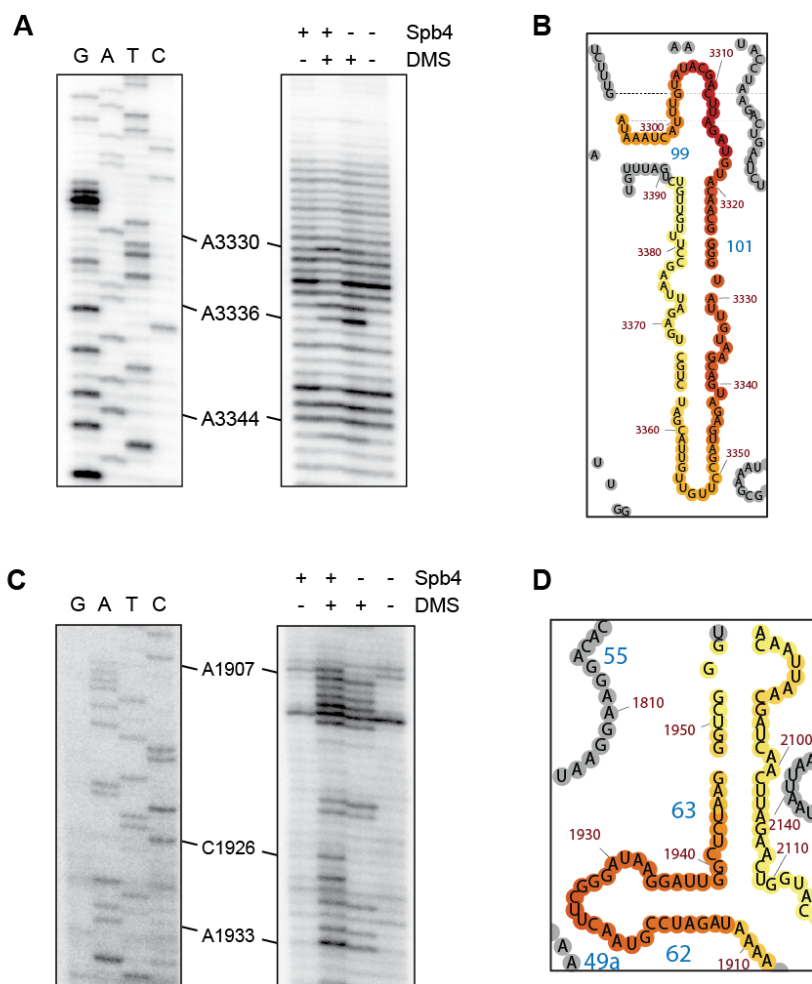
Figure 3.17: DMS structure probing to confirm Spb4 binding at two distinct sites within the 25S rRNA sequence. The yeast Spb4 depletion strain containing genomically HTP-tagged Nop2 was cultivated for the appropriate depletion time of 12 h in permissive or non-permissive medium (+Spb4; -Spb4). After cell lysis, pre-60S complexes were co-immunoprecipitated using IgG-sepharose. On beads, complexes were treated with DMS (+DMS) and RNA was extracted, which was used as template for primer extension analyses, starting from a radiolabelled oligonucleotide downstream of the detected Spb4 crosslinking sites. Reaction products were subjected to denaturing PAGE, so that fragments, which derived from stops in transcription due to DMS modifications, could be detected using a phosphorimager. As a reference, primer extensions were performed on total RNA after spiking in individual ddNTPs, which created a sequencing ladder as indicated above. **(A)** DMS structure probing analysis of Spb4 crosslinking site at the 3' end of 25S rRNA. **(B)** Spb4 PAR-CRAC data mapped to the secondary structure of LSU with focus on 3' end of 25S rRNA (as shown in Fig. 3.14. **(C)** DMS structure probing analysis of Spb4 crosslinking site at helices 62 and 63 within 25S rRNA. **(D)** Spb4 PAR-CRAC data mapped to the secondary structure of LSU with focus on helices 62 and 63 within 25S rRNA (as shown in Fig. 3.14).

3.8 Mak5 is involved in structural rearrangements of helices 37 - 39 of the 25S rRNA that are ultimately bound by Rpl10

To better understand the functional relevance of the crosslinking sites identified in the 25S rRNA sequence for Mak5 (Fig. 3.4D), the Mak5 PAR-CRAC data was mapped onto the secondary structure of mature LSU rRNAs, which showed that the two peaks, which were

distant on the primary sequence, came into close proximity at helices 37 – 39 in domain II of 25S rRNA (Fig. 3.18). To gain a more detailed view of the interactions Mak5 forms with pre-ribosomal complexes, mapping was also carried out onto the available 3D structure of the Nog2-particle (Wu *et al.*, 2016; PDB-ID: 3JCT).
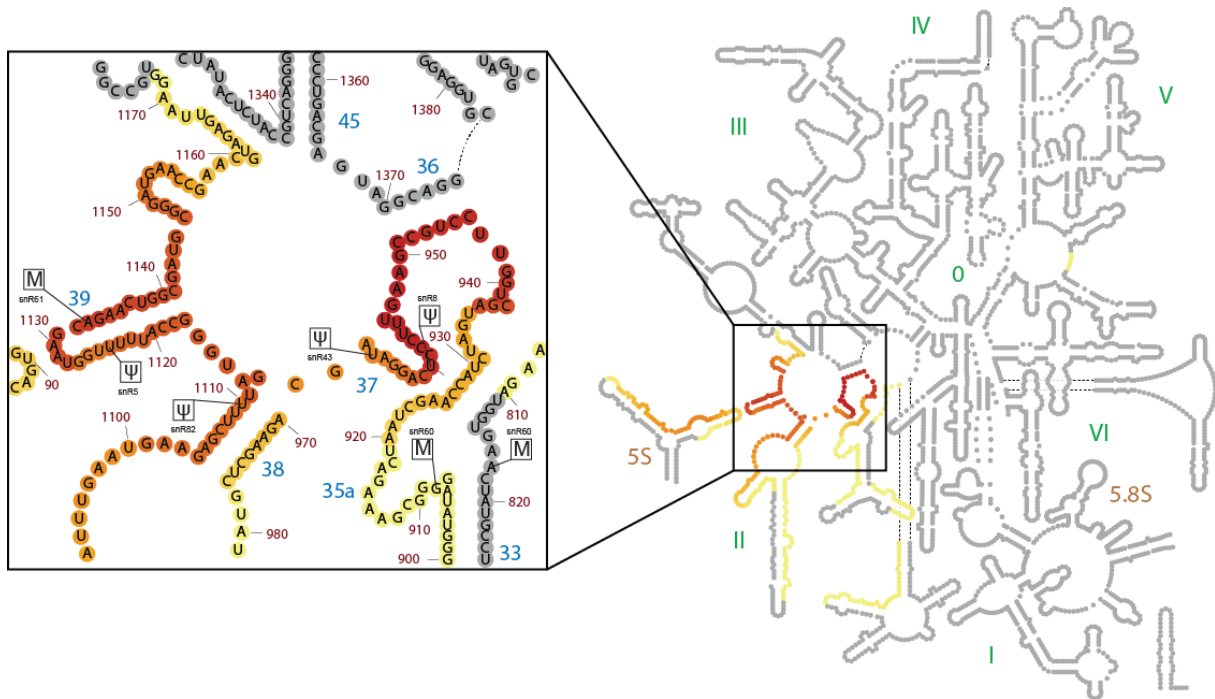
Figure 3.18: Mak5 crosslinks at helices 37 – 39 of domain II in the 25S rRNA sequence. Mak5 PAR-CRAC data depicted as colour-coded hit representation above a 10 % threshold from yellow (low value) to red (highest value) in correlation to all hits across *RDN37*. Mapping onto the secondary structure of mature LSU is shown (Petrov *et al.*, 2014a). Secondary structure elements of 25S rRNA are indicated in green. 5S and 5.8S rRNA are labelled in brown.

Not surprisingly, the two distant peaks from the primary transcript cluster together in this pre-ribosomal particle as well (Fig. 3.19A), indicative for a single binding site of the Mak5 RNA helicase. Mutations in *MAK5* have been shown to supress the phenotype of mutations in *NSA1*, suggesting that these proteins are functionally linked (Pratte *et al.*, 2013), and interestingly, the essential *trans*-acting ribosome biogenesis factor Nsa1 binds to pre-60S complexes in close proximity to the Mak5 binding site (Fig. 3.19B). Mak5 was additionally proposed to be involved in a functional cluster with Ebp2, Nop16 and promoting the formation of a certain structural surface of pre-60S complexes including assembly of ribosomal proteins Rpl6 (eL6), Rpl14 (eL14) and Rpl16 (uL13; Pratte *et al.*, 2013). Although none of the ribosomal proteins directly contacts the Mak5 crosslinking site, they are present on the surface of the pre-60S complex in close proximity to the identified Mak5 crosslinking site.

Analogous to the analysis of Spb4, DMS structure probing experiments were performed in order to confirm the crosslinking sites of Mak5 identified by CRAC as *bona-fide* protein binding sites and to explore rRNA structural changes in this region caused by lack of the helicase. Pull-

down analysis of Nop2-HTP particles had shown co-immunoprecipitation of Mak5 and late pre-rRNA precursors with these complexes, making them suitable also for analysis of Mak5 function (Fig. 3.16B/C). Primer extension analysis on DMS-treated and non-treated pre-rRNA isolated from cells in which Mak5 was present or absent, were initiated downstream of helix 39.
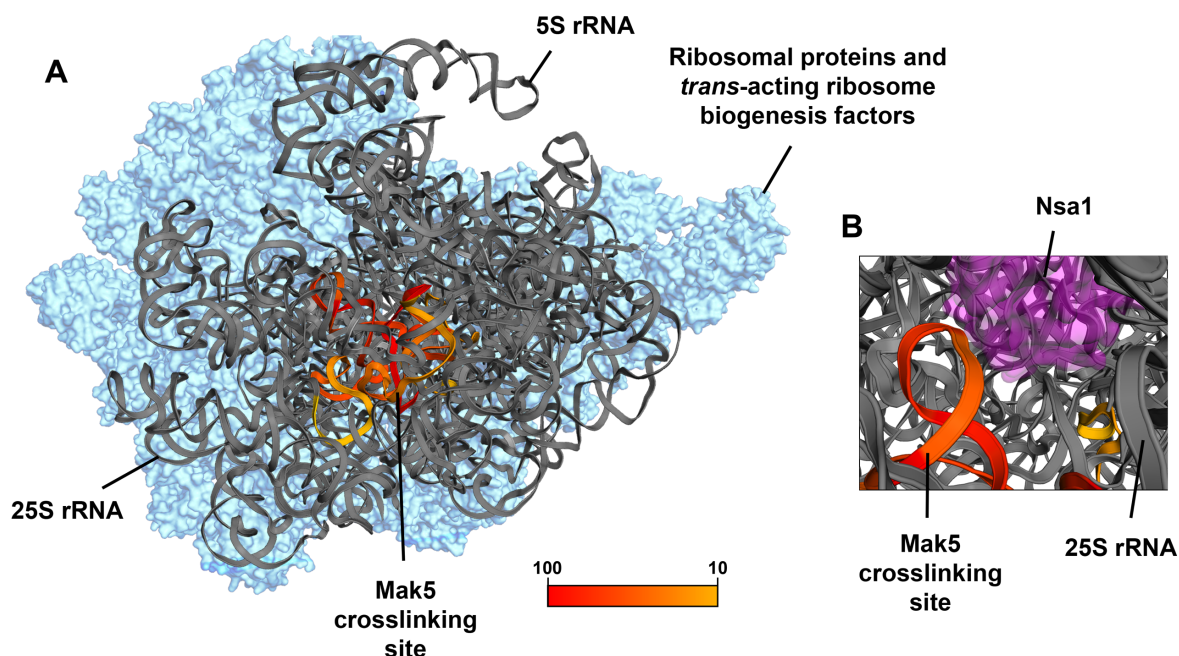
Figure 3.19: Mak5 crosslinks at helices 37 – 39 of domain II in the Nog2 pre-60S particle. (A) Mak5 PAR-CRAC data was mapped onto the 3D structure of the pre-LSU Nog2-particle (Wu *et al.*, 2016; PDB-ID: 3JCT). Colour-code reflects peak height above a 10 % threshold from yellow (low value) to red (highest value). **(B)** The magnified view shows the close proximity of the *trans*-acting ribosome biogenesis factor Nsa1 (magenta) to the Mak5 crosslinking site.

Two nucleotides in the loop of helix 39 were highly accessible for DMS modification when Mak5 was present, leading to the detection of strong primer extension stops at positions A1129 and A1130 of the 25S rRNA sequence (Fig. 3.20). Interestingly, the observed signal (and therefore the extent of DMS-mediated modification) decreased significantly in the absence of Mak5, which suggests that these nucleotides are involved in basepairing or protein-RNA interactions in earlier pre-ribosomal complexes that are dissolved if the RNA helicase is present.

Therefore, the question arose of how the DMS accessibility of these nucleotides is affected during the process of ribosome biogenesis. For this reason, a series of pre-60S particles along the pathway of LSU maturation was isolated and structure probing analysis was performed. The pre-60S biogenesis factors Ssf1, Nip7, Nop2, Erb1 and Rpf2 were selected as bait proteins for the analysis of early and middle pathway intermediate particles and Arx1 as well as Rlp24 were chosen for the affinity purification of late nuclear/cytoplasmic pre-60S

complexes. First, yeast strains expressing HTP- or TAP-tagged versions of these *trans*-acting ribosome biogenesis factors were generated. After cultivation, harvesting, cell disruption and affinity purification using IgG-sepharose, these particles were subjected to DMS treatment (or left untreated for comparison) in order to investigate the modification behaviour and therefore accessibility of A1129 and A1130 along the time line of ribosome biogenesis (Fig. 2.21).
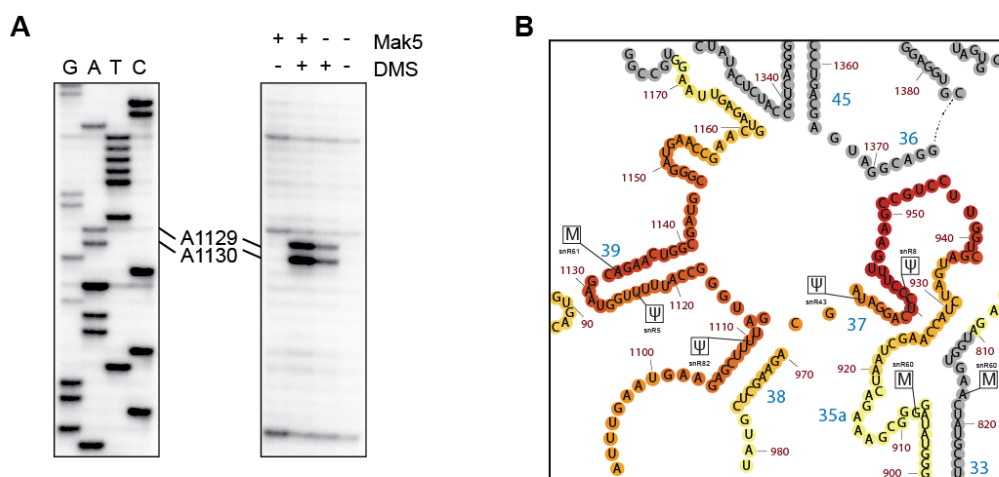
Figure 3.20: DMS structure probing confirmed Mak5 binding to helix 39 in domain II in 25S rRNA. The yeast Mak5 depletion strain containing genomically HTP-tagged Nop2 was cultivated for the appropriate depletion time of 10 h in permissive or non-permissive medium (+Mak5; -Mak5). After cell lysis, pre-60S complexes were co-immunoprecipitated using IgG-sepharose. On beads, complexes were treated with DMS (+DMS) if applicable and RNA was extracted, which was used as template for primer extension analysis, starting from a radiolabelled oligonucleotide downstream of the detected Mak5 crosslinking site. Reaction products were subjected to denaturing PAGE, so that fragments, which derived from stops in transcription due to DMS modifications, could be detected using a phosphorimager. As a reference, primer extensions were performed on total RNA after spiking in individual ddNTPs, which created a sequencing ladder. **(A)** DMS structure probing analysis of Mak5 crosslinking site in domain II of 25S rRNA. **(B)** Mak5 PAR-CRAC data mapped to the secondary structure of LSU with focus on domain II of 25S rRNA (as shown in Fig. 3.18).

Interestingly, the extent of DMS-mediated modification of A1129 and A1130 changed twice over the time-course of pre-60S biogenesis. In early particles, these nucleotides were protected from DMS treatment, suggesting that they are either basepaired or protected by the presence of a protein. However, in the case of intermediate particles, starting with the Nop2-HTP particle in which Mak5 is present and that was used in the previously described DMS structure probing experiment, these nucleotides became readily accessible for modification. This suggests that the observed transition of accessibility of A1129 and A1130 to DMS, which occurs in Nop2-HTP particles, was triggered by Mak5. Interestingly, in late pre-60S particles after their export to the cytoplasm, as well as in the mature LSU, these nucleotides again became inaccessible for modification, indicating another structural or compositional change in this region of the pre-ribosome.
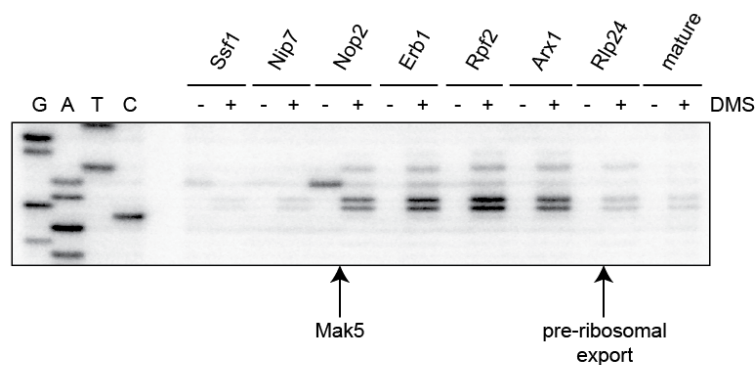
Figure 3.21: A1129 and A1130 in domain II of 25S rRNA are temporarily accessible for DMS during ribosome biogenesis. Several strains with different ProteinA-tagged *trans*-acting ribosome biogenesis factors were grown to mid-log phase. After harvesting and cell disruption, lysates were subjected to pull-down analysis and subsequent DMS treatment (-DMS; +DMS). The modification level of extracted RNA was monitored by primer extension analyses using an oligonucleotide annealing downstream of helix 39 in domain II of 25S rRNA (analogous to Fig. 3.20). Primer extensions on total RNA in the presence of ddNTPs provided the sequencing ladder on the left. Baits for co-immunoprecipitations are indicated above and arrows indicate pre-ribosomal export as well as the Nop2-particle, which contains Mak5.

Excitingly, analysis of the location of A1129 and A1130 in the structure of the mature LSU revealed that these two nucleotides are directly bound by Rpl10 (uL16; Fig. 3.22). This ribosomal protein is known to assemble late into pre-60S particles, only joining after they have been exported to the cytoplasm. Taken together, this suggests that the RNA helicase Mak5 is required at a relatively late step of LSU biogenesis for a structural rearrangement that makes helix 39 in domain II of 25S rRNA accessible for the recruitment of Rpl10 after the export of the pre-60S complex to the cytoplasm.
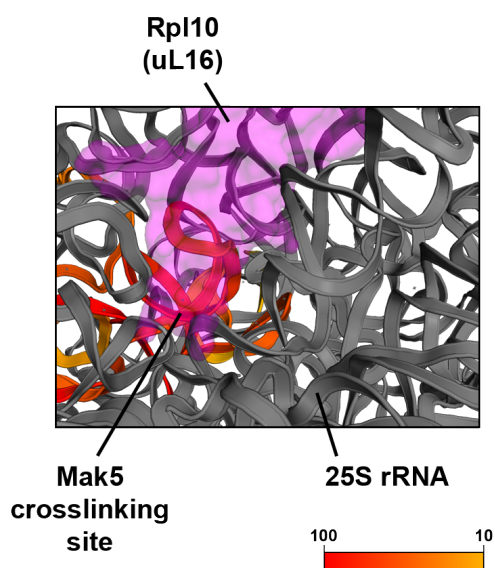
Figure 3.22: Rpl10 (uL16) binds to A1129 and A1130 in domain II of 25S rRNA in the mature large ribosomal subunit. The 3D structure of mature LSU is shown (Ben-Shem *et al*., 2011; PDB-ID: 4V88). The ribosomal protein Rpl10 is indicated in magenta and binds to the tip of helix 39, where nucleotides A1129 and A1130 are located, explaining the loss of accessibility of these residues (Fig. 3.21), when pre-60S particles are exported to the cytoplasm and Rpl10 is recruited to pre-ribosomes.

4 Discussion

4.1 Identification of the binding sites of RNA-binding proteins on cellular RNAs

RNA-binding proteins (RBPs) play key roles in the formation of ribonucleoprotein (RNP) complexes required for gene expression, such as the ribosome and the spliceosome, as well as in the regulation of different aspects of the gene expression process. Furthermore, RBPs can determine the fate of cellular RNAs by influencing their processing, assembly into RNP complexes and functions. Many RBPs contain characterised RNA-binding domains that have common structures and are relatively low in diversity. Amongst the best characterised RNA-binding domains are the RNA recognition motif (RRM), the zinc finger (ZNF), the KH domain, the S1 fold, the dsRBD and the R3H domain (Lunde *et al.*, 2007). Interestingly, many of the known RNA-binding domains are limited in their RNA sequence specificity but often particular domains favour interactions with specific types of RNAs, e.g. single-stranded RNAs, double-stranded RNAs, RNAs with 5' or 3' overhangs, etc. Furthermore, numerous enzymes that mediate processing, folding or modification of RNAs, such as nucleases, methyltransferases and helicases, form direct contacts with substrate RNAs via their catalytic sites. Often RBPs make multiple contacts with their RNA substrates via different RNA-binding motifs, which are presented in a particular structural topology, improving specific target recognition and extending the functional repertoire of RBPs.

The increasing knowledge about the importance of non-coding RNAs in gene expression and the extensive regulation of both coding and non-coding RNAs that takes place, has stimulated research into the proteins that interact with RNAs. While techniques such as RNA-seq can be used to identify transcripts that are affected by the lack of a particular protein and RIP-seq providing information about protein-RNA complexes, in order to identify targets directly contacted by RNA-binding proteins, a variety of different crosslinking and immunoprecipitation (CLIP)-based techniques with subsequent analyses of high-throughput sequencing data were established (CLIP: Ule *et al.*, 2003; HITS-CLIP: Licatalosi *et al.*, 2008; PAR-CLIP: Hafner *et al.*, 2010; iCLIP: König *et al.*, 2010). All these methods involve covalent crosslinking of associated RNAs and proteins followed by the isolation of these complexes using protein specific antibodies, which bind the RNA-binding protein of interest with high affinity. In contrast, the UV crosslinking and analysis of cDNA (CRAC) approach does not require protein specific antibodies and makes use of a His_6-TEV cleavage site-ProteinA epitope fused to the RNA-binding protein of interest enabling a tandem affinity purification including a purification step under very stringent and denaturing conditions. The CRAC approach is therefore especially useful to gain information about protein-RNA interactions in complex ribonucleoprotein

particles, such as pre-ribosomal particles or intermediates of the spliceosome, as the inclusion of the purification step under denaturing conditions ensures that only RNAs directly contacted by the protein of interest are isolated (Bohnsack *et al.*, 2012). Importantly, both the CLIP and CRAC approaches include a partial RNase digestion step in which RNAs co-purified with the protein of interest are trimmed to leave a specific footprint of the protein on its target RNA. This means that as well as identifying RNAs bound by the protein of interest, the precise binding sites of the proteins on the RNAs can be determined, which is especially relevant for proteins that bind to long RNAs, such as rRNAs and mRNAs, as it provides important insight into the potential functions of the protein binding to the RNA. For CRAC, a variety of different techniques have been reported that differ in the preparation of yeast cultures and the crosslinking wavelength. *In vivo* crosslinking describes that yeast cells were harvested, resuspended and spread onto a petri dish, where they can be irradiated on ice. *In culturo* crosslinking is carried out on actively growing yeast cells that are irradiated without harvesting, which has the advantage of capturing transient interactions and avoiding triggering stress responses that might lead to the formation of non-typical protein-RNA interactions. Irradiation can be applied at 254 nm, whereas incorporation of photoactivatable ribonucleosides like 4-thiouridine (4SU) or 6-thioguanosine (6SG) allows irradiation at 365 nm, which was shown to increase the efficiency of nucleic acid crosslinking (Hafner *et al.*, 2010). In both cases, covalent links are primarily formed between uridines in the RNAs and aromatic amino acids (e.g. tryptophan, tyrosine and phenylalanine) in the proteins, meaning that the close proximity of these features is essential for efficient protein-RNA crosslinking. For some modification enzymes like 5-methylcytosine RNA methyltransferases, alternatively, chemical crosslinking can be used. Incorporation of 5-azacytidine (5-AzaC) into nascent RNAs, traps the methyltransferase in a covalent intermediate with its target RNA during the catalytic step of the methylation reaction (Haag *et al.*, 2017). This approach has the advantage that crosslinked protein-RNA complexes are only formed during catalysis, meaning that the identified RNAs represent methylation substrates not just RNAs that are contacted by the methyltransferase. Several different alternatives for cDNA library preparation prior to next generation sequencing have also been developed for such CLIP/CRAC approaches. Typically, this involves ligation of adaptors to the 3' and 5' ends of the co-purified RNAs, which serve as a platform for reverse transcription and PCR amplification. Alternatively, following reverse transcription, a circularisation step of cDNA products using a single adapter sequence can be used to circumvent the problem of frequently occurring premature stops at the introduced crosslinking sites (König *et al.*, 2010). During the process of reverse transcription, the reverse transcriptase is prone to stalling or pausing at nucleotides that are crosslinked to amino acids remaining after protease digestion. This behaviour can be advantageous if the reverse transcriptase overcomes this site by misincorporation of a random nucleotide, which is most likely an

adenine, or by skipping the lesion, thereby generating a specific reverse transcriptase signature that can be detected during the subsequent bioinformatics analysis. In the PAR-CRAC approach, it was shown that at sites of crosslinking, which are restricted to the PAR-CRAC specific 4SU residue, the reverse transcriptase incorporates an adenine because it reads this nucleotide as a thymine. This characteristic can be selected for bioinformatically during analysis of the obtained sequence reads allowing to differentiate reads that are derived from specific crosslinking events from reads that come from background RNAs (Ascano *et al*., 2012).

With UV-CRAC and PAR-CRAC, two alternative crosslinking methods were applied in this study. For technical reasons, the UV-CRAC protocol was coupled to *in culturo* irradiation, whereas the PAR-CRAC approach was performed using *in vivo* irradiation. For Spb4, both the PAR- and UV-CRAC had similar crosslinking efficiencies and also, mapping of the sequence reads indicated the same crosslinking sites on the 25S rRNA. However, for both Has1 and Mak5, only the PAR-CRAC method crosslinked the proteins efficiently to their RNA target and allowed subsequent data analysis. Spb4 is proposed to be recruited to early pre-ribosomal complexes but remains associated until the later stages of pre-60S maturation. In contrast, the interactions of Has1 and Mak5 with pre-ribosomal complexes is thought to be much more transient. This hypothesis is supported by our observations that in a series of pull-down experiments, which represented a time course of the pathway of ribosome biogenesis, Has1 and Mak5 could hardly be detected in different pre-ribosomal particles whereas Spb4 could readily be detected (data not shown). It is possible therefore that the transient interactions of Mak5 and Has1 with pre-ribosomes prevented efficient crosslinking with UV, but that the increased crosslinking efficiency of the PAR-CRAC approach (Hafner *et al*., 2010) enabled Has1 and Mak5 to be stably bound to their substrate RNAs. Studies analysing the behaviour of mutant RNA helicases indicated that some mutants, e.g. the DEAD mutant used in this study, cannot be recycled from their substrates, suggesting that an alternative version of the CRAC protocol using a catalytically inactive protein could increase the crosslinking efficiency of helicases that normally only transiently bind to RNA. Additionally, if applied in parallel to CRAC of a WT helicase, the RNA sites that are contacted by the helicase core or by ancillary domains, which do not rely on the helicase function, could be differentiated. Interestingly, such an approach was applied to investigate the binding sites of the translocating human SF1-RNA helicase MOV10 (Gregersen *et al*., 2014). In contrast to DEAD-box proteins, translocating RNA helicases show a more dispersed distribution along their target RNAs, with the majority of sequence reads corresponding to their starting and end positions on the RNA substrate, where they have an increased residence time. Using a MOV10 helicase deficient mutant in PAR-CLIP analysis revealed an enrichment of sequence reads upstream of highly structured

3'UTRs of mRNAs, implying that these structures are resolved by the translocation of MOV10 along the RNA (Gregersen *et al*., 2014).

In the case of Has1, Spb4 and Mak5, the target RNAs could already be anticipated from the finding that these proteins are required for biogenesis of the large ribosomal subunit. However, the genome-wide characteristic of the CRAC approach enables an unbiased search for substrate RNAs of an uncharacterised protein without prior knowledge. Such unbiased approaches recently allowed the identification of the target sites of the uncharacterised human methyltransferases NSUN3 and NSUN6, which methylate the mitochondrial tRNA^{Met} and generate m^{5}C72 on a subset of cytoplasmic tRNAs, respectively (Haag *et al*., 2015; Haag *et al*., 2016). In the case of mRNA-interacting proteins, hits on specific subsets of mRNAs can be identified using the CRAC approach coupled with a bioinformatics peak calling approach and the relative distribution of crosslinking sites in mRNA features (e.g. 5'UTR, start codon, ORF, stop codon, introns and 3'UTR) can be monitored. For example, a novel level of translational control of gene expression was uncovered, where the DEAD-box RNA helicase Dhh1 unwinds highly structured regions especially in the 5'UTR and beginning of ORFs in order to facilitate ribosome translocation on mRNAs mainly encoding secreted or membrane proteins (Jungfleisch *et al*., 2017).

4.2   Recruitment and regulation of RNA helicases

In particular for multifunctional RNA helicases that have more than one target RNA, the mechanism of recruitment to its RNA targets remains an important question. Although RNA helicases are predicted to have almost no sequence specificity as their core domains primarily interact with the RNA backbone, a sequence motif within its target RNA of 23S rRNA was reported for the *E. coli* DEAD-box RNA helicase DbpA (Fuller-Pace *et al*., 1993). N- and C-terminal extensions of RNA helicases in proximity to the helicase core are proposed to mediate substrate specificity, potentially by forming sequence specific interactions with RNA substrates. Therefore, for multifunctional proteins for which many target RNAs can be identified, nucleotide motifs within the retrieved CRAC sequence reads can be examined using bioinformatics software tools. Additionally, other possible mechanisms of recruitment and enzymatic regulation are thought to be mediated through specific secondary or tertiary structural features of RNA substrates and/or cofactor interactions.

Several RNA helicase cofactors have been identified so far although it is likely that many more remain to be discovered. For example, in yeast ribosome biogenesis, Rrp5 was proposed to interact with the DEAD-box RNA helicase Rok1, which is implicated in the release of snR30 from pre-ribosomes (Vos *et al*., 2004; Bohnsack *et al*., 2008; Young *et al*., 2013) and the RNA helicase Dbp8 was shown to be recruited to pre-ribosomal complexes by its interaction with Esf2, which additionally also stimulates the ATPase activity of the protein (Granneman *et al*.,

2006a). In contrast, the mRNA binding protein Yra1 was reported to inhibit the unwinding activity of Dbp2 (Ma *et al.*, 2013). A common structural fold that is present in numerous RNA helicase cofactors is the MIF4G-domain that mediates interactions with DEAD-box helicases of the eIF4A-like family. Synergistic stimulating effects were observed for the interaction between eIF4A and its cofactors eIF4G and eIF4B in the context of translation initiation (Nielsen *et al.*, 2011; Andreou and Klostermeier, 2014). Interestingly, the MIF4G-domain containing protein Gle1 was reported to independently modulate the activity of two RNA helicases, Ded1 and Dbp5, playing a role in translation initiation as well as in mRNA export (Weirich *et al.*, 2006; Aryanpur *et al.*, 2017). G-patch proteins are another known family of cofactors, which regulate the recruitment and activity of RNA helicases by interactions formed between their characteristic glycine-rich region and the OB-fold of DEAH-box helicases. Excitingly, several G-patch proteins were shown to compete for the interaction with the multifunctional DEAH-box RNA helicase Prp43, influencing its subcellular localisation for directing the protein to its different functional sites (Heininger *et al.*, 2016). Another interesting model of helicase recruitment was reported for the mitochondrial DEAD-box protein Mss116, which is implicated in splicing of group I and group II introns (Huang *et al.*, 2005). This protein contains a basic tail containing several positively charged amino acids at the C-terminus, which was proposed to tether the helicase to structured RNA substrates, which promotes unwinding activities of neighbouring RNA duplexes (Mohr *et al.*, 2008; Mallam *et al.*, 2011). Due to the multitude of *trans*-acting factors that are present on pre-ribosomes at the same time, the identification of RNA helicase cofactors in the context of ribosome biogenesis remains a major challenge. In addition to the action of dedicated protein cofactors, the activity of RNA helicases can be regulated in other ways. For example, the activity of the human DEAD-box protein DDX21 was recently shown to be regulated by binding of the SLERT lncRNA (Xing *et al.*, 2017). Also, the action of DDX21 on R-loops was shown to be post-translationally regulated by acetylation, which is carried out by CBP for inhibition and deacetylation mediated by SIRT7 activates the protein (Song *et al.*, 2017).

By applying CRAC, we were able to determine the interaction sites of Has1, Spb4 and Mak5 on pre-ribosomal complexes. Identification of distinct crosslinking sites of Has1 on the 18S rRNA as well as on the 25S rRNA, to which Has1 likely binds at separate times during ribosome biogenesis, suggests specific recruitment mechanisms for its functions in the biogenesis of each of the ribosomal subunits. A dedicated protein cofactor has not been identified for Has1 so far, but it is likely that the association of Has1 with pre-40S and pre-60S complexes involves specific protein interactions, which may either be formed on the pre-ribosome or Has1 may be recruited as part of a protein subcomplex. It is proposed that Mak5 interacts only very transiently with its target site in 25S rRNA suggesting that recruitment to the pre-ribosome is concomitant with the use of its RNA helicase activity, thereby triggering its rapid recycling.

Genetic interaction studies defined a functional cluster of proteins composed of Mak5, Ebp2, Nop16, Rpf1 and Rpl14 (eL14) and it was suggested that these proteins provide a structural interface promoting the recruitment of Mak5 to its RNA substrate (Pratte *et al.*, 2013). Mapping the Mak5 binding site on the Nog2 pre-60S particle revealed that Rpl14 does not directly contact the rRNA sequence bound by Mak5, but it is located in close proximity at the surface of this particle. Given the relatively large size of the Mak5 protein, it is likely that Mak5 and Rpl14 may contact each other on the pre-ribosome, which would be consistent with their inter-dependent recruitment to pre-60S particles.

In contrast to the transient pre-ribosome binding of Mak5, Spb4 is recruited early to pre-ribosomal particles and is released relatively late in the pathway, but prior to export of pre-60S particles. This suggests that the recruitment and RNA helicase activity of Spb4 are uncoupled. Spb4 was proposed to be part of a hierarchical recruitment pathway for factors involved in pre-60S biogenesis; Spb4 needs the Rpf2-subcomplex to be recruited to pre-ribosomes and in turn, Spb4 is required for the recruitment of the GTPase Nog2 (Talkish *et al.*, 2012). Interestingly, the binding site of Spb4 in helices 62 and 63 of the 25S rRNA is in close proximity to the position of Nog2 determined in a recent cryo-EM structure of a pre-ribosomal complex, suggesting a direct link between Spb4 and Nog2. In line with this, it was further proposed that Nog2 might regulate the activity of Spb4 (Talkish *et al.*, 2012), but it remains to be determined if this is the case.

Interestingly, sequence analysis of Mak5 and Spb4 revealed that both proteins contain numerous positively charged amino acids at their C-terminus beyond the conserved helicase core domain, reminiscent of the C-terminal end of Mss116, which provides a platform for interactions with a helix structure in its RNA substrate. This raises the possibility that the basic tails of Spb4 and Mak5 similarly contribute to the interactions of these proteins with their ribosomal RNA substrates. For Mak5 it was shown in truncation experiments that its C-terminal tail is essential for the function of Mak5, but it is still unclear if the C-terminus is involved in recognition of the RNA target or if it is involved in mediating cofactor interactions (Pratte *et al.*, 2013). Interestingly, the interaction site of Spb4 at the 3' end of 25S rRNA (Fig. 3.14) constitutes a helical secondary structure, similar to the structure bound by the C-terminus of Mss116, making this a likely candidate for such an RNA interaction platform. This model is further supported by our structure probing analysis, which indicates that this region of the 25S rRNA might be bound, but not remodelled by Spb4. To determine the regions/amino acids of Spb4 that contact the rRNA, a mass spectrometry-based approach focusing on protein components crosslinked or bound to the RNA could provide additional information about the 25S rRNA-Spb4 interaction sites on the protein level and further support our hypothesis that the two Spb4 crosslinking sites on the 25S RNA represent a binding platform and a functional site. It is possible that Spb4 is recruited to its binding platform with the help of the Rpf2-

subcomplex and its basic C-terminal end to rRNA as soon as the 3' end of 25S rRNA is synthesised. Spb4 would then remain bound until the helicase core has access to its functional site, which could be prevented during the early stages of pre-60S biogenesis by steric hindrance. The interaction of Spb4 with its functional site could promote the recruitment of Nog2 and stimulate ATP hydrolysis by Spb4, triggering its release from pre-60S.

4.3 Diverse functions of RNA helicases in ribosome biogenesis

Regulating snoRNA levels on pre-ribosomes is the best described function of RNA helicases involved in ribosome biogenesis and links these proteins to the functions carried out by the interacting snoRNPs. As box C/D snoRNAs form long basepairing interactions with their target rRNA (up to 21 nts), the release of some snoRNAs after they have successfully performed their functions has been suggested to require the unwinding activity of RNA helicases. This can influence rRNA modification either by releasing snoRNAs that have overlapping basepairing sites to enable modification of adjacent or nearby sites by successive snoRNAs. Alternatively, as some snoRNAs guide modifications at more than one site in the rRNAs, helicase-mediated release of such snoRNAs may help efficient recycling, ensuring that sufficient amounts of snoRNAs are available for modification of newly synthesised pre-rRNA. Finally, RNA helicases may also remodel rRNA-rRNA interactions that prevent efficient basepairing of snoRNAs with their target sites in the pre-rRNA. Such pre-ribosome remodelling by the RNA helicase Prp43 has been suggested to enable the pre-ribosomal recruitment of the snoRNAs snR64 and snR67 (Bohnsack *et al*., 2009), and a corresponding decrease in the extent of 2'-*O*-methylation at C2337 guided by snR64 in cells lacking Prp43 was reported (Leeds *et al*., 2006). Interestingly, a sequencing based method for monitoring the levels of 2'-*O*-methylation in rRNA (RiboMeth-Seq) revealed partial modification of several residues targeted by box C/D snoRNAs (Birkedal *et al*., 2015). By regulating the levels of snoRNAs on pre-ribosomes, RNA helicases contribute to regulating the modification pattern of rRNAs. Together with alternative pre-rRNA processing and incorporation of different RP paralogs, the detection of substoichiometic rRNA modifications strengthens the model of ribosome heterogeneity. This model suggests the presence of ribosomes with different composition and specificity, to promote expression of specific mRNAs in response to different cellular stresses, during particular developmental phases and to modulate protein expression levels in different tissues or subcellular localisations.

In addition to their functions in guiding snoRNP-mediated rRNA modifications, snoRNAs are also implicated in maintaining an open rRNA conformation in early pre-ribosomes to allow efficient recruitment of other snoRNPs, *trans*-acting ribosome biogenesis factors and ribosomal proteins. However, binding of snoRNAs to sites within the rRNAs also affects secondary and tertiary structure formation. For example, basepairing interactions by the

snoRNA U3 are required for central pseudoknot formation, which is a conserved structural fold in the small ribosomal subunit essential for translation (Dutca *et al*., 2011). Furthermore, binding of other snoRNAs to sites in rRNA, which are distant on the primary sequence, establishes long-range rRNA interactions that bring rRNA sequences in close proximity to form new basepairing interactions (Martin *et al*., 2014). The RNA helicases Dhr1 and Rok1 are required for the release of U3 and snR30 respectively from pre-40S complexes, enabling progress of the pre-40S maturation pathway once these structural features have been established (Martin *et al*., 2014; Sardana *et al*., 2015). In this study, the identification of the binding sites of the DEAD-box RNA helicase Has1 on 18S rRNA and U14 (Fig. 3.4 – 3.7) supported its proposed function in mediating the release of U14 (Liang and Fournier, 2006). Interestingly, U14 has maintained both snoRNA functions in 2'-*O*-methylation of 18S-C414 and bringing distant 18S rRNA helices of the 18S rRNA 5' domain into close proximity and it therefore forms several basepairing interactions with the 18S rRNA. CLASH hybrids within the obtained CRAC data provided evidence for a basepairing interaction between U14 and 18S rRNA while Has1 is present on the pre-40S complex (Fig. 3.6). Taken together with the crosslinking of Has1 to the 18S rRNA and U14 sequences involved in forming basepairing interactions, this suggests that the observation of U14 accumulation on pre-ribosomes in the absence of Has1 (Fig. 3.13) could be a direct effect. The RNA helicase Dbp4 was also reported to be required for the release of the U14 snoRNA from pre-ribosomes (Liang *et al*., 1997), which could suggest either a partial redundancy with Has1 in directly releasing U14 or that an indirect effect is responsible for U14 accumulation on pre-ribosomes in the absence of Dbp4. Notably, a second identified crosslinking site of Has1 on the 18S rRNA, which is distant on the mature small ribosomal subunit (Fig. 3.4, 3.5 and 3.7) was also identified. On the one hand, it is possible that this region of the 18S rRNA is closer to the U14 basepairing sites in a pre-SSU conformation and that these two separate crosslinking sites actually represent binding of a single protein, and that crosslinking of Has1 to this site also reflects the role of this protein in mediating U14 release. Similar to the model for Spb4, it is possible that the two binding sites correspond to rRNA interactions made by different domains of Has1. On the other hand, the crosslinking sites of Has1 at helices 30 - 35 in the 3' major domain of the 18S rRNA could derive from a second hitherto unknown function of Has1 during pre-40S biogenesis.

RNA helicase function is typically connected to structural transitions in RNAs. As well as mediating the release of snoRNAs, which triggers conformational changes in the rRNA, structural transitions in the context of rRNA-rRNA interactions are another proposed function for RNA helicases, and this can lead to a variety of consequences during biogenesis of the ribosomal subunit. Like this, the DEAH-box RNA helicase Prp43 is required for efficient D site cleavage by the endonuclease Nob1 (Pertschy *et al*., 2009). Structural transitions in rRNA as a result of RNA helicase action also can induce compositional changes in pre-ribosomal

complexes, if the affected structure promotes efficient binding, or triggers release, of *trans*-acting ribosome biogenesis factors or ribosomal proteins.

The function of the DEAD-box RNA helicase Has1 in LSU biogenesis appears to be uncoupled from its snoRNA release function in SSU biogenesis. In previous publications, Has1 was suggested to mediate the release of several *trans*-acting ribosome biogenesis factors from pre-60S particles (Dembowski *et al.*, 2013). The six affected biogenesis factors, including a trimeric subcomplex composed of Nop7-Erb1-Ytm1, functionally cluster together and are required after pre-rRNA cleavage at site A_3 for downstream steps of ribosome biogenesis (Miles *et al.*, 2005). Interestingly, Ytm1 is homologous to Rsa4 and both proteins share a structural motif that mediates their interaction with the MIDAS domain of the AAA-ATPase Rea1 and it was shown that Rea1 removes both proteins from pre-60S particles (Baßler *et al.*, 2010; Thoms *et al.*, 2016). It was further proposed that the removal of Ytm1 triggers the release of its interaction partner Erb1 (Thoms *et al.*, 2016), whereas, in contrast, the removal of Rsa4 does not induce the release of its interaction partner Nsa2, which was predicted to form stronger pre-rRNA interactions (Baßler *et al.*, 2010). These observations, together with our data showing that the 25S rRNA crosslinking site of Has1 overlaps with the binding site of Erb1 (Fig. 3.8; Granneman *et al.*, 2011), suggest a model where the RNA helicase Has1 weakens the pre-rRNA interactions of Erb1, ultimately leading to its release from the pre-60S particle through its interactions with Ytm1 and Rea1. Removal of these "A_3-cluster" factors was proposed to allow pre-rRNA rearrangements and subsequent binding of other *trans*-acting ribosome biogenesis factors promoting turnover of ITS2 (Konikkat *et al.*, 2017).

The identified binding site of Spb4 in helices 62 and 63 of the 25S rRNA could also indicate a structural transition during late pre-60S biogenesis (Fig. 3.14). This Spb4 crosslinking site is located at the base of a eukaryotic expansion segment (ES27), which appears to be very flexible at earlier stages of ribosome biogenesis (Bradatsch *et al.*, 2012), whereas its position on the pre-ribosome is restricted during pre-60 export by its interaction with the export adaptor Arx1. Our DMS structure probing experiment of this region in the presence of Spb4 resembles the structural composition in mature large ribosomal subunits. However, in the absence of Spb4, the mature rRNA structure of this region seems not to be formed yet, allowing a higher degree of flexibility for ES27 (Fig. 3.17). Co-immunoprecipitation experiments from various publications indicate that Arx1 and Spb4 are not present in the same pre-60S particles, suggesting that the remodelling activity of Spb4 at helices 62 and 63 of 25S rRNA and the subsequent release of Spb4 might be required for efficient recruitment of Arx1 to pre-ribosomal particles. To test this hypothesis, we have generated yeast strains that allow the isolation of late pre-60S complexes from cells that contain Spb4 or where Spb4 is depleted. With these strains, we will monitor the level of Arx1 on pre-60S complexes upon depletion of Spb4 and a decrease in the amount of Arx1 detected would support the hypothesis that Spb4 is required

for Arx1 recruitment to ES27. As mentioned earlier, Spb4 is required for the pre-ribosome recruitment of Nog2, which also associates in close proximity to ES27. Interestingly, Nog2 acts as a placeholder for the essential export factor Nmd3 meaning that the action of Spb4 on helices 62 and 63 of the 25S rRNA might facilitate recruitment of another export factor, Arx1. Thus, Spb4 might play an important function in generating export competence of pre-ribosomal particles. How these processes are physically and/or regulatory interconnected should be addressed by further research. This model is proposed based on the proximity of the identified Spb4 crosslinking site and the binding sites of Arx1 and Nog2 as shown by cryo-EM structures of pre-60S complexes. However, it is also possible that remodelling of helices 62 and 63 of the 25S rRNA by Spb4 leads to long range conformational changes that affect other regions of the pre-ribosome. Therefore, an experiment combining DMS structure probing and next generation sequencing to monitor changes in the DMS modification pattern along the entire length of the 25S rRNA in the presence or absence of Spb4 would be a powerful tool to analyse the conformational changes in a whole range of pre-60S particles. A similar approach was already used in order to define the flexibility of pre-rRNA in late pre-40S particles, which could not be detected by the use of cryo-EM reconstructions (Hector *et al.*, 2014).

The Mak5 binding site in 25S rRNA identified in this study allowed further functional studies into the structural and compositional transitions that take place within domain I of pre-60S ribosomal subunits. After confirmation of the putative Mak5 binding site in helix 39 of the 25S rRNA by DMS structure probing (Fig. 3.20), the observed changes in the intensity of DMS-specific modification of A1129 and A1130 at the very tip of helix 39 upon depletion of Mak5 prompted us to further investigate the interactions of these two nucleotides in the temporal context of ribosome synthesis. Intriguingly, applying DMS structure probing to a series of purified pre-60S complexes revealed two structural transitions involving A1129 and A1130 along the pathway of 60S biogenesis (Fig. 3.21). The two adenines were protected from DMS modification during the early stages of LSU biogenesis until the Nop2-particle was formed. Importantly, this is the pre-60S particle where it could be shown that the accessibility of A1129 and A1130 is dependent on the presence of Mak5 (Fig. 3.20). As helix 39 in mature ribosomes constitutes a stem-loop structure, rather than being composed of sequences from distance regions of the pre-rRNA transcript, it is unlikely that this sequence participates in alternative basepair interactions, which would need additional help for being formed. In contrast, we speculate that Mak5 might rather be involved in the release of an unidentified *trans*-acting ribosome biogenesis factor, which binds to helix 39 during the early steps of ribosome assembly. However, in cytoplasmic pre-ribosomal complexes, as well as in mature ribosomes, A1129 and A1130 were no longer exposed to modification by DMS (Fig. 3.21). Investigating the position of these nucleotides in the available crystal structures of mature 60S subunits revealed that A1129 and A1130 are buried within a binding pocket of Rpl10 (uL16), a ribosomal

protein, which is known to be recruited to pre-ribosomes at a very late and cytoplasmic step (Fig. 3.22; Hedges *et al*., 2005). Therefore, we concluded that the presence, and most likely the unwinding activity, of the DEAD-box protein Mak5 during the nuclear steps of ribosome biogenesis is required for efficient binding of Rpl10 to domain I of 25S rRNA. Interestingly, as well as being an essential component of the mature LSU, together with the cytoplasmic GTPase Lsg1, binding of Rpl10 facilitates the release of Nmd3 and preventing the stable association of Rpl10 was suggested to affect the dynamics of Nmd3 loading, which impairs the export of pre-ribosomal particles (West *et al*., 2005; Hofer *et al*., 2007). It was also shown that mutations in Mak5 are able to suppress the phenotype of mutations in the essential *trans*-acting ribosome biogenesis factor Nsa1 (Pratte *et al*., 2013). Excitingly, Nsa1 binds to pre-60S complexes in very close proximity to the identified binding site of Mak5, suggesting a potential interplay between these proteins (Fig. 3.19). Future experiments will investigate on the one hand, which ribosome biogenesis factor binds to helix 39 during the early stages of 60S biogenesis and requires the help of Mak5 to be efficiently released from pre-ribosomes, and, on the other hand, explore how Mak5 and Nsa1 might be functionally linked.

In eukaryotes, 21 RNA helicases, including 16 DEAD-box proteins, are implicated in ribosome biogenesis and this work alongside various other studies, suggests that the action of these enzymes has diverse effects on pre-ribosome assembly. In general, the suggested helicase functions in the biogenesis of the large ribosomal subunit are related to conformational and compositional changes that promote a more compact pre-60S structure, i.e. the release of snoRNAs that help maintain an open pre-rRNA structure and the release of *trans*-acting biogenesis factors. However, it is likely that all these enzymes have the same functions on a molecular level. This raises the question of why so many different helicases are required during ribosome biogenesis. It is likely that each helicase is optimised for a specific task through its interactions with other proteins. Although the ATPase activity of Mak5 and Spb4 was found to be essential for their functions in pre-60S biogenesis, the presence of these proteins is probably also important for subunit maturation. The large number of RNA helicases required for eukaryotic ribosome biogenesis compared to prokaryotic ribosome biogenesis, likely reflects that complexity of this process. This is due to the larger size of the rRNAs and the numerous additional ribosomal proteins that are present on eukaryotic ribosomes, meaning numerous structural transitions are required during subunit assembly.

It is important that this complicated pathway takes place correctly as ribosome biogenesis has a high metabolic cost (Warner, 1999) and only functional ribosomes should be produced so that translation of cellular proteins is efficient and accurate. The structural transitions induced by energy-driven enzymes such as RNA helicases promote the progression and directionality of the pathway, and can therefore provide a platform for quality control checkpoints. Quality control mechanisms for pre-ribosomal subunits have been suggested; a model was proposed

where degradation of ribosome biogenesis intermediates is kinetically controlled and RNA in kinetically trapped pre-ribosomal particles gets oligoadenylated by the TRAMP complex, which activates rRNA degradation by the nuclear exosome (Houseley *et al*., 2006; Karbstein, 2009). Once in the cytoplasm, non-functional ribosomes trapped on mRNAs are identified as stalled translation machineries, and are resolved with the help of Hbs1 and Dom34, which promotes subsequent degradation of the ribosomal subunits and the bound mRNA by exonucleases in a pathway called NRD (non-functional ribosome decay) (reviewed in Lafontaine *et al*., 2010).

4.4   Analysis of structural transitions during LSU biogenesis

Innovative technical advances like new direct detectors in cryo-EM have significantly improved the resolution and number of available structures of mature ribosomes and pre-ribosomal complexes, which has significantly enhanced our understanding of structural composition and transitions taking place at late stages during LSU biogenesis. During the late stages of LSU biogenesis, a more compact pre-60S structure is formed ready for nucleo-cytoplasmic transport, minimising the heterogeneity of purified pre-ribosomal complexes and making determination of their structures possible. The already available structures of late pre-60S complexes have revealed the 5S RNP rotation as a prerequisite for export of pre-ribosomal particles and identified the positions of still attached ITS2 sequences and their interactions with associated factors, providing valuable insights into the structural dynamics of these particles (Biedka *et al*., 2017). Notably, the pre-ribosomal complexes purified via a given bait protein constitute a non-homogenous mixture of several pre-60S intermediates. Of the to date earliest resolved pre-60S structure, the Nog2-particle, three major structural forms were detected and could be differentiated by advanced computational analysis (Wu *et al*., 2016). The appearance and loss of additional masses, which clustered around the subunit interface and could be assigned as specific *trans*-acting ribosome biogenesis factors by crosslinking coupled with mass spectrometry, revealed the dynamic association and dissociation of assembly factors during this phase of LSU biogenesis. Together with the conformational changes observed in ITS2 and its subsequent removal, these structures provided insights into the construction of important functional regions within 60S subunits, namely the peptidyl transferase centre and the peptidyl exit tunnel (Biedka *et al*., 2017).

Structure determination of even earlier pre-ribosomal particles represents a major challenge, as the rRNA exhibits more flexibility and multiple conformational and compositional changes occur at the same time at different sites across the pre-ribosome. Nevertheless, further structural information regarding earlier ribosome biogenesis intermediates can also be obtained by structural methods with lower resolution (e.g. negative stain electron microscopy) as well as classical genetic and biochemical approaches, such as genetic interaction screens, co-immunoprecipitations of pre-ribosomal particles, protein-protein interaction studies,

purification and structural analysis of pre-assembled pre-ribosomal subcomplexes, identification of protein-rRNA interaction sites by CRAC and chemical structure probing of pre-rRNA. Since structural transitions are frequently co-ordinated by the function of energy-consuming enzymes such as RNA helicases, the identification of the binding sites of such factors on pre-ribosomes provides important information regarding transitions they might regulate, and enables further functional studies to understand the transitions to be carried out.

In this study, the binding sites of three RNA helicases, Has1, Spb4 and Mak5 on pre-ribosomal complexes were identified. Although these proteins carry out the same biochemical activity on a molecular level, namely unwinding of RNA duplexes, the physiological consequences of their actions in ribosome biogenesis differ. Has1 was shown to crosslink to 18S rRNA and to the U14 snoRNA indicating a direct role in releasing U14 from pre-40S particles (Fig. 3.6; Liang and Fournier, 2006). The overlapping binding site of Has1 with the *trans*-acting ribosome biogenesis factor Erb1 supports the observation that Has1 is involved in the release of the Erb1-Ytm1 subcomplex from pre-60S subunits, a step which also involves the AAA-ATPase Rea1 and is required for subsequent C_2-cleavage and turnover of the ITS2 sequence (Fig. 3.8; Konikkat *et al*., 2017). Identification of the binding sites of Spb4, together with DMS structure probing experiments, indicates a structural rearrangement involving the expansion segment ES27, which is subsequently tethered by Arx1 for efficient export of pre-ribosomal particles into the cytoplasm (Fig. 3.14 and 3.17) and also provides mechanistic insight into the role of Spb4 in recruitment of Nog2 to pre-60S particles. Structural probing addressing the pre-rRNA structure in vicinity of the identified Mak5 binding site revealed that Mak5 is required for a structural rearrangement that is important for efficient recruitment of Rpl10 in the cytoplasm (Fig. 3.21 and 3.22). Together, these findings expand the knowledge of the functions of RNA helicases in ribosome biogenesis as well as the structural and compositional changes that occur during the biogenesis of ribosomal subunits.

References

Alcazar-Roman AR, Tran EJ, Guo S, Wente SR (2006) Inositol hexakisphosphate and Gle1 activate the DEAD-box protein Dbp5 for nuclear mRNA export. *Nature cell biology* **8**: 711-716.

Alexander RD, Barrass JD, Dichtl B, Kos M, Obtulowicz T, Robert MC, Koper M, Karkusiewicz I, Mariconti L, Tollervey D et al. (2010) RiboSys, a high-resolution, quantitative approach to measure the in vivo kinetics of pre-mRNA splicing and 3'-end processing in Saccharomyces cerevisiae. *RNA (New York, NY)* **16**: 2570-2580.

Allmang C, Kufel J, Chanfreau G, Mitchell P, Petfalski E, Tollervey D (1999) Functions of the exosome in rRNA, snoRNA and snRNA synthesis. *The EMBO journal* **18**: 5399-5410.

Andreou AZ, Klostermeier D (2014) eIF4B and eIF4G jointly stimulate eIF4A ATPase and unwinding activities by modulation of the eIF4A conformational cycle. *Journal of molecular biology* **426**: 51-61.

Arenas JE, Abelson JN (1997) Prp43: An RNA helicase-like factor involved in spliceosome disassembly. *Proceedings of the National Academy of Sciences of the United States of America* **94**: 11798-11802.

Armache JP, Jarasch A, Anger AM, Villa E, Becker T, Bhushan S, Jossinet F, Habeck M, Dindar G, Franckenberg S et al. (2010a). Cryo-EM structure and rRNA model of a translating eukaryotic 80S ribosome at 5.5-A resolution. *Proceedings of the National Academy of Sciences of the United States of America* **107**: 19748-19753.

Armache JP, Jarasch A, Anger AM, Villa E, Becker T, Bhushan S, Jossinet F, Habeck M, Dindar G, Franckenberg S et al. (2010b). Localization of eukaryote-specific ribosomal proteins in a 5.5-A cryo-EM map of the 80S eukaryotic ribosome. *Proceedings of the National Academy of Sciences of the United States of America* **107**: 19754-19759.

Aryanpur PP, Regan CA, Collins JM, Mittelmeier TM, Renner DM, Vergara AM, Brown NP, Bolger TA (2017) Gle1 regulates RNA binding of the DEAD-box helicase Ded1 in its complex role in translation initiation. *Molecular and cellular biology*.

Ascano M, Hafner M, Cekan P, Gerstberger S, Tuschl T (2012) Identification of RNA-protein interaction networks using PAR-CLIP. *Wiley interdisciplinary reviews RNA* **3**: 159-177.

Banroques J, Cordin O, Doere M, Linder P, Tanner NK (2008). A conserved phenylalanine of motif IV in superfamily 2 helicases is required for cooperative, ATP-dependent binding of RNA substrates in DEAD-box proteins. *Molecular and cellular biology* **28**: 3359-3371.

Barrio-Garcia C, Thoms M, Flemming D, Kater L, Berninghausen O, Bassler J, Beckmann R, Hurt E (2016). Architecture of the Rix1-Rea1 checkpoint machinery during pre-60S-ribosome remodeling. *Nature structural & molecular biology* **23**: 37-44.

Baßler J, Kallas M, Pertschy B, Ulbrich C, Thoms M, Hurt E (2010) The AAA-ATPase Rea1 drives removal of biogenesis factors during multiple stages of 60S ribosome assembly. *Molecular cell* **38**: 712-721.

Baudin-Baillieu A, Fabret C, Liang XH, Piekna-Przybylska D, Fournier MJ, Rousset JP (2009) Nucleotide modifications in three functionally important regions of the Saccharomyces cerevisiae ribosome affect translation accuracy. *Nucleic acids research* **37**: 7665-7677.

Ben-Shem A, Garreau de Loubresse N, Melnikov S, Jenner L, Yusupova G, Yusupov M (2011) The structure of the eukaryotic ribosome at 3.0 A resolution. *Science (New York, NY)* **334**: 1524-1529.

Bernstein KA, Granneman S, Lee AV, Manickam S, Baserga SJ (2006) Comprehensive mutational analysis of yeast DEXD/H box RNA helicases involved in large ribosomal subunit biogenesis. *Molecular and cellular biology* **26**: 1195-1208.

Biedka S, Wu S, LaPeruta AJ, Gao N, Woolford Jr. JL (2017) Insights into remodeling events during eukaryotic large ribosomal subunit assembly provided by high resolution cryo-EM structures. *RNA biology*: 1-8.

Birkedal U, Christensen-Dalsgaard M, Krogh N, Sabarinathan R, Gorodkin J, Nielsen H (2015) Profiling of ribose methylations in RNA by high-throughput sequencing. *Angewandte Chemie (International ed in English)* **54**: 451-455.

Bizebard T, Ferlenghi I, Iost I, Dreyfus M (2004) Studies on three E. coli DEAD-box helicases point to an unwinding mechanism different from that of model DNA helicases. *Biochemistry* **43**: 7857-7866.

Bohnsack MT, Kos M, Tollervey D (2008) Quantitative analysis of snoRNA association with pre-ribosomes and release of snR30 by Rok1 helicase. *EMBO reports* **9**: 1230-1236.

Bohnsack MT, Martin R, Granneman S, Ruprecht M, Schleiff E, Tollervey D. 2009. Prp43 bound at different sites on the pre-rRNA performs distinct functions in ribosome synthesis. *Molecular cell* **36**: 583-592.

Bohnsack MT, Tollervey D, Granneman S (2012) Identification of RNA helicase target sites by UV cross-linking and analysis of cDNA. *Methods in enzymology* **511**: 275-288.

Bond AT, Mangus DA, He F, Jacobson A (2001) Absence of Dbp2p alters both nonsense-mediated mRNA decay and rRNA processing. *Molecular and cellular biology* **21**: 7366-7379.

Brachmann CB, Davies A, Cost GJ, Caputo E, Li J, Hieter P, Boeke JD (1998) Designer deletion strains derived from Saccharomyces cerevisiae S288C: a useful set of strains and plasmids for PCR-mediated gene disruption and other applications. *Yeast (Chichester, England)* **14**: 115-132.

Bradatsch B, Leidig C, Granneman S, Gnadig M, Tollervey D, Bottcher B, Beckmann R, Hurt E (2012) Structure of the pre-60S ribosomal subunit with nuclear export factor Arx1 bound at the exit tunnel. *Nature structural & molecular biology* **19**: 1234-1241.

Briggs MW, Burkard KT, Butler JS (1998) Rrp6p, the yeast homologue of the human PM-Scl 100-kDa autoantigen, is essential for efficient 5.8 S rRNA 3' end formation. *The Journal of biological chemistry* **273**: 13255-13263.

Buchwald G, Schussler S, Basquin C, Le Hir H, Conti E (2013) Crystal structure of the human eIF4AIII-CWC22 complex shows how a DEAD-box protein is inhibited by a MIF4G domain. *Proceedings of the National Academy of Sciences of the United States of America* **110**: E4611-4618.

Burger F, Daugeron MC, Linder P (2000) Dbp10p, a putative RNA helicase from Saccharomyces cerevisiae, is required for ribosome biogenesis. *Nucleic acids research* **28**: 2315-2323.

Caruthers JM, Johnson ER, McKay DB (2000) Crystal structure of yeast initiation factor 4A, a DEAD-box RNA helicase. *Proceedings of the National Academy of Sciences of the United States of America* **97**: 13080-13085.

Chaker-Margot M, Hunziker M, Barandun J, Dill BD, Klinge S (2015) Stage-specific assembly events of the 6-MDa small-subunit processome initiate eukaryotic ribosome biogenesis. *Nature structural & molecular biology* **22**: 920-923.

Chen Y, Potratz JP, Tijerina P, Del Campo M, Lambowitz AM, Russell R (2008) DEAD-box proteins can completely separate an RNA duplex using a single ATP. *Proceedings of the National Academy of Sciences of the United States of America* **105**: 20203-20208.

Chen YL, Capeyrou R, Humbert O, Mouffok S, Kadri YA, Lebaron S, Henras AK, Henry Y (2014) The telomerase inhibitor Gno1p/PINX1 activates the helicase Prp43p during ribosome biogenesis. *Nucleic acids research* **42**: 7330-7345.

Choque E, Marcellin M, Burlet-Schiltz O, Gadal O, Dez C (2011) The nucleolar protein Nop19p interacts preferentially with Utp25p and Dhr2p and is essential for the production of the 40S ribosomal subunit in Saccharomyces cerevisiae. *RNA biology* **8**: 1158-1172.

Cloutier SC, Ma WK, Nguyen LT, Tran EJ (2012) The DEAD-box RNA helicase Dbp2 connects RNA quality control with repression of aberrant transcription. *The Journal of biological chemistry* **287**: 26155-26166.

Colley A, Beggs JD, Tollervey D, Lafontaine DL (2000) Dhr1p, a putative DEAH-box RNA helicase, is associated with the box C+D snoRNP U3. *Molecular and cellular biology* **20**: 7238-7246.

Combs DJ, Nagel RJ, Ares M, Jr., Stevens SW (2006) Prp43p is a DEAH-box spliceosome disassembly factor essential for ribosome biogenesis. *Molecular and cellular biology* **26**: 523-534.

Cordin O, Banroques J, Tanner NK, Linder P (2006) The DEAD-box protein family of RNA helicases. *Gene* **367**: 17-37.

Cordin O, Beggs JD (2013) RNA helicases in splicing. *RNA biology* **10**: 83-95.

Cordin O, Tanner NK, Doere M, Linder P, Banroques J (2004) The newly discovered Q motif of DEAD-box RNA helicases regulates RNA-binding and helicase activity. *The EMBO journal* **23**: 2478-2487.

Daugeron MC, Kressler D, Linder P (2001) Dbp9p, a putative ATP-dependent RNA helicase involved in 60S-ribosomal-subunit biogenesis, functionally interacts with Dbp6p. *RNA (New York, NY)* **7**: 1317-1334.

Daugeron MC, Linder P (1998) Dbp7p, a putative ATP-dependent RNA helicase from Saccharomyces cerevisiae, is required for 60S ribosomal subunit assembly. *RNA (New York, NY)* **4**: 566-581.

Daugeron MC, Linder P (2001) Characterization and mutational analysis of yeast Dbp8p, a putative RNA helicase involved in ribosome biogenesis. *Nucleic acids research* **29**: 1144-1155.

de la Cruz J, Kressler D, Rojo M, Tollervey D, Linder P (1998) Spb4p, an essential putative RNA helicase, is required for a late step in the assembly of 60S ribosomal subunits in Saccharomyces cerevisiae. *RNA (New York, NY)* **4**: 1268-1281.

Decatur WA, Fournier MJ (2002) rRNA modifications and ribosome function. *Trends in biochemical sciences* **27**: 344-351.

Dembowski JA, Kuo B, Woolford Jr. JL (2013) Has1 regulates consecutive maturation and processing steps for assembly of 60S ribosomal subunits. *Nucleic acids research* **41**: 7889-7904.

Dunbar DA, Baserga SJ (1998) The U14 snoRNA is required for 2'-O-methylation of the pre-18S rRNA in Xenopus oocytes. *RNA (New York, NY)* **4**: 195-204.

Dutca LM, Gallagher JE, Baserga SJ (2011) The initial U3 snoRNA:pre-rRNA base pairing interaction required for pre-18S rRNA folding revealed by in vivo chemical probing. *Nucleic acids research* **39**: 5164-5180.

Emery B, de la Cruz J, Rocak S, Deloche O, Linder P (2004) Has1p, a member of the DEAD-box family, is required for 40S ribosomal subunit biogenesis in Saccharomyces cerevisiae. *Molecular microbiology* **52**: 141-158.

Enright CA, Maxwell ES, Eliceiri GL, Sollner-Webb B (1996) 5'ETS rRNA processing facilitated by four small RNAs: U14, E3, U17, and U3. *RNA (New York, NY)* **2**: 1094-1099.

Esguerra J, Warringer J, Blomberg A (2008) Functional importance of individual rRNA 2'-O-ribose methylations revealed by high-resolution phenotyping. *RNA (New York, NY)* **14**: 649-656.

Faber AW, Vos HR, Vos JC, Raue HA (2006) 5'-end formation of yeast 5.8SL rRNA is an endonucleolytic event. *Biochemical and biophysical research communications* **345**: 796-802.

Fairman-Williams ME, Guenther UP, Jankowsky E (2010) SF1 and SF2 helicases: family matters. *Current opinion in structural biology* **20**: 313-324.

Fatica A, Oeffinger M, Dlakic M, Tollervey D (2003a) Nob1p is required for cleavage of the 3' end of 18S rRNA. *Molecular and cellular biology* **23**: 1798-1807.

Fatica A, Oeffinger M, Tollervey D, Bozzoni I (2003b) Cic1p/Nsa3p is required for synthesis and nuclear export of 60S ribosomal subunits. *RNA (New York, NY)* **9**: 1431-1436.

Faza MB, Chang Y, Occhipinti L, Kemmler S, Panse VG (2012) Role of Mex67-Mtr2 in the nuclear export of 40S pre-ribosomes. *PLoS genetics* **8**: e1002915.

Ferreira-Cerca S, Poll G, Kuhn H, Neueder A, Jakob S, Tschochner H, Milkereit P (2007). Analysis of the in vivo assembly pathway of eukaryotic 40S ribosomal proteins. *Molecular cell* **28**: 446-457.

Fourmann JB, Schmitzova J, Christian H, Urlaub H, Ficner R, Boon KL, Fabrizio P, Luhrmann R (2013) Dissection of the factor requirements for spliceosome disassembly and the elucidation of its dissociation products using a purified splicing system. *Genes & development* **27**: 413-428.

Fromont-Racine M, Senger B, Saveanu C, Fasiolo F (2003) Ribosome assembly in eukaryotes. *Gene* **313**: 17-42.

Fuller-Pace FV, Nicol SM, Reid AD, Lane DP (1993) DbpA: a DEAD box protein specifically activated by 23s rRNA. *The EMBO journal* **12**: 3619-3626.

Gadal O, Strauss D, Kessl J, Trumpower B, Tollervey D, Hurt E (2001) Nuclear export of 60s ribosomal subunits depends on Xpo1p and requires a nuclear export sequence-containing factor, Nmd3p, that associates with the large subunit protein Rpl10p. *Molecular and cellular biology* **21**: 3405-3415.

Gamalinda M, Jakovljevic J, Babiano R, Talkish J, de la Cruz J, Woolford Jr. JL (2013) Yeast polypeptide exit tunnel ribosomal proteins L17, L35 and L37 are necessary to recruit late-assembling factors required for 27SB pre-rRNA processing. *Nucleic acids research* **41**: 1965-1983.

Gamalinda M, Ohmayer U, Jakovljevic J, Kumcuoglu B, Woolford J, Mbom B, Lin L, Woolford Jr. JL (2014) A hierarchical model for assembly of eukaryotic 60S ribosomal subunit domains. *Genes & development* **28**: 198-210.

Garcia-Gomez JJ, Lebaron S, Froment C, Monsarrat B, Henry Y, de la Cruz J (2011) Dynamics of the putative RNA helicase Spb4 during ribosome assembly in Saccharomyces cerevisiae. *Molecular and cellular biology* **31**: 4156-4164.

Gasse L, Flemming D, Hurt E (2015) Coordinated Ribosomal ITS2 RNA Processing by the Las1 Complex Integrating Endonuclease, Polynucleotide Kinase, and Exonuclease Activities. *Molecular cell* **60**: 808-815.

Geerlings TH, Vos JC, Raue HA (2000) The final step in the formation of 25S rRNA in Saccharomyces cerevisiae is performed by 5'-->3' exonucleases. *RNA (New York, NY)* **6**: 1698-1703.

Gerhardy S, Menet AM, Pena C, Petkowski JJ, Panse VG (2014) Assembly and nuclear export of pre-ribosomal particles in budding yeast. *Chromosoma* **123**: 327-344.

Gorbalenya AE, Koonin EV (1993) Helicases: amino acid sequence comparisons and structure-function relationships. *Current opinion in structural biology* **3**: 419-429.

Grandi P, Rybin V, Bassler J, Petfalski E, Strauss D, Marzioch M, Schafer T, Kuster B, Tschochner H, Tollervey D et al. (2002) 90S pre-ribosomes include the 35S pre-rRNA, the U3 snoRNP, and 40S subunit processing factors but predominantly lack 60S synthesis factors. *Molecular cell* **10**: 105-115.

Granneman S, Bernstein KA, Bleichert F, Baserga SJ (2006a) Comprehensive mutational analysis of yeast DEXD/H box RNA helicases required for small ribosomal subunit synthesis. *Molecular and cellular biology* **26**: 1183-1194.

Granneman S, Kudla G, Petfalski E, Tollervey D (2009) Identification of protein binding sites on U3 snoRNA and pre-rRNA by UV cross-linking and high-throughput analysis of cDNAs. *Proceedings of the National Academy of Sciences of the United States of America* **106**: 9613-9618.

Granneman S, Lin C, Champion EA, Nandineni MR, Zorca C, Baserga SJ (2006b) The nucleolar protein Esf2 interacts directly with the DExD/H box RNA helicase, Dbp8, to stimulate ATP hydrolysis. *Nucleic acids research* **34**: 3189-3199.

Granneman S, Petfalski E, Tollervey D (2011) A cluster of ribosome synthesis factors regulate pre-rRNA folding and 5.8S rRNA maturation by the Rat1 exonuclease. *The EMBO journal* **30**: 4006-4019.

Greber BJ, Gerhardy S, Leitner A, Leibundgut M, Salem M, Boehringer D, Leulliot N, Aebersold R, Panse VG, Ban N (2016) Insertion of the Biogenesis Factor Rei1 Probes the Ribosomal Tunnel during 60S Maturation. *Cell* **164**: 91-102.

Gregersen LH, Schueler M, Munschauer M, Mastrobuoni G, Chen W, Kempa S, Dieterich C, Landthaler M (2014) MOV10 Is a 5' to 3' RNA helicase contributing to UPF1 mRNA target degradation by translocation along 3' UTRs. *Molecular cell* **54**: 573-585.

Gross T, Siepmann A, Sturm D, Windgassen M, Scarcelli JJ, Seedorf M, Cole CN, Krebber H (2007) The DEAD-box RNA helicase Dbp5 functions in translation termination. *Science (New York, NY)* **315**: 646-649.

Haag S, Kretschmer J, Sloan KE, Bohnsack MT (2017) Crosslinking Methods to Identify RNA Methyltransferase Targets In Vivo. *Methods in molecular biology (Clifton, NJ)* **1562**: 269-281.

Haag S, Sloan KE, Ranjan N, Warda AS, Kretschmer J, Blessing C, Hubner B, Seikowski J, Dennerlein S, Rehling P et al. (2016) NSUN3 and ABH1 modify the wobble position of mt-tRNAMet to expand codon recognition in mitochondrial translation. *The EMBO journal* **35**: 2104-2119.

Haag S, Warda AS, Kretschmer J, Gunnigmann MA, Hobartner C, Bohnsack MT (2015) NSUN6 is a human RNA methyltransferase that catalyzes formation of m5C72 in specific tRNAs. *RNA (New York, NY)* **21**: 1532-1543.

Hafner M, Landthaler M, Burger L, Khorshid M, Hausser J, Berninger P, Rothballer A, Ascano M, Jungkamp AC, Munschauer M et al. (2010) PAR-CliP--a method to identify transcriptome-wide the binding sites of RNA binding proteins. *Journal of visualized experiments : JoVE*.

Halls C, Mohr S, Del Campo M, Yang Q, Jankowsky E, Lambowitz AM (2007) Involvement of DEAD-box proteins in group I and group II intron splicing. Biochemical characterization of Mss116p, ATP hydrolysis-dependent and -independent mechanisms, and general RNA chaperone activity. *Journal of molecular biology* **365**: 835-855.

He Y, Andersen GR, Nielsen KH (2010) Structural basis for the function of DEAH helicases. *EMBO reports* **11**: 180-186.

Hector RD, Burlacu E, Aitken S, Le Bihan T, Tuijtel M, Zaplatina A, Cook AG, Granneman S (2014) Snapshots of pre-rRNA structural flexibility reveal eukaryotic 40S assembly dynamics at nucleotide resolution. *Nucleic acids research* **42**: 12138-12154.

Hedges J, West M, Johnson AW (2005) Release of the export adapter, Nmd3p, from the 60S ribosomal subunit requires Rpl10p and the cytoplasmic GTPase Lsg1p. *The EMBO journal* **24**: 567-579.

Heininger AU, Hackert P, Andreou AZ, Boon KL, Memet I, Prior M, Clancy A, Schmidt B, Urlaub H, Schleiff E et al. (2016) Protein cofactor competition regulates the action of a multifunctional RNA helicase in different pathways. *RNA biology* **13**: 320-330.

Helm M (2006) Post-transcriptional nucleotide modification and alternative folding of RNA. *Nucleic acids research* **34**: 721-733.

Henn A, Cao W, Licciardello N, Heitkamp SE, Hackney DD, De La Cruz EM (2010) Pathway of ATP utilization and duplex rRNA unwinding by the DEAD-box helicase, DbpA. *Proceedings of the National Academy of Sciences of the United States of America* **107**: 4046-4050.

Henras AK, Plisson-Chastang C, O'Donohue MF, Chakraborty A, Gleizes PE (2015) An overview of pre-ribosomal RNA processing in eukaryotes. *Wiley interdisciplinary reviews RNA* **6**: 225-242.

Henry Y, Wood H, Morrissey JP, Petfalski E, Kearsey S, Tollervey D (1994) The 5' end of yeast 5.8S rRNA is generated by exonucleases from an upstream cleavage site. *The EMBO journal* **13**: 2452-2463.

Hilbert M, Karow AR, Klostermeier D (2009) The mechanism of ATP-dependent RNA unwinding by DEAD box proteins. *Biological chemistry* **390**: 1237-1250.

Hoang T, Peng WT, Vanrobays E, Krogan N, Hiley S, Beyer AL, Osheim YN, Greenblatt J, Hughes TR, Lafontaine DL (2005) Esf2p, a U3-associated factor required for small-subunit processome assembly and compaction. *Molecular and cellular biology* **25**: 5523-5534.

Hofer A, Bussiere C, Johnson AW (2007) Mutational analysis of the ribosomal protein Rpl10 from yeast. *The Journal of biological chemistry* **282**: 32630-32639.

Hong B, Brockenbrough JS, Wu P, Aris JP (1997) Nop2p is required for pre-rRNA processing and 60S ribosome subunit synthesis in yeast. *Molecular and cellular biology* **17**: 378-388.

Houseley J, Tollervey D (2006) Yeast Trf5p is a nuclear poly(A) polymerase. *EMBO reports* **7**: 205-211.

Houseles J, Tollervey D (2010) Apparent non-canonical trans-splicing is generated by reverse transcriptase in vitro. *PloS one* **5**: e12271.

Huang HR, Rowe CE, Mohr S, Jiang Y, Lambowitz AM, Perlman PS (2005) The splicing of yeast mitochondrial group I and group II introns requires a DEAD-box protein with RNA chaperone function. *Proceedings of the National Academy of Sciences of the United States of America* **102**: 163-168.

Hurt E, Hannus S, Schmelzl B, Lau D, Tollervey D, Simos G (1999) A novel in vivo assay reveals inhibition of ribosomal nuclear export in ran-cycle and nucleoporin mutants. *The Journal of cell biology* **144**: 389-401.

Jankowsky E (2011) RNA helicases at work: binding and rearranging. *Trends in biochemical sciences* **36**: 19-29.

Jankowsky E, Bowers H (2006) Remodeling of ribonucleoprotein complexes with DExH/D RNA helicases. *Nucleic acids research* **34**: 4181-4188.

Jankowsky E, Gross CH, Shuman S, Pyle AM (2000) The DExH protein NPH-II is a processive and directional motor for unwinding RNA. *Nature* **403**: 447-451.

Jarmoskaite I, Russell R (2011) DEAD-box proteins as RNA helicases and chaperones. *Wiley interdisciplinary reviews RNA* **2**: 135-152.

Jarmoskaite I, Russell R (2014) RNA helicase proteins as chaperones and remodelers. *Annual review of biochemistry* **83**: 697-725.

Jenner L, Melnikov S, Garreau de Loubresse N, Ben-Shem A, Iskakova M, Urzhumtsev A, Meskauskas A, Dinman J, Yusupova G, Yusupov M (2012) Crystal structure of the 80S yeast ribosome. *Current opinion in structural biology* **22**: 759-767.

Jensen TH, Boulay J, Rosbash M, Libri D (2001) The DECD box putative ATPase Sub2p is an early mRNA export factor. *Current biology : CB* **11**: 1711-1715.

Jungfleisch J, Nedialkova DD, Dotu I, Sloan KE, Martinez-Bosch N, Brüning L, Raineri E, Navarro P, Bohnsack MT, Leidel SA et al. (2017) A novel translational control mechanism involving RNA structures within coding sequences. *Genome research* **27**: 95-106.

Karbstein K (2009) Eukaryotic ribosome assembly. Wiley encyclopedia of chemical biology. John wiley and sons: 222-230.

Karbstein K, Jonas S, Doudna JA (2005) An essential GTPase promotes assembly of preribosomal RNA processing complexes. *Molecular cell* **20**: 633-643.

Kempers-Veenstra AE, Oliemans J, Offenberg H, Dekker AF, Piper PW, Planta RJ, Klootwijk J (1986) 3'-End formation of transcripts from the yeast rRNA operon. *The EMBO journal* **5**: 2703-2710.

Khoshnevis S, Askenasy I, Johnson MC, Dattolo MD, Young-Erdos CL, Stroupe ME, Karbstein K (2016) The DEAD-box Protein Rok1 Orchestrates 40S and 60S Ribosome Assembly by Promoting the Release of Rrp5 from Pre-40S Ribosomes to Allow for 60S Maturation. *PLoS biology* **14**: e1002480.

Kiianitsa K, Solinger JA, Heyer WD (2003) NADH-coupled microplate photometric assay for kinetic studies of ATP-hydrolyzing enzymes with low and high specific activities. *Analytical biochemistry* **321**: 266-271.

King TH, Liu B, McCully RR, Fournier MJ (2003) Ribosome structure and activity are altered in cells lacking snoRNPs that form pseudouridines in the peptidyl transferase center. *Molecular cell* **11**: 425-435.

Kistler AL, Guthrie C (2001) Deletion of MUD2, the yeast homolog of U2AF65, can bypass the requirement for sub2, an essential spliceosomal ATPase. *Genes & development* **15**: 42-49.

Klinge S, Voigts-Hoffmann F, Leibundgut M, Arpagaus S, Ban N (2011) Crystal structure of the eukaryotic 60S ribosomal subunit in complex with initiation factor 6. *Science (New York, NY)* **334**: 941-948.

Klinge S, Voigts-Hoffmann F, Leibundgut M, Ban N (2012) Atomic structures of the eukaryotic ribosome. *Trends in biochemical sciences* **37**: 189-198.

Koch B, Mitterer V, Niederhauser J, Stanborough T, Murat G, Rechberger G, Bergler H, Kressler D, Pertschy B (2012) Yar1 protects the ribosomal protein Rps3 from aggregation. *The Journal of biological chemistry* **287**: 21806-21815.

König J, Zarnack K, Rot G, Curk T, Kayikci M, Zupan B, Turner DJ, Luscombe NM, Ule J (2010) iCLIP reveals the function of hnRNP particles in splicing at individual nucleotide resolution. *Nature structural & molecular biology* **17**: 909-915.

Konikkat S, Biedka S, Woolford Jr. JL (2017) The assembly factor Erb1 functions in multiple remodeling events during 60S ribosomal subunit assembly in S. cerevisiae. *Nucleic acids research* **45**: 4853-4865.

Kornprobst M, Turk M, Kellner N, Cheng J, Flemming D, Kos-Braun I, Kos M, Thoms M, Berninghausen O, Beckmann R et al. (2016) Architecture of the 90S Pre-ribosome: A Structural View on the Birth of the Eukaryotic Ribosome. *Cell* **166**: 380-393.

Kos M, Tollervey D (2005) The Putative RNA Helicase Dbp4p Is Required for Release of the U14 snoRNA from Preribosomes in Saccharomyces cerevisiae. *Molecular cell* **20**: 53-64.

Kos M, Tollervey D (2010) Yeast pre-rRNA processing and modification occur cotranscriptionally. *Molecular cell* **37**: 809-820.

Kressler D, de la Cruz J, Rojo M, Linder P (1997) Fal1p is an essential DEAD-box protein involved in 40S-ribosomal-subunit biogenesis in Saccharomyces cerevisiae. *Molecular and cellular biology* **17**: 7283-7294.

Kressler D, de la Cruz J, Rojo M, Linder P (1998) Dbp6p is an essential putative ATP-dependent RNA helicase required for 60S-ribosomal-subunit assembly in Saccharomyces cerevisiae. *Molecular and cellular biology* **18**: 1855-1865.

Kressler D, Doere M, Rojo M, Linder P (1999) Synthetic lethality with conditional dbp6 alleles identifies rsa1p, a nucleoplasmic protein involved in the assembly of 60S ribosomal subunits. *Molecular and cellular biology* **19**: 8633-8645.

Kudla G, Granneman S, Hahn D, Beggs JD, Tollervey D (2011) Cross-linking, ligation, and sequencing of hybrids reveals RNA-RNA interactions in yeast. *Proceedings of the National Academy of Sciences of the United States of America* **108**: 10010-10015.

Laemmli UK (1970) Cleavage of structural proteins during the assembly of the head of bacteriophage T4. *Nature* **227**: 680-685.

Lafontaine DL (2010) A 'garbage can' for ribosomes: how eukaryotes degrade their ribosomes. *Trends in biochemical sciences* **35**: 267-277.

Lafontaine DL, Bousquet-Antonelli C, Henry Y, Caizergues-Ferrer M, Tollervey D (1998) The box H + ACA snoRNAs carry Cbf5p, the putative rRNA pseudouridine synthase. *Genes & development* **12**: 527-537.

Lardelli RM, Thompson JX, Yates JR, 3rd, Stevens SW (2010) Release of SF3 from the intron branchpoint activates the first step of pre-mRNA splicing. *RNA (New York, NY)* **16**: 516-528.

Lebaron S, Froment C, Fromont-Racine M, Rain JC, Monsarrat B, Caizergues-Ferrer M, Henry Y (2005) The splicing ATPase prp43p is a component of multiple preribosomal particles. *Molecular and cellular biology* **25**: 9269-9282.

Lebaron S, Papin C, Capeyrou R, Chen YL, Froment C, Monsarrat B, Caizergues-Ferrer M, Grigoriev M, Henry Y (2009) The ATPase and helicase activities of Prp43p are stimulated by the G-patch protein Pfa1p during yeast ribosome biogenesis. *The EMBO journal* **28**: 3808-3819.

Lebaron S, Schneider C, van Nues RW, Swiatkowska A, Walsh D, Bottcher B, Granneman S, Watkins NJ, Tollervey D (2012) Proofreading of pre-40S ribosome maturation by a translation initiation factor and 60S subunits. *Nature structural & molecular biology* **19**: 744-753.

Leeds NB, Small EC, Hiley SL, Hughes TR, Staley JP (2006) The splicing factor Prp43p, a DEAH box ATPase, functions in ribosome biogenesis. *Molecular and cellular biology* **26**: 513-522.

Leidig C, Thoms M, Holdermann I, Bradatsch B, Berninghausen O, Bange G, Sinning I, Hurt E, Beckmann R (2014) 60S ribosome biogenesis requires rotation of the 5S ribonucleoprotein particle. *Nature communications* **5**: 3491.

Li B, Nierras CR, Warner JR (1999) Transcriptional elements involved in the repression of ribosomal protein synthesis. *Molecular and cellular biology* **19**: 5393-5404.

Liang WQ, Clark JA, Fournier MJ (1997) The rRNA-processing function of the yeast U14 small nucleolar RNA can be rescued by a conserved RNA helicase-like protein. *Molecular and cellular biology* **17**: 4124-4132.

Liang WQ, Fournier MJ (1995) U14 base-pairs with 18S rRNA: a novel snoRNA interaction required for rRNA processing. *Genes & development* **9**: 2433-2443.

Liang XH, Fournier MJ (2006) The helicase Has1p is required for snoRNA release from pre-rRNA. *Molecular and cellular biology* **26**: 7437-7450.

Liang XH, Liu Q, Fournier MJ (2007) rRNA modifications in an intersubunit bridge of the ribosome strongly affect both ribosome biogenesis and activity. *Molecular cell* **28**: 965-977.

Liang XH, Liu Q, Fournier MJ (2009) Loss of rRNA modifications in the decoding center of the ribosome impairs translation and strongly delays pre-rRNA processing. *RNA (New York, NY)* **15**: 1716-1728.

Licatalosi DD, Mele A, Fak JJ, Ule J, Kayikci M, Chi SW, Clark TA, Schweitzer AC, Blume JE, Wang X et al. (2008) HITS-CLIP yields genome-wide insights into brain alternative RNA processing. *Nature* **456**: 464-469.

Lin J, Lai S, Jia R, Xu A, Zhang L, Lu J, Ye K (2011) Structural basis for site-specific ribose methylation by box C/D RNA protein complexes. *Nature* **469**: 559-563.

Linder P, Jankowsky E (2011) From unwinding to clamping - the DEAD box RNA helicase family. *Nature reviews Molecular cell biology* **12**: 505-516.

Liu F, Putnam A, Jankowsky E (2008) ATP hydrolysis is required for DEAD-box protein recycling but not for duplex unwinding. *Proceedings of the National Academy of Sciences of the United States of America* **105**: 20209-20214.

Liu F, Putnam AA, Jankowsky E (2014) DEAD-box helicases form nucleotide-dependent, long-lived complexes with RNA. *Biochemistry* **53**: 423-433.

Long EO, Dawid IB (1980) Repeated genes in eukaryotes. *Annual review of biochemistry* **49**: 727-764.

Longtine MS, McKenzie A, 3rd, Demarini DJ, Shah NG, Wach A, Brachat A, Philippsen P, Pringle JR (1998) Additional modules for versatile and economical PCR-based gene deletion and modification in Saccharomyces cerevisiae. *Yeast (Chichester, England)* **14**: 953-961.

Ma C, Wu S, Li N, Chen Y, Yan K, Li Z, Zheng L, Lei J, Woolford JL, Jr., Gao N (2017) Structural snapshot of cytoplasmic pre-60S ribosomal particles bound by Nmd3, Lsg1, Tif6 and Reh1. *Nature structural & molecular biology* **24**: 214-220.

Ma WK, Cloutier SC, Tran EJ (2013) The DEAD-box protein Dbp2 functions with the RNA-binding protein Yra1 to promote mRNP assembly. *Journal of molecular biology* **425**: 3824-3838.

Mallam AL, Jarmoskaite I, Tijerina P, Del Campo M, Seifert S, Guo L, Russell R, Lambowitz AM (2011) Solution structures of DEAD-box RNA chaperones reveal conformational changes and nucleic acid tethering by a basic tail. *Proceedings of the National Academy of Sciences of the United States of America* **108**: 12254-12259.

Manikas RG, Thomson E, Thoms M, Hurt E (2016) The K(+)-dependent GTPase Nug1 is implicated in the association of the helicase Dbp10 to the immature peptidyl transferase centre during ribosome maturation. *Nucleic acids research* **44**: 1800-1812.

Martin R (2014) Functional characterisation of ribosome biogenesis cofactors on Saccharomyces cerevisiae. PhD thesis, Georg-August-Universität Göttingen.

Martin R, Hackert P, Ruprecht M, Simm S, Brüning L, Mirus O, Sloan KE, Kudla G, Schleiff E, Bohnsack MT (2014) A pre-ribosomal RNA interaction network involving snoRNAs and the Rok1 helicase. *RNA (New York, NY)* **20**: 1173-1182.

Matsuo Y, Granneman S, Thoms M, Manikas RG, Tollervey D, Hurt E (2014) Coupled GTPase and remodelling ATPase activities form a checkpoint for ribosome export. *Nature* **505**: 112-116.

Melnikov S, Ben-Shem A, Garreau de Loubresse N, Jenner L, Yusupova G, Yusupov M (2012) One core, two shells: bacterial and eukaryotic ribosomes. *Nature structural & molecular biology* **19**: 560-567.

Miles TD, Jakovljevic J, Horsey EW, Harnpicharnchai P, Tang L, Woolford Jr. JL (2005) Ytm1, Nop7, and Erb1 form a complex necessary for maturation of yeast 66S preribosomes. *Molecular and cellular biology* **25**: 10419-10432.

Mitchell P, Petfalski E, Tollervey D (1996) The 3' end of yeast 5.8S rRNA is generated by an exonuclease processing mechanism. *Genes & development* **10**: 502-513.

Mohr G, Del Campo M, Mohr S, Yang Q, Jia H, Jankowsky E, Lambowitz AM (2008) Function of the C-terminal domain of the DEAD-box protein Mss116p analyzed in vivo and in vitro. *Journal of molecular biology* **375**: 1344-1364.

Montpetit B, Thomsen ND, Helmke KJ, Seeliger MA, Berger JM, Weis K (2011) A conserved mechanism of DEAD-box ATPase activation by nucleoporins and InsP6 in mRNA export. *Nature* **472**: 238-242.

Morrissey JP, Tollervey D (1993) Yeast snR30 is a small nucleolar RNA required for 18S rRNA synthesis. *Molecular and cellular biology* **13**: 2469-2477.

Myong S, Ha T (2010) Stepwise translocation of nucleic acid motors. *Current opinion in structural biology* **20**: 121-127.

Nemeth A, Perez-Fernandez J, Merkl P, Hamperl S, Gerber J, Griesenbeck J, Tschochner H (2013) RNA polymerase I termination: Where is the end? *Biochimica et biophysica acta* **1829**: 306-317.

Neumann B, Wu H, Hackmann A, Krebber H (2016) Nuclear Export of Pre-Ribosomal Subunits Requires Dbp5, but Not as an RNA-Helicase as for mRNA Export. *PloS one* **11**: e0149571.

Nielsen KH, Behrens MA, He Y, Oliveira CL, Jensen LS, Hoffmann SV, Pedersen JS, Andersen GR (2011) Synergistic activation of eIF4A by eIF4B and eIF4G. *Nucleic acids research* **39**: 2678-2689.

O'Day CL, Chavanikamannil F, Abelson J (1996) 18S rRNA processing requires the RNA helicase-like protein Rrp3. *Nucleic acids research* **24**: 3201-3207.

Oberer M, Marintchev A, Wagner G (2005) Structural basis for the enhancement of eIF4A helicase activity by eIF4G. *Genes & development* **19**: 2212-2223.

Oeffinger M, Zenklusen D, Ferguson A, Wei KE, El Hage A, Tollervey D, Chait BT, Singer RH, Rout MP (2009) Rrp17p is a eukaryotic exonuclease required for 5' end processing of Pre-60S ribosomal RNA. *Molecular cell* **36**: 768-781.

Ohmayer U, Gamalinda M, Sauert M, Ossowski J, Poll G, Linnemann J, Hierlmeier T, Perez-Fernandez J, Kumcuoglu B, Leger-Silvestre I et al. (2013) Studies on the assembly characteristics of large subunit ribosomal proteins in S. cerevisae. *PloS one* **8**: e68412.

Ohmayer U, Gil-Hernandez A, Sauert M, Martin-Marcos P, Tamame M, Tschochner H, Griesenbeck J, Milkereit P (2015) Studies on the Coordination of Ribosomal Protein Assembly Events Involved in Processing and Stabilization of Yeast Early Large Ribosomal Subunit Precursors. *PloS one* **10**: e0143768.

Ohtake Y, Wickner RB (1995) Yeast virus propagation depends critically on free 60S ribosomal subunit concentration. *Molecular and cellular biology* **15**: 2772-2781.

Pause A, Methot N, Sonenberg N (1993) The HRIGRXXR region of the DEAD box RNA helicase eukaryotic translation initiation factor 4A is required for RNA binding and ATP hydrolysis. *Molecular and cellular biology* **13**: 6789-6798.

Pause A, Sonenberg N (1992) Mutational analysis of a DEAD box RNA helicase: the mammalian translation initiation factor eIF-4A. *The EMBO journal* **11**: 2643-2654.

Pertschy B, Saveanu C, Zisser G, Lebreton A, Tengg M, Jacquier A, Liebminger E, Nobis B, Kappel L, van der Klei I et al. (2007) Cytoplasmic recycling of 60S preribosomal factors depends on the AAA protein Drg1. *Molecular and cellular biology* **27**: 6581-6592.

Pertschy B, Schneider C, Gnadig M, Schafer T, Tollervey D, Hurt E (2009) RNA helicase Prp43 and its co-factor Pfa1 promote 20 to 18 S rRNA processing catalyzed by the endonuclease Nob1. *The Journal of biological chemistry* **284**: 35079-35091.

Petrov AS, Bernier CR, Gulen B, Waterbury CC, Hershkovits E, Hsiao C, Harvey SC, Hud NV, Fox GE, Wartell RM et al. (2014a) Secondary structures of rRNAs from all three domains of life. *PloS one* **9**: e88222.

Petrov AS, Bernier CR, Hsiao C, Norris AM, Kovacs NA, Waterbury CC, Stepanov VG, Harvey SC, Fox GE, Wartell RM et al. (2014b) Evolution of the ribosome at atomic resolution. *Proceedings of the National Academy of Sciences of the United States of America* **111**: 10251-10256.

Phipps KR, Charette J, Baserga SJ (2011) The small subunit processome in ribosome biogenesis-progress and prospects. *Wiley interdisciplinary reviews RNA* **2**: 1-21.

Pillet B, Garcia-Gomez JJ, Pausch P, Falquet L, Bange G, de la Cruz J, Kressler D (2015) The Dedicated Chaperone Acl4 Escorts Ribosomal Protein Rpl4 to Its Nuclear Pre-60S Assembly Site. *PLoS genetics* **11**: e1005565.

Pratte D, Singh U, Murat G, Kressler D (2013) Mak5 and Ebp2 act together on early pre-60S particles and their reduced functionality bypasses the requirement for the essential pre-60S factor Nsa1. *PloS one* **8**: e82741.

Rabl J, Leibundgut M, Ataide SF, Haag A, Ban N (2011) Crystal structure of the eukaryotic 40S ribosomal subunit in complex with initiation factor 1. *Science (New York, NY)* **331**: 730-736.

Ray P, Basu U, Ray A, Majumdar R, Deng H, Maitra U (2008) The Saccharomyces cerevisiae 60 S ribosome biogenesis factor Tif6p is regulated by Hrr25p-mediated phosphorylation. *The Journal of biological chemistry* **283**: 9681-9691.

Ripmaster TL, Vaughn GP, Woolford Jr. JL (1992) A putative ATP-dependent RNA helicase involved in Saccharomyces cerevisiae ribosome assembly. *Proceedings of the National Academy of Sciences of the United States of America* **89**: 11131-11135.

Ripmaster TL, Vaughn GP, Woolford Jr. JL (1993) DRS1 to DRS7, novel genes required for ribosome assembly and function in Saccharomyces cerevisiae. *Molecular and cellular biology* **13**: 7901-7912.

Rocak S, Emery B, Tanner NK, Linder P (2005) Characterization of the ATPase and unwinding activities of the yeast DEAD-box protein Has1p and the analysis of the roles of the conserved motifs. *Nucleic acids research* **33**: 999-1009.

Rogers GW, Jr., Richter NJ, Merrick WC (1999) Biochemical and kinetic characterization of the RNA helicase activity of eukaryotic initiation factor 4A. *The Journal of biological chemistry* **274**: 12236-12244.

Rosado IV, Dez C, Lebaron S, Caizergues-Ferrer M, Henry Y, de la Cruz J (2007) Characterization of Saccharomyces cerevisiae Npa2p (Urb2p) reveals a low-molecular-mass complex containing Dbp6p, Npa1p (Urb1p), Nop8p, and Rsa3p involved in early steps of 60S ribosomal subunit biogenesis. *Molecular and cellular biology* **27**: 1207-1221.

Rout MP, Blobel G, Aitchison JD (1997) A distinct nuclear import pathway used by ribosomal proteins. *Cell* **89**: 715-725.

Ruby SW, Chang TH, Abelson J (1993) Four yeast spliceosomal proteins (PRP5, PRP9, PRP11, and PRP21) interact to promote U2 snRNP binding to pre-mRNA. *Genes & development* **7**: 1909-1925.

Russell R (2008) RNA misfolding and the action of chaperones. *Frontiers in bioscience : a journal and virtual library* **13**: 1-20.

Sachs AB, Davis RW (1989) The poly(A) binding protein is required for poly(A) shortening and 60S ribosomal subunit-dependent translation initiation. *Cell* **58**: 857-867.

Sachs AB, Davis RW (1990) Translation initiation and ribosomal biogenesis: involvement of a putative rRNA helicase and RPL46. *Science (New York, NY)* **247**: 1077-1079.

Sahasranaman A, Dembowski J, Strahler J, Andrews P, Maddock J, Woolford Jr. JL (2011) Assembly of Saccharomyces cerevisiae 60S ribosomal subunits: role of factors required for 27S pre-rRNA processing. *The EMBO journal* **30**: 4020-4032.

Samarsky DA, Fournier MJ (1998) Functional mapping of the U3 small nucleolar RNA from the yeast Saccharomyces cerevisiae. *Molecular and cellular biology* **18**: 3431-3444.

Sambrook J, Russell DW (2001) Molecular cloning a laboratory manual. 3. Cold Spring Harbor Laboratory Press, Cold Spring Harbor, NY.

Sardana R, Liu X, Granneman S, Zhu J, Gill M, Papoulas O, Marcotte EM, Tollervey D, Correll CC, Johnson AW (2015) The DEAH-box helicase Dhr1 dissociates U3 from the pre-rRNA to promote formation of the central pseudoknot. *PLoS biology* **13**: e1002083.

Saveanu C, Namane A, Gleizes PE, Lebreton A, Rousselle JC, Noaillac-Depeyre J, Gas N, Jacquier A, Fromont-Racine M (2003) Sequential protein association with nascent 60S ribosomal particles. *Molecular and cellular biology* **23**: 4449-4460.

Schäfer T, Maco B, Petfalski E, Tollervey D, Bottcher B, Aebi U, Hurt E (2006) Hrr25-dependent phosphorylation state regulates organization of the pre-40S subunit. *Nature* **441**: 651-655.

Schuch B, Feigenbutz M, Makino DL, Falk S, Basquin C, Mitchell P, Conti E (2014) The exosome-binding factors Rrp6 and Rrp47 form a composite surface for recruiting the Mtr4 helicase. *The EMBO journal* **33**: 2829-2846.

Schütz P, Bumann M, Oberholzer AE, Bieniossek C, Trachsel H, Altmann M, Baumann U (2008) Crystal structure of the yeast eIF4A-eIF4G complex: an RNA-helicase controlled by protein-protein interactions. *Proceedings of the National Academy of Sciences of the United States of America* **105**: 9564-9569.

Seiser RM, Sundberg AE, Wollam BJ, Zobel-Thropp P, Baldwin K, Spector MD, Lycan DE (2006) Ltv1 is required for efficient nuclear export of the ribosomal small subunit in Saccharomyces cerevisiae. *Genetics* **174**: 679-691.

Sharma S, Langhendries JL, Watzinger P, Kötter P, Entian KD, Lafontaine DL (2015) Yeast Kre33 and human NAT10 are conserved 18S rRNA cytosine acetyltransferases that modify tRNAs assisted by the adaptor Tan1/THUMPD1. *Nucleic acids research* **43**: 2242-2258.

Sharma S, Yang J, van Nues R, Watzinger P, Kötter P, Lafontaine DLJ, Granneman S, Entian KD (2017) Specialized box C/D snoRNPs act as antisense guides to target RNA base acetylation. *PLoS genetics* **13**: e1006804.

Simoff I, Moradi H, Nygard O (2009) Functional characterization of ribosomal protein L15 from Saccharomyces cerevisiae. *Current genetics* **55**: 111-125.

Singh SK, Gurha P, Gupta R (2008) Dynamic guide-target interactions contribute to sequential 2'-O-methylation by a unique archaeal dual guide box C/D sRNP. *RNA (New York, NY)* **14**: 1411-1423.

Singleton MR, Dillingham MS, Wigley DB (2007) Structure and mechanism of helicases and nucleic acid translocases. *Annual review of biochemistry* **76**: 23-50.

Sloan KE, Warda AS, Sharma S, Entian KD, Lafontaine DLJ, Bohnsack MT (2016) Tuning the ribosome: The influence of rRNA modification on eukaryotic ribosome biogenesis and function. *RNA biology*: 1-16.

Soltanieh S, Osheim YN, Spasov K, Trahan C, Beyer AL, Dragon F (2015) DEAD-box RNA helicase Dbp4 is required for small-subunit processome formation and function. *Molecular and cellular biology* **35**: 816-830.

Song C, Hotz-Wagenblatt A, Voit R, Grummt I (2017) SIRT7 and the DEAD-box helicase DDX21 cooperate to resolve genomic R loops and safeguard genome stability. *Genes & development*.

Stage-Zimmermann T, Schmidt U, Silver PA (2000) Factors affecting nuclear export of the 60S ribosomal subunit in vivo. *Molecular biology of the cell* **11**: 3777-3789.

Staley JP, Guthrie C (1999) An RNA switch at the 5' splice site requires ATP and the DEAD box protein Prp28p. *Molecular cell* **3**: 55-64.

Steffen KK, McCormick MA, Pham KM, MacKay VL, Delaney JR, Murakami CJ, Kaeberlein M, Kennedy BK (2012) Ribosome deficiency protects against ER stress in Saccharomyces cerevisiae. *Genetics* **191**: 107-118.

Strunk BS, Karbstein K (2009) Powering through ribosome assembly. *RNA (New York, NY)* **15**: 2083-2104.

Strunk BS, Loucks CR, Su M, Vashisth H, Cheng S, Schilling J, Brooks CL, 3rd, Karbstein K, Skiniotis G (2011) Ribosome assembly factors prevent premature translation initiation by 40S assembly intermediates. *Science (New York, NY)* **333**: 1449-1453.

Strunk BS, Novak MN, Young CL, Karbstein K (2012) A translation-like cycle is a quality control checkpoint for maturing 40S ribosome subunits. *Cell* **150**: 111-121.

Swiatkowska A, Wlotzka W, Tuck A, Barrass JD, Beggs JD, Tollervey D (2012) Kinetic analysis of pre-ribosome structure in vivo. *RNA (New York, NY)* **18**: 2187-2200.

Talkish J, Biedka S, Jakovljevic J, Zhang J, Tang L, Strahler JR, Andrews PC, Maddock JR, Woolford Jr. JL (2016) Disruption of ribosome assembly in yeast blocks cotranscriptional pre-rRNA processing and affects the global hierarchy of ribosome biogenesis. *RNA (New York, NY)* **22**: 852-866.

Talkish J, Zhang J, Jakovljevic J, Horsey EW, Woolford Jr. JL (2012) Hierarchical recruitment into nascent ribosomes of assembly factors required for 27SB pre-rRNA processing in Saccharomyces cerevisiae. *Nucleic acids research* **40**: 8646-8661.

Tanner JA, Watt RM, Chai YB, Lu LY, Lin MC, Peiris JS, Poon LL, Kung HF, Huang JD (2003) The severe acute respiratory syndrome (SARS) coronavirus NTPase/helicase belongs to a distinct class of 5' to 3' viral helicases. *The Journal of biological chemistry* **278**: 39578-39582.

Thiry M, Lafontaine DL (2005) Birth of a nucleolus: the evolution of nucleolar compartments. *Trends in cell biology* **15**: 194-199.

Thoms M, Ahmed YL, Maddi K, Hurt E, Sinning I (2016) Concerted removal of the Erb1-Ytm1 complex in ribosome biogenesis relies on an elaborate interface. *Nucleic acids research* **44**: 926-939.

Thoms M, Thomson E, Bassler J, Gnadig M, Griesel S, Hurt E (2015) The Exosome Is Recruited to RNA Substrates through Specific Adaptor Proteins. *Cell* **162**: 1029-1038.

Torchet C, Hermann-Le Denmat S (2000) Bypassing the rRNA processing endonucleolytic cleavage at site A2 in Saccharomyces cerevisiae. *RNA (New York, NY)* **6**: 1498-1508.

Travis AJ, Moody J, Helwak A, Tollervey D, Kudla G (2014) Hyb: a bioinformatics pipeline for the analysis of CLASH (crosslinking, ligation and sequencing of hybrids) data. *Methods (San Diego, Calif)* **65**: 263-273.

Tsai RT, Tseng CK, Lee PJ, Chen HC, Fu RH, Chang KJ, Yeh FL, Cheng SC (2007) Dynamic interactions of Ntr1-Ntr2 with Prp43 and with U5 govern the recruitment of Prp43 to mediate spliceosome disassembly. *Molecular and cellular biology* **27**: 8027-8037.

Tseng SS, Weaver PL, Liu Y, Hitomi M, Tartakoff AM, Chang TH (1998) Dbp5p, a cytosolic RNA helicase, is required for poly(A)+ RNA export. *The EMBO journal* **17**: 2651-2662.

Turner AJ, Knox AA, Prieto JL, McStay B, Watkins NJ (2009) A novel small-subunit processome assembly intermediate that contains the U3 snoRNP, nucleolin, RRP5, and DBP4. *Molecular and cellular biology* **29**: 3007-3017.

Turowski TW, Tollervey D (2015) Cotranscriptional events in eukaryotic ribosome synthesis. *Wiley interdisciplinary reviews RNA* **6**: 129-139.

Ule J, Jensen KB, Ruggiu M, Mele A, Ule A, Darnell RB (2003) CLIP identifies Nova-regulated RNA networks in the brain. *Science (New York, NY)* **302**: 1212-1215.

van Nues RW, Granneman S, Kudla G, Sloan KE, Chicken M, Tollervey D, Watkins NJ (2011) Box C/D snoRNP catalysed methylation is aided by additional pre-rRNA base-pairing. *The EMBO journal* **30**: 2420-2430.

Vanrobays E, Leplus A, Osheim YN, Beyer AL, Wacheul L, Lafontaine DL (2008) TOR regulates the subcellular distribution of DIM2, a KH domain protein required for cotranscriptional ribosome assembly and pre-40S ribosome export. *RNA (New York, NY)* **14**: 2061-2073.

Venema J, Bousquet-Antonelli C, Gelugne JP, Caizergues-Ferrer M, Tollervey D (1997) Rok1p is a putative RNA helicase required for rRNA processing. *Molecular and cellular biology* **17**: 3398-3407.

von Moeller H, Basquin C, Conti E (2009) The mRNA export protein DBP5 binds RNA and the cytoplasmic nucleoporin NUP214 in a mutually exclusive manner. *Nature structural & molecular biology* **16**: 247-254.

Vos HR, Bax R, Faber AW, Vos JC, Raue HA (2004) U3 snoRNP and Rrp5p associate independently with Saccharomyces cerevisiae 35S pre-rRNA, but Rrp5p is essential for association of Rok1p. *Nucleic acids research* **32**: 5827-5833.

Walker JE, Saraste M, Runswick MJ, Gay NJ (1982) Distantly related sequences in the alpha- and beta-subunits of ATP synthase, myosin, kinases and other ATP-requiring enzymes and a common nucleotide bining fold. *EMBO J* **8**: 945-951.

Warkocki Z, Odenwalder P, Schmitzova J, Platzmann F, Stark H, Urlaub H, Ficner R, Fabrizio P, Luhrmann R (2009) Reconstitution of both steps of Saccharomyces cerevisiae splicing with purified spliceosomal components. *Nature structural & molecular biology* **16**: 1237-1243.

Warner JR. (1999) The economics of ribosome biosynthesis in yeast. *Trends in biochemical sciences* **24**: 437-440.

Wasmuth EV, Zinder JC, Zattas D, Das M, Lima CD (2017) Structure and reconstitution of yeast Mpp6-nuclear exosome complexes reveals that Mpp6 stimulates RNA decay and recruits the Mtr4 helicase. *eLife* **6**.

Watkins NJ, Bohnsack MT (2012) The box C/D and H/ACA snoRNPs: key players in the modification, processing and the dynamic folding of ribosomal RNA. *Wiley interdisciplinary reviews RNA* **3**: 397-414.

Weaver PL, Sun C, Chang TH (1997) Dbp3p, a putative RNA helicase in Saccharomyces cerevisiae, is required for efficient pre-rRNA processing predominantly at site A3. *Molecular and cellular biology* **17**: 1354-1365.

Webb S, Hector RD, Kudla G, Granneman S (2014) PAR-CLIP data indicate that Nrd1-Nab3-dependent transcription termination regulates expression of hundreds of protein coding genes in yeast. *Genome biology* **15**: R8.

Weirich CS, Erzberger JP, Flick JS, Berger JM, Thorner J, Weis K (2006) Activation of the DExD/H-box protein Dbp5 by the nuclear-pore protein Gle1 and its coactivator InsP6 is required for mRNA export. *Nature cell biology* **8**: 668-676.

Wells GR, Weichmann F, Colvin D, Sloan KE, Kudla G, Tollervey D, Watkins NJ, Schneider C (2016) The PIN domain endonuclease Utp24 cleaves pre-ribosomal RNA at two coupled sites in yeast and humans. *Nucleic acids research* **44**: 5399-5409.

Wells SE, Hughes JM, Igel AH, Ares Jr. M (2000) Use of dimethyl sulfate to probe RNA structure in vivo. *Methods in enzymology* **318**: 479-493.

West M, Hedges JB, Chen A, Johnson AW (2005) Defining the order in which Nmd3p and Rpl10p load onto nascent 60S ribosomal subunits. *Molecular and cellular biology* **25**: 3802-3813.

Woodson SA (2008) RNA folding and ribosome assembly. *Current opinion in chemical biology* **12**: 667-673.

Wu S, Tutuncuoglu B, Yan K, Brown H, Zhang Y, Tan D, Gamalinda M, Yuan Y, Li Z, Jakovljevic J et al. (2016) Diverse roles of assembly factors revealed by structures of late nuclear pre-60S ribosomes. *Nature* **534**: 133-137.

Xing YH, Yao RW, Zhang Y, Guo CJ, Jiang S, Xu G, Dong R, Yang L, Chen LL (2017) SLERT Regulates DDX21 Rings Associated with Pol I Transcription. *Cell* **169**: 664-678.e616.

Yang Q, Del Campo M, Lambowitz AM, Jankowsky E (2007) DEAD-box proteins unwind duplexes by local strand separation. *Molecular cell* **28**: 253-263.

Yang Q, Jankowsky E (2005) ATP- and ADP-dependent modulation of RNA unwinding and strand annealing activities by the DEAD-box protein DED1. *Biochemistry* **44**: 13591-13601.

Yang Q, Jankowsky E (2006) The DEAD-box protein Ded1 unwinds RNA duplexes by a mode distinct from translocating helicases. *Nature structural & molecular biology* **13**: 981-986.

Yang Z, Lin J, Ye K (2016) Box C/D guide RNAs recognize a maximum of 10 nt of substrates. *Proceedings of the National Academy of Sciences of the United States of America* **113**: 10878-10883.

Yao W, Roser D, Kohler A, Bradatsch B, Bassler J, Hurt E (2007) Nuclear export of ribosomal 60S subunits by the general mRNA export receptor Mex67-Mtr2. *Molecular cell* **26**: 51-62.

Young CL, Khoshnevis S, Karbstein K (2013) Cofactor-dependent specificity of a DEAD-box protein. *Proceedings of the National Academy of Sciences of the United States of America* **110**: E2668-2676.

Zagulski M, Kressler D, Becam AM, Rytka J, Herbert CJ (2003) Mak5p, which is required for the maintenance of the M1 dsRNA virus, is encoded by the yeast ORF YBR142w and is involved in the biogenesis of the 60S subunit of the ribosome. *Molecular genetics and genomics : MGG* **270**: 216-224.

Zemp I, Wild T, O'Donohue MF, Wandrey F, Widmann B, Gleizes PE, Kutay U (2009) Distinct cytoplasmic maturation steps of 40S ribosomal subunit precursors require hRio2. *The Journal of cell biology* **185**: 1167-1180.

Zhang J, Harnpicharnchai P, Jakovljevic J, Tang L, Guo Y, Oeffinger M, Rout MP, Hiley SL, Hughes T, Woolford Jr. JL (2007) Assembly factors Rpf2 and Rrs1 recruit 5S rRNA and ribosomal proteins rpL5 and rpL11 into nascent ribosomes. *Genes & development* **21**: 2580-2592.

Zhu J, Liu X, Anjos M, Correll CC, Johnson AW (2016) Utp14 Recruits and Activates the RNA Helicase Dhr1 To Undock U3 snoRNA from the Preribosome. *Molecular and cellular biology* **36**: 965-978.

Publications associated with this thesis

Jungfleisch J, Nedialkova DD, Dotu I, Sloan KE, Martinez-Bosch N, <u>Brüning L</u>, Raineri E, Navarro P, Bohnsack MT, Leidel SA, Diez J (2017) A novel translational control mechanism involving RNA structures within coding sequences. *Genome research* **27**: 95 – 106.

Martin R, Hackert P, Ruprecht M, Simm S, <u>Brüning L</u>, Mirus O, Sloan KE, Kudla G, Schleiff E & Bohnsack MT (2014) A pre-ribosomal RNA interaction network involving snoRNAs and the Rok1 helicase. *RNA (New York, NY)* **20**: 1173–1182.

<u>Acknowledgments</u>

For the opportunity to work on such an exciting topic, which enabled me to extend my range of skills on various levels, I would like to thank my supervisor Prof. Dr. Markus Bohnsack. Constructive discussions along with excellent supervision and guidance kept a high level of motivation throughout my time in the Bohnsack lab.

I am thankful for the support of the additional members of my thesis committee, Prof. Dr. Ralf Ficner and Prof. Dr. Jörg Enderlein. Besides my thesis committee, I would like to thank Prof. Dr. Jörg Stülke, Prof. Dr. Michael Thumm and Prof. Dr. Gerhard Braus for their willingness to become members of my examination board.

My sincere and special thanks go to Dr. Katherine Sloan for her constant support, helpful suggestions, interesting discussions and useful comments during the whole PhD and also during the preparation of this thesis.

I would like to express my gratitude to Prof. Dr. Blanche Schwappach-Pignataro, head of the Department of Molecular Biology, and all former and present colleagues in the institute who contributed to creating a nice working atmosphere and making my time here so pleasant.

I would like to thank all members of the Bohnsack lab, who I shared a significant amount of time with during the last four years. First of all, Philipp Hackert for his never-ending sense of support, including reading this thesis very carefully. Dr. Roman Martin and Jens Kretschmer, who introduced me to a previously unknown world of programming and bioinformatics. The members of our "yeast lab": Dr. Annika Heininger, Jimena Davila Gallesio, Gerald Aquino and Benedikt Hübner, as well as those colleagues focusing on projects in the "human lab": Dr. Sara Haag, Dr. Carmen Döbele, Ahmed Warda, Indira Memet and Priyanka Choudhury.

Special thanks go to my girlfriend Svenja for being such a lovely and important person in my life. Without her, all this would not have happened.

Finally, I want to express my gratitude to both my and Svenja's family for their caring and ongoing support along my studies.